Propagating Waves in Reaction Cross-Diffusion Systems

Submitted by **Abdullah Mohammed Aldurayhim,**
to the University of Exeter as a thesis for the degree of
Doctor of Philosophy in Mathematics, in **October 2017.**

I certify that all material in this thesis which is not my own work has been identified and that no material has previously been submitted and approved for the award of a degree by this or any other University.

Signature: .....

Abstract

This research focuses on the reaction diffusion systems where the matrix of diffusion coefficients is not diagonal. We call these systems reaction cross-diffusion systems. These systems possess interesting solutions that do not appear in the reaction self-diffusion systems that have a diagonal diffusion matrix. Compared to research conducted on reaction self-diffusion systems, the reaction cross-diffusion systems have received little attentions.

The aim of this research is to extend existing literature on these systems. In this thesis we considered two-components reaction cross-diffusion systems. We find an analytical solution of reaction diffusion system with replacing FitzHugh-Nagumo kinetics by quartic polynomial. Finding the analytical solution is extends analytical results presented in [9]. This analytical solution is presented in a wave front profile. We study the possibility of imitating Fisher-KPP and ZFK-Nagumo front waves by our analytical solution which we have introduced.

The existence of a quartic polynomial yields four different cases with respect to the positions of the roots of the quartic polynomial and the resting states of the wave front. We solve the problem numerically and compare the numerical solution to the analytical solution for those four cases.

Finally, we extend the analysis of the different wave regimes in reaction cross-diffusion system with FitzHugh-Nagumo kinetics by varying parameters in the system using numerical continuation. We compute the speed of propagating waves in this system and show the corresponding eigenvalues of equilibrium which gives an indication about the profile of the propagating waves. We find a stable propagating wave that is not obtained by direct numerical simulation in [55]. We investigate the stability of propagating waves by using direct numerical simulation.

ACKNOWLEDGEMENT

The success and the final outcome of this research required a lot of guidance and assistance from many people and I extremely fortunate to have got this all along the completion of this work.

I would first like to thank my supervisor Professor Vadim Biktashev for his encouragement, expertise, understanding and invaluable guidance through the process of researching and writing this thesis. This PhD thesis would not be possible without his support. I am really appreciated his patience and quick replies to my queries even on the days of his vacation.

I am also grateful for the contribution and advices of my second supervisor Professor Peter Ashwin and my mentor Dr. Chris Ferro.

I would like to thank my dad, my mum and my brothers and sisters for their supports. Special thanks to my wife Abrar and my lovely daughters Sarah, Jana and my newly born baby Maram for their love and patience through the rough road we have been on together.

I would like to thank my colleagues in Room H201, Saad Almuadi, Hassan Alkhayuon, Lamees Felemban, Courtney Quinn, Paul Ritchie and Damian Smug.

Finally, I would like to express my deepest gratitude to every single member of my family for helping me survive all the stress. I owe them much more than I would ever be able to express.

CONTENTS

List of Tables

List of Figures

CHAPTER 1

INTRODUCTION

In 1836, John Scott Russell, observed a wave and his observation was described in [44]. He said in his description of this wave

" I followed it on horseback, and overtook it still rolling an at rate of some eight or nine miles an hour, preserving its original figure some thirty feet long ⋯"

This wave is called *soliton* wave by Kruskal and Zabusky [64]. This wave falls within a field of so-called Travelling (Propagating) waves. The travelling wave solution becomes a significant technique to solve partial differential equations. The importance of dealing with problems by using waves is that many topics in science could be interpreted by waves.

Partial differential equations (PDEs) are an enormous topic in mathematics often used in most of the fields of science. As a consequence of the nonlinearity of the world, much research seeks to understand nonlinear processes. These nonlinear processes are usually expressed by PDEs. So, the PDE is an active topic in applied mathematics. The facilities that we have now gained by computers to solve PDE will keep the research in this topic alive for longer.

There are different classifications for PDEs, but the classification of interest for this

thesis is linear PDEs and nonlinear PDEs. The partial differential equations considered in this thesis are composed of linear *diffusion* terms and nonlinear *reaction* terms. The name of such a model is a reaction diffusion system. They fall within nonlinear parabolic PDEs.

1.1 Reaction Diffusion Systems

The common form for reaction diffusion systems is

$$u_t^\alpha = \sum_{\beta=1}^{n} \sum_{j=1}^{3} \frac{\partial}{\partial x_j} \left(D^{\alpha\beta} \frac{\partial u^\beta}{\partial x_j} \right) + f^\alpha(u^\beta), \tag{1.1}$$

where t denotes the time, n is the number of components in the system , x_j is the spatial variable and D is the matrix of diffusion coefficients. Unknown variable $u \in \mathbb{R}^n$ is a state variable that represents density, saturation or concentration at position x at time t for one dimension or at position (x, y) at time t for two dimensions or at position (x, y, z) at time t for three dimensions. The action of diffusion terms in reaction diffusion systems is to find a connection between the differences between concentrations of components along the domain of the space.

In various areas such as physics, chemistry, biology, ecology, neurology etc., we observe phenomena that can be described by such systems (1.1). There are many problems that are exhibited by reaction diffusion systems [61].

The combination of reaction terms and diffusion terms covers all surrounding factors of the phenomenon in real-world problems. For example, the movement of a herbivorous animal in a field is described by a diffusion term and a reaction term. The random motion of the animal in the field is presented by the diffusion term and the reaction term presents the competition for the source of the food and/or the interaction between prey and predators.

The reaction terms $f(u)$ determines the specification of the system. The following are selections of some well-known reaction diffusion models taken from [37] , [38] and [24].

Fisher model:

$$u_t = Du_{xx} + u(1-u).$$

Fisher [21] built his model to present the spread of advantageous genes in a population living in one dimension.

Bistable (Nagumo) model:

$$u_t = Du_{xx} + u(u-\alpha)(1-u), \quad 0 < \alpha < 1\,,$$

This model, revealed in [66], was created to describe flame propagation theory. Later, this model was used to simulate electrical pulses in a nerve axon.

The solutions of Fisher and Nagumo models will be discussed later in more detail as we will consider them in the thesis.

Newell-Whitehead-Segel model:

$$u_t = u_{xx} + au - bu^3, \quad a, b \in \mathbb{R},$$

[45]. This model studies the thermal convection of shallow fluid in two plates heated from below.

Under rescaling, the Fisher model and when $a = b = 1$ in the Newell-Whitehead model, we see that both are special case of the Kolmogorov-Petrovskii-Piskunov (KPP) model [31]. KPP model is written as

$$u_t = u_{xx} + F(u),$$

where $F(u)$ is a continuous function and satisfies the following conditions:

$$F(0) = F(1) = 0; \quad F(u) > 0 \text{ for } 0 < u < 1;$$

$$F'(0) = 1; \quad \text{and} \quad F'(u) < 1, 0 < u \leq 1.$$

The above models appeared with one component system, i.e. $u \in \mathbb{R}$.

For more than one component system, $u \in \mathbb{R}^n$, $(n \geq 2)$, there is an additional classification for the system (1.1). If the matrix of diffusion coefficients is diagonal, then we call

the system (1.1) a reaction *self*-diffusion system; otherwise, we call it a reaction *cross*-diffusion system. Indeed, all the systems of reaction diffusion with one component are examples of reaction self-diffusion system. In the next sections, we will explain more about both cases.

1.1.1 Reaction Self-Diffusion Systems

Reaction self-diffusion systems have received huge attention. The diffusion in these systems represents random motion only. The mechanism of the diffusion here is that the species moves from a high concentration area to a low concentration area.

In 1952, Turing [58] introduced reaction diffusion system with two components when he studied a chemical reaction between two morphogens. We could say that Turing's model is a seminal system of a reaction diffusion system with more than one component. In that year, there was also an equally important research by Hodgkin and Huxley [25], who used the reaction self-diffusion system to model the propagation of electrical impulse nerves along the axon. Hodgkin and Huxley's model was simplified to the activator-inhibitor model as presented by FitzHugh [22], that is so-called FitzHugh-Nagumo model (FHN). The FHN model has the following form :

$$\begin{aligned} u_t &= f(u,v) + D_u u_{xx}\,, \\ v_t &= \epsilon g(u,v) + D_v v_{xx}\,, \end{aligned} \tag{1.2}$$

where $f(u,v)$ is a cubic function while $g(u,v)$ is a linear function. If the curve $f(u,v)=0$ is S-shaped in the $(u,v)-$plane, and $g(u,v)$ is negative on its left branch and positive on its right branch then the system (1.2) is called an activator-inhibitor system or propagator and controller system as Fife [20] called this system.

The mechanisms in such systems (1.2) are described in several papers. For example, Murray [37] has introduced an enjoyable unrealistic description about fired grass and the reaction of grasshoppers. The example, that Murray has given, helping us to understand the reason for calling u as an activator and v as an inhibitor.

1.1.2 Reaction cross-diffusion System

The random motion presented in reaction self-diffusion systems does not reflect the motion in all problems in the real world. For example, taxis motion is not random. *Taxis* movement designates the biased movement of organisms away from or towards a stimulant. This stimulant can be chemical as described in chemotaxis or biological as in predator-prey (pursuit-evasion waves). An explanation of how chemotaxis works can be found in [23], [29] and [43].

The early model of the reaction cross-diffusion system has originated by Keller and Segel in 1969 [29]. The model describes the motion of the cells when they are affected by molecules stimulated by chemical reaction. The model of Keller and Segel is simplified to a system with two equations. One equation presents the density of the cells and its variation over time. The second equation relates to the chemical stimulant and its variation over time. Therefore, this system is represented as follows

$$u_t = \nabla(D_u \nabla u - \chi u \nabla v) + f(u),$$
$$v_t = D_v \Delta v + g(v),$$

where u designates for the density of the cells and v is the concentration of the chemical attractant and χ represents the chemotatic coefficient.

Another example that shows the demand of a reaction cross-diffusion system is the interaction between predators and prey. The mechanism in a prey-predator system could be considered as directed movement not random movements as follows. In this case, the prey is an external stimulus for the predator and vice versa. The prey is moving away from a high-concentration area of predator to a low-concentration area, that is presented by negative taxis. On the other hand, the predator will move from a low-concentration area of prey to a high-concentration area, that is presented by positive taxis. In general, the gradient of one component affects the flux direction of the other component. This mechanism will not be described adequately by considering only a reaction self-diffusion system.

The early work that applied cross-reaction diffusion system on population dynamics

was done by Shigesada et al. 1979 [49]. This model described Morisita's experiment, that studied ant-lion's tendency to pit formation in the fine sand rather than coarse sand depends on the population density. Shigesada et al. provided mathematical model that describes the behaviour of ant-lion

$$u_t = \frac{\partial}{\partial x}\left[\frac{\partial}{\partial x}\{(\alpha_1 + \beta_{11}u + \beta_{12}v)u\} + \gamma_1 \frac{dU(x)}{dx}u\right],$$
$$v_t = \frac{\partial}{\partial x}\left[\frac{\partial}{\partial x}\{(\alpha_2 + \beta_{21}u + \beta_{22}v)v\} + \gamma_2 \frac{dU(x)}{dx}v\right],$$

where u and v designates the ant-lions that settled in fine sand and coarse sand, respectively. Parameters $\alpha_{1,2}$ are the dispersion coefficients and $\beta_{1,2}$ are the coefficients of population pressure while the function $U(x)$ represents value of habitat at position x. We could see that Morisita's model is expressed in cross-diffusion form.

Moreover, in seismology, Burridge-Knopoff [12] model describes the contact region between two plates, which could be used to understand the interaction between two faces of a fault in the earthquake case. From this model, Cartwright et al [15] obtained the continuum version of the Burridge-Knopoff model

$$\frac{\partial^2 \chi}{\partial t^2} = c^2 \frac{\partial^2 \chi}{\partial x^2} - (\chi - vt) - \frac{\gamma}{3}(\frac{\partial \chi}{\partial t})^3 + \gamma \frac{\partial \chi}{\partial t}, \tag{1.3}$$

where $\chi(x,t)$ represents local longitudinal deformation of the surface of the upper plate, c is the longitudinal speed, v is the pulling velocity and γ measures magnitude of the system.

It is found that in [14], by introducing $\psi = \frac{\partial \chi}{\partial t}$, the system (1.3) presents in a similar manner as the cross-diffusion system,

$$\frac{\partial \psi}{\partial t} = \gamma[\eta - \frac{1}{3}\psi^3 + \psi],$$
$$\frac{\partial \eta}{\partial t} = -\frac{1}{\gamma}(\psi - v - c^2 \frac{\partial^2 \psi}{\partial x^2}),$$

where ψ represents the time derivative of the local longitudinal deformation of the surface of the upper plate.

Recently, the dynamics of diffusion of genes in the early vertebrate embryo was presented in a similar style of reaction cross-diffusion system [4]. The dynamics of somitogenesis, in the case when the FGF8 (Fibroblast growth factor 8) gene is produced only

in the tail region of the embryo, was described by the following system

$$\begin{aligned}
\frac{\partial u}{\partial t} &= \frac{\left(u+\mu v\right)^2}{\gamma+u^2}\chi_u - u,\\
\frac{\partial v}{\partial t} &= \kappa\left(\frac{\chi_v}{\epsilon+u} - v\right) + D_v\frac{\partial^2 v}{\partial x^2},\\
\frac{\partial w}{\partial t} &= \chi_w - \mu w + D_v\frac{\partial^2 v}{\partial x^2},
\end{aligned} \tag{1.4}$$

where u is a somitic factor, v is a signalling molecule and w is FGF8. The parameters $\mu,\gamma,\kappa,\epsilon,\mu,D_v$ and D_w are positive and χ_u,χ_v and χ_w are functions that control the production of u,v and w, respectively. The formulae of these functions and more details could be found in [4]. We see in the system (1.4) that the diffusion term in the second equation is self-diffusion, in the third equation it is cross-diffusion.

The experimental results, that focus on how the feather patterns are aligned from stripes to spots, are simulated by reaction cross-diffusion model [34].

$$\begin{aligned}
n_t &= D_n n_{xx} - \chi\nabla\cdot(n\nabla c),\\
c_t &= D_c c_{xx} + \frac{sn}{\beta+n} - \gamma c,
\end{aligned} \tag{1.5}$$

where n is a cell density and c is chemical (activator) concentration. The parameters D_n,D_c,χ,s,β and γ are positive. In the system (1.5), the diffusion term in the second equation is self-diffusion while in the first equation there is nonlinear cross-diffusion.

From this collection of examples, we see the demand to understand the reaction cross-diffusion system. In fact, the reaction cross-diffusion system has not received as much attention as the reaction self-diffusion system. This alone is enough to motivate us to explore some properties in such systems.

1.2 Propagating Waves

As seen previously, most (if not all) reaction terms that appear in reaction diffusion systems are not linear. Thus, not all techniques of solving linear systems are applicable here.

The components in a reaction diffusion system spatially disperse, so this dispersion could be presented in a travelling wave manner. The travelling wave solution is one of the methods used to solve nonlinear PDEs. A collection of methods to solve nonlinear PDEs with brief explanations are listed in [35]. In this thesis, we used a lot the propagating (travelling) wave solution technique.

The travelling wave solution for PDEs is a solution with specific properties. These properties are that the travelling wave is advancing with fixed speed and preserving its profile, somewhat similar to the properties of a travelling wave observed by John Russell in 1836.

The beginning work on travelling wave was in the 1930s by Fisher and Kolomogrov, Petrovskii and Piskunov. This travelling wave with these mentioned properties is a phenomenon that is observed in many fields of science. It is found in chemical reactions [60],[27]. Also, it is found in fluid mechanics [16]. Travelling waves appear also in combustion theory, as it is used to study the propagation of flame from a burnt area towards an unburnt area [65].

Biology is a rich field for the travelling wave phenomenon. Most things that happen in a single species such as growth, distribution or competition can be presented as a travelling wave. This is also true for the interaction between two or more species of populations, such as a predator-prey model, mutualism or epidemiology, which reveals how a disease diffuses in a single population, [37], [38], [60] [19].

The first step to solving reaction diffusion systems with travelling wave technique is, applying the wave variable such as $\xi = x \pm ct$. Indeed, this form of wave variable is applicable for a reaction diffusion system in one dimension. Substituting a wave variable in a reaction diffusion system yields an ordinary differential equation (ODE) as we will see later.

The common form for reaction diffusion system for one component is

$$\frac{\partial u}{\partial t} = \frac{\partial}{\partial x}\left(D\frac{\partial}{\partial x}u\right) + f(u) \tag{1.6}$$

The travelling wave solution for a reaction diffusion system in one dimension has the

form

$$U(\xi) = u(x,t), \qquad \xi = x \pm ct\,,$$

where c is the speed of the propagating wave that advances in the right direction for $\xi = x - ct$ or to the left for $\xi = x + ct$. By applying the wave variable on the reaction diffusion system (1.6), we have the following ODE

$$c\frac{dU}{d\xi} + \frac{d}{d\xi}\left(D\frac{d}{d\xi}U\right) + f(U) = 0\,. \tag{1.7}$$

The only condition that is demanded for a travelling wave to have meaning is that the wave solution has to be bounded. The travelling wave solution $U(\xi)$ in one dimension satisfies the following boundary condition

$$U(-\infty) = v_1 \text{ and } U(+\infty) = v_2 \qquad \text{where} \quad v_{1,2} \in \mathbb{R}, \tag{1.8}$$

for *front wave* when $v_1 > v_2$, for *back wave* when $v_1 < v_2$ and for *pulse wave* when $v_1 = v_2$. Satisfying (1.8), yields the boundedness of the wave solution.

For *periodic travelling wave*, the travelling wave solution $U(\xi)$ satisfies the following

$$U(\xi) = U(\xi + L), \qquad L > 0, \tag{1.9}$$

that requires boundedness condition to have meaning, i.e.

$$\left|U(\xi)\right| < \omega, \qquad \omega \in \mathbb{R}.$$

The plot of these different profiles is shown in figure 1.1.

1.3 Models with Analytical Solutions

There are a few models of nonlinear reaction diffusion systems that have known exact analytical propagating wave solutions. However, there are a few analytical solutions known for reaction diffusion systems with two or more components. Rodrigo and Mimura [41] presented three models with analytical solutions. For two components

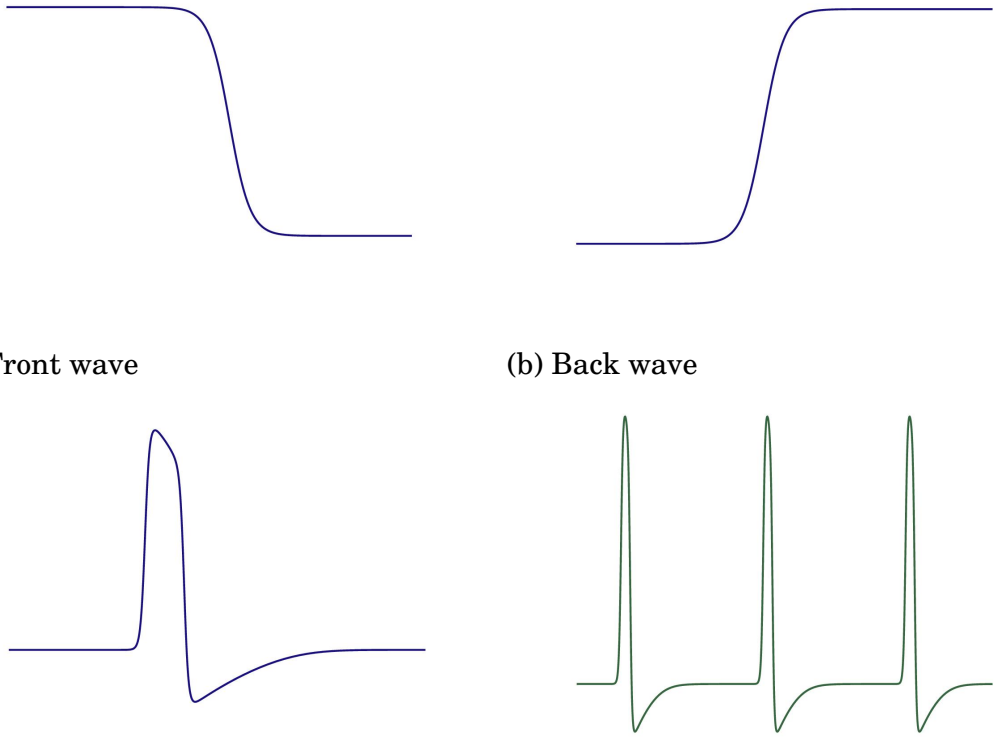

(a) Front wave (b) Back wave

(c) Pulse wave (d) Periodic travelling wave

Figure 1.1: Different profiles of propagating waves.

cases, we consider the FHN model (cubic nonlinearity) which has no analytical solution known yet.

In this section, we will present some details about propagating wave solutions of Fisher-KPP model and and Zeldovich and Frank-Kamenetzki [66] or Nagumo [36] models (ZFK-Nagumo) with one component in one space dimension as we will recall them later in this thesis.

1.3.1 Fisher-KPP model

Fisher described the spread of advantageous genes in a population living in one dimensional by the following model

$$u_t = \rho u(1-u) + D u_{xx} \qquad \rho > 0 \quad , \quad D > 0\,. \tag{1.10}$$

This model has two equilibria with respect to time evolution: $u = 0$ that is unstable and $u = 1$ which is stable [38].

The stationary travelling wave solution for (1.10) is given by introducing the wave variable $\xi = x - ct$, that yields

$$U(\xi) = u(x,t), \qquad \text{where } \xi = x - ct\,.$$

Substituting the wave variable into Fisher model (1.10) yields

$$cU_\xi + DU_{\xi\xi} + \rho U(1-U) = 0\,. \tag{1.11}$$

Thus, from equation (1.8), the solution of (1.11), $U(\xi)$ satisfies the following

$$\lim_{\xi\to\infty} U(\xi) = 0 \qquad , \qquad \lim_{\xi\to-\infty} U(\xi) = 1\,.$$

As we have two distinct equilibria, it is clear that the solution here is forming a wave front. Note that the notion of stability of these equilibria in (1.11) is not same as notion of stability of the equilibria in equation (1.10).

Despite the simple appearance of equation (1.11), the formula of an exact propagating wave solution of (1.11) is not yet known. However, analytical proof shows that there are stable monotonic travelling wave solutions of Fisher-KPP for $c \geq 2\sqrt{\rho D}$ [38]. In fact, there is a travelling wave for $c < 2\sqrt{\rho D}$ but it is unstable and not monotonic. Moreover, for $c < 2\sqrt{\rho D}$, some values of u are negative which is infeasible from the application point of view as the u component represents the density of population.

Here is an indication of some attempts to solve the Fisher model analytically. In 1979, Ablowitz and Zeppetella [2] found the exact propagating wave solution of the Fisher model (1.10) where $\rho = D = 1$ and for special wave speed $c = \pm 5/\sqrt{6} \approx 2.0412$. The formula of that solution is

$$u(x,t) = U(\xi) = \frac{1}{(1 + r\exp(\xi/\sqrt{6})^2}, \qquad r > 0\,, \tag{1.12}$$

which is presented graphically in figure 1.2

The analytical solution is computed for a generalised Fisher equation where the generalised Fisher equation is

$$u'' + cu' + u - u^n = 0, \qquad n \in (1,\infty)\,,$$

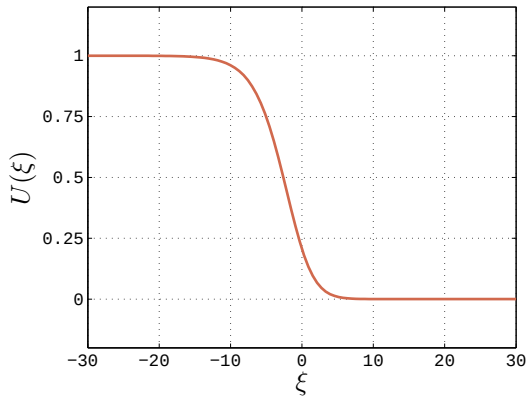

Figure 1.2: The plot of Fisher-KPP front wave obtained by the formula (1.12) where $r = 1.2$

where there is a relation between the minimal speed c and the exponent n as given by the following formula

$$c = \frac{n+3}{(2n+2)^{\frac{1}{2}}}.$$

As $n > 1$ then $c \in (2, \infty)$. The Fisher model is a special case that is obtained for $n = 2$. This solution was found in 1984 by Kaliappan [26], whereby

$$u(x,t) = U(\xi) = \frac{1}{\left[1 - Ae^{m\xi}\right]^{2/(n-1)}},$$

where c formula is given previously while

$$m = \frac{n-1}{(2n+2)^{\frac{1}{2}}}.$$

Similar work and similar results were found in 1982 by Abdelkader [1]. So, in general, the analytical solution for the Fisher model is known for special wave speed but not for continuous wave speeds.

The properties of the propagating wave in Fisher-KPP is summarised as follows: there is a stable monotonic wave front for a continuous spectrum of speed $c \geq 2$. Also, the travelling wave solution $U(\xi)$ for Fisher-KPP model shows a transition between an unstable rest state to a stable rest state.

1.3.2 ZFK-Nagumo

ZFK-Nagumo's model is used to describe flame propagation. In one component in one dimension, this model has the following form:

$$u_t = u_{xx} + u(u-\alpha)(1-u) \quad , \qquad \alpha \in (0,1). \tag{1.13}$$

This equation is known as the ZFK-Nagumo model and describes also the propagation of an electrical signal in a nerve axon.

By applying the wave variable $\xi = x - ct$ on (1.13) we obtain the following:

$$cU_\xi + U_{\xi\xi} + U(U-\alpha)(1-U) = 0\,. \tag{1.14}$$

The solution $U(\xi)$ represents a front travelling wave that is similar to the wave front in Fisher-KPP 1.2. The difference is that $U(\xi)$ for the ZFK-Nagumo model shows the transition between two stable resting states: so this system is a so-called bistable system. The exact analytical solution of (1.14) could be found in literature, i.e. [36]. The analytical solution in this case is known for the only value of c for which it exists, unlike Fisher-KPP for which solutions exist for a continuous spectrum of c but analytical solutions are known only for selected.

The method that has been applied to solve (1.14)is a reduction of order. In the Appendix, Section 6.1, we showed in detail how the solution of the ZFK-Nagumo model is analytically computed.

The formula of the analytical solution is

$$U(\xi) = \frac{1}{1 + C\,\exp\,(\xi/\sqrt{2})}\,, \tag{1.15}$$

where the speed is given by the following function;
$c(\alpha) = \sqrt{2}(\frac{1}{2} - \alpha)$, where positive $c > 0$, implies the requirement that the parameter $\alpha \in (0, 1/2)$. This formula (1.15) represents the front that connects the steady states $U = 0$ and $U = 1$.

There is another solution for this problem. For example, Kawahara and Tanaka [28] show three formulae of analytical solutions for (1.14). Each formula represents one of

the three possibilities of the connection of the resting states in the travelling front of ZFK. These possibilities are that, the connection between $[u = 0$ with $u = \alpha]$, $[u = 0$ with $u = 1]$ and $[u = \alpha$ with $u = 1]$.

The properties of the propagating wave solutions of ZFK-Nagumo model is summarised as follows. It shows a transition between two stable resting states. Also, the spectrum of speed is discrete as it is depends on a parameter α.

1.4 Comparison between reaction self-diffusion with reaction cross-diffusion

The reaction diffusion system with two or more components gives rise to more features than can be presented in one component system. For example, limit cycle or period orbit is impossible to represent in a one-component system. Moreover, all one-component systems show a reaction self-diffusion system whereas two- or more component systems could appear as a reaction system with self-diffusion or/and cross-diffusion. The diffusion matrix D in (1.1) has significant effects on the propagating wave's behaviour.

Here we identify the most notable differences between propagating waves in reaction self-diffusion systems (diagonal diffusion matrix D) and those in a reaction cross-diffusion system (not diagonal diffusion matrix D).

The propagating waves of reaction cross-diffusion system waves are capable of penetrating each other. As a result of that they reflect from a no-flux boundary. This attribute is observed in reaction cross-diffusion systems with the Truscott and Brindely model as a reaction kinetic terms [56]. Also, it is observed in reaction cross-diffusion systems with the FHN kinetics [9]. When two evasion waves collide, they merge into one wave with the highest amplitude. This wave lasts for a short moment before splitting into two waves with small amplitude that propagate in different direction, see figure 1.3.

Those splitting propagating waves take some time to recover their features before the collision. These features reflect the nature of waves in reality, as observed in the interaction of bacterial populations [57].

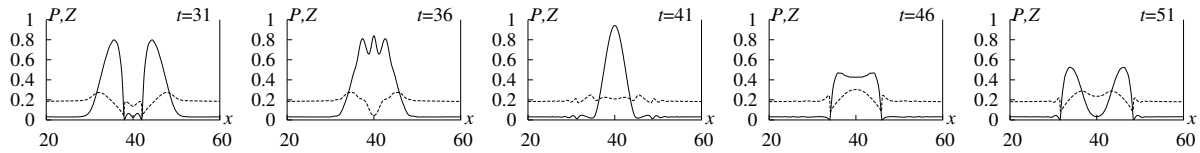

Figure 1.3: The waves of reaction cross-diffusion system penetrate each other on collision. This figure is taken from [56] with permission. P and Z are two components in Truscott and Brindley model.

However, the survival of propagating waves after a collision in one dimension is conditioned by the equality of the width of the waves. In the case when the propagating waves are different, then there is the possibility to have half-soliton behaviour, that is after the collision one of the wave will annihilate and the other one will keep propagating [54].

On the contrary, the reaction self-diffusion system waves are destroyed on collision, so they are not capable of reflecting from an impermeable boundary.

Another difference is that, the waves of reaction diffusion system with FHN model as kinetic term has a monotonic front in self-diffusion while it has an oscillatory front in cross-diffusion. Moreover, from this oscillation, this system could represent a quasi soliton envelope [8].

Last but not least, a difference between reaction cross-diffusion waves and those from self-diffusion waves is that there is a periodic propagating wave appearing spontaneously for the reaction cross-diffusion system [7]. This attribute has appeared in the spatially extended version of Truscott-Brindley model and the Rosenzweig-MacArthur model as well. The spontaneous periodic travelling wave happens only when there is a non-zero element at a non-diagonal position in the matrix of diffusion D in (1.1).

1.5 Numerical Methods

The numerical solution is very important when solving mathematical problems. The need for a numerical solution increases when there are nonlinear problems and the analytical solutions are not known. The numerical solution helps us to approximate with high accuracy the solutions of those problems.

Another reason is that the analytical solution addresses for a specific problem formula. So, we need to find the analytical solution every time we do a small change in the formula of the problem. This process takes a long time and might end with obstacles that prevent getting the analytical solution. However, the numerical solution can be applicable for various problems. Moreover, applying a numerical solution for a known analytical solution is a good way to validate a numerical method.

However, the numerical solution requires discretisation so some of the accuracy is lost.

There are three well-known methods that are used for nonlinear PDEs, listed in [53], that are Finite Difference Methods (1950s), Finite Element Methods (1960s) and Spectral Methods (1970s). We give a brief definition of the finite difference methods as they are used in the thesis.

Also, we need a numerical continuation when we study the bifurcation of the system. We admit that this analysis will consume a great deal of time if one would do it by hand; thus, we use software to do this step for us.

Last but not least, our need for numerical interpolation appeared when we obtained a solution vector organised into irregular gridded points. In fact, the software, that we used for numerical continuation, produced a solution array that is irregularly gridded. There is a demand to make the discretisation regular gridded. To solve this problem, we apply a cubic spline interpolation method.

1.5.1 Finite Difference Method

The finite difference method is a well-known method to solve PDEs. The basic idea of this method is to approximate the partial derivatives in PDEs as expressed by finite difference approximation [51] [52].

As common in all the numerical methods, applying a finite difference method changes the problem from continuous intervals to discontinuous intervals. Moreover, applying this method to an infinite domain and infinite time is practically impossible. So, for the finite domains, i.e. $0 \leq t \leq T$ and $0 \leq x \leq L$, $L \in \mathbb{R}^+$, we introduce two integers j and k

and define space step discretisation Δx and time step discretisation as

$$\Delta x = \frac{L}{j} \quad , \quad \Delta t = \frac{T}{k}$$

As a result, we have mesh grid points (x_m, t_n) where $x_m = m\Delta x$ and $t_n = n\Delta t$ for $m = \{0, 1, \cdots, j\}$ and $n = \{0, 1, \cdots, k\}$.

The partial derivative is defined on this mesh grid by a finite difference method. For this thesis regarding a reaction diffusion system, we apply the central difference method for spatial derivative and forward or backward Euler method for time. That is expressed as follows, the second spatial derivative of term $u(x_m, t_n)$ approximates to

$$\frac{\partial^2 u(x_m, t_n)}{\partial x^2} = \frac{u^n_{m-1} - 2u^n_m + u^n_{m+1}}{\Delta x^2}$$

where $\left(u^n_m\right)$ denotes $u(x_m, t_n)$.
For the first time derivative we used forward Euler, that is

$$\frac{\partial u^n_m}{\partial t} = \frac{u^{n+1}_m - u^n_m}{\Delta t}$$

where the backward Euler which is expressed as

$$\frac{\partial u^n_m}{\partial t} = \frac{u^n_m - u^{n-1}_m}{\Delta t}$$

As a finite difference method provides an approximation solution, there are errors. Those errors are summarised in two errors: truncation error and round-off error. The truncation error is the difference between the exact solution and an approximated solution at (m, n)th mesh point [50]. Round-off errors only happen when there is more than one arithmetic operation [40]. Indeed, for a small number of operations, round-off errors do not have an obvious effect on the result. The effect of the round-off error could be found in [13].

In fact, we have not discussed this in the thesis, but we should be aware of the existence of such errors that may affect our numerical simulation.

1.5.2 Spline interpolation

In our case, the need for interpolation appears when we want turn irregular grid points on a finite domain to regular grid points. To achieve that, we should insert regular grid points between those points in the domain. Therefore, we need to apply interpolation.

By interpolation, one could find a smooth curve that passes through points on a finite domain. In our problem, those finite number of points are irregular grid points. So, by interpolation, we will connect those points by curve that composed of regular grid points.

There is more than one way to identify a curve. However, we apply cubic spline interpolation. Because we need to apply the interpolation on the propagating wave with oscillation as we will see later. The best curve to fit the oscillation should not be linear, so cubic is better. The details of this method are outside the field of this study. Some interpolation functions are already defined in MATLAB [62] from which we have benefited in our work.

1.5.3 Parameter Continuation (Bifurcation Analysis)

One of the objects when studying the dynamics of a system is to investigate the local behaviour around the equilibrium that corresponds to the resting states of propagating wave in reaction diffusion systems. Often, the qualitative behaviour of the system depends heavily on the parameters.

In terms of solving a reaction diffusion system by travelling waves, we have seen that there is a system of ODEs which result from applying a wave variable on a reaction diffusion system. This resulting ODE system contains at least one parameter c. In fact, usually, the reaction terms contain parameters. Also there are diffusion coefficients which are parameters as well. Thus usually we have an ODE system with several parameters. Varying the values of parameters would change the behaviour of the system and provides interesting results. Indeed, it is valuable to study how each parameter influences the solution separately.

In bifurcation analysis, we study the behaviour of the equilibria of a system as a function of parameter. The plot that provides information of different behaviours of the system corresponding to different values of parameters, is called bifurcation diagram. The well-known tool for implementing this computation falls under the numerical continuation field.

The main reason to do a numerical continuation on a reaction diffusion system is to gain insight into the understanding of a system such as the stability of the solution of the system as well as the bifurcation analysis. Furthermore, the results that are obtained by numerical continuation could be compared to what we know in dynamical systems.

However, it is exhausting to do numerical continuation by hand. There are several continuation softwares designed for this purpose, such as AUTO, XPPAUT, CONTENT, MATCONT etc. Such software is built on various numerical methods. The explanation of these methods is outside of the scope of the study but it can be found in chapter 10 in [33].

1.6 Periodic Travelling Waves

The existence of oscillator model in reaction diffusion system leads to the presence of periodic travelling wave [32]. According to Kopell and Howard if there is a Hopf point in the kinetic term in a reaction diffusion system, then there is a guarantee of existence of periodic travelling wave solution (PTW).

PTW has applications in different fields of science. Some of the problems in science present periodic waves. For example, in biology, PTW presents in the competition model between water and vegetation [47]. In chemistry, PTW presents in the CHD-BZ reaction [10]. In ecology, the interaction between predator and prey populations could be analysed by PTW [48]. Most of the works on PTW consider reaction self diffusion system.

The existence of PTWs depends on the parameters in the system. Most of PTW is

difficult to compute analytically. The following system

$$u_t = \lambda(r)u - \omega(r)v + u_{xx}$$

$$v_t = \lambda(r)v + \omega(r)u + v_{xx}$$

where $r = \sqrt{\omega^2 + \lambda^2}$, is called Lambda-Omega system is used commonly as a prototype of studying PTW as it is one of the few systems that has analytical PTW [32] . One of the methods to compute the PTW for reaction diffusion system is to introduce travelling wave variable. After applying travelling wave variable, the system of PDE turns into a system of ODEs. PTW in PDE corresponds with limit cycle in ODE. So, the first step in this case is to compute the Hopf bifurcation point, that giving birth of limit cycle which presents a family of periodic solution. The aforementioned is about finding the PTW but the stability of PTW is another topic.

1.7 Stability of Stationary Solutions

As mentioned above reaction diffusion systems are difficult to solve analytically. So, the travelling wave solution is one technique to facilitate this problem. In this case, the travelling wave solution is of interest of us.

Suppose we know the travelling wave solution. The following problematic question appears. If we substitute this travelling wave solution into the reaction diffusion system the question arises: will it travel in a fixed shape and constant speed or this is not the case. In other words, if we perturb the stationary solution, will it go far away or stay close to the stationary solution? Thus we should study the stability of the travelling wave solution.

To represent this problem in mathematical notations, we are looking for travelling wave solution

$$U(\xi, \tau) = u(x - ct, t)\ , \tau = t\ , \xi = x - ct \tag{1.16}$$

that satisfies

$$u_t = Du_{xx} + f(u), \qquad u \in \mathbb{R}^n\ . \tag{1.17}$$

Applying $U(\xi,\tau)$ in 1.17 yields

$$U_\tau = DU_{\xi\xi} + cU_\xi + F(U). \tag{1.18}$$

At $\tau = 0$, we obtain the stationary solution, $\underline{U}(\xi) = U(\xi,0)$, that is

$$0 = D\underline{U}_{\xi\xi} + c\underline{U}_\xi + F(\underline{U}). \tag{1.19}$$

As we are studying the stability of the stationary solution, we will perturb the solution (1.19) and explore what will happen then. So, for the perturbation, we introduce

$$\hat{u}(\xi,\tau) = \underline{U}(\xi) + \tilde{v}(\xi,\tau), \tag{1.20}$$

and $\tilde{v}(\xi,\tau)$ is considered to be a small function.
Therefore, to study the stability of the travelling wave solution of reaction diffusion equation (1.17), we need to study the behaviour of the perturbation term $\tilde{v}(\xi,\tau)$. If for every $\tau \geq 0$

$$\|\tilde{v}(\xi,\tau)\| < \epsilon, \tag{1.21}$$

where $\epsilon > 0$, then the reaction diffusion system (1.17) has a stable travelling wave solution. To be precise, this condition coincides with the definition of Lyapunov stability [39].

Obviously, we call the propagating wave stable too if it satisfies the asymptotic stable condition, that is

$$\|\tilde{v}(\xi,t)\| \to 0 \qquad \text{as } t \to \infty. \tag{1.22}$$

Also, it is stable if it satisfies the exponential stability condition, that is

$$\|\tilde{v}(\xi,\tau)\| \leq \alpha \|\tilde{v}(\xi,\tau)\| \mathrm{e}^{-\beta t}, \tag{1.23}$$

where α and β are positive.

The first step towards this investigation is to linearise the system (1.18) about the solution of interest, that is a stationary solution $U(\xi)$, thus, we substitute (1.20) in (1.18) which gives

$$\tilde{v}(\xi,\tau)_\tau = D\underline{U}_{\xi\xi} + D\tilde{v}_{\xi\xi} + c\underline{U}_\xi + c\tilde{v}_\xi + f(\underline{U} + \tilde{v}). \tag{1.24}$$

By linearising nonlinear term $f(\underline{U}+\tilde{v})$ about the stationary solution

$$f(\underline{U}+\tilde{v}) = f(\underline{U}) + \left.\frac{\partial f}{\partial U}\right|_{U=\underline{U}} \tilde{v}\,. \tag{1.25}$$

Substituting (1.25) in (1.24) yields the following equation

$$\tilde{v}_\tau = \mathscr{L}\tilde{v}\,, \tag{1.26}$$

where

$$\mathscr{L} = D\frac{\partial^2}{\partial\xi^2} + c\frac{\partial}{\partial\xi} + \left.\frac{\partial f}{\partial U}\right|_{U=\underline{U}}. \tag{1.27}$$

The spectrum of the linear operator $\mathscr{L}$ gives us an indication about the stability of the travelling wave solution with the nonlinear terms. The spectrum in our case can be computed from the following equation

$$\lambda\tilde{v} = \mathscr{L}\tilde{v} = \left(D\frac{\partial^2}{\partial\xi^2} + c\frac{\partial}{\partial\xi} + \left.\frac{\partial f}{\partial U}\right|_{U=\underline{U}}\right)\tilde{v}\,. \tag{1.28}$$

This is an eigenvalue problem which could be cast to the following system

$$\begin{bmatrix}\tilde{v}_\xi\\ \tilde{z}_\xi\end{bmatrix} = \begin{bmatrix}\tilde{z}\\ D^{-1}(\lambda\tilde{v} - c\tilde{z} - \left.\frac{\partial f}{\partial U}\right|_{U=\underline{U}}\tilde{v})\end{bmatrix} = \begin{bmatrix}0 & I\\ D^{-1}(\lambda - \left.\frac{\partial f}{\partial U}\right|_{U=\underline{U}}) & -cD^{-1}\end{bmatrix}\begin{bmatrix}\tilde{v}\\ \tilde{z}\end{bmatrix}. \tag{1.29}$$

In most of reaction cross-diffusion system, the minimum size of D is (2×2). This leads to that the smallest size of the matrix being in the right hand side of the system (1.29) at (4×4). This matrix depends on ξ, which shows one side of the difficulty of computing λ.

The above is a theoretical approach to investigate the stability of a travelling wave solution. As can be deduced from (1.29), the values of parameters of the system are playing a significant role in these computation. However, determining the locus of spectrum of the linear operator of PDE analytically is out of the scope of this thesis. Most of the explanation in this section is taken from [5] and [42] where more details can be found.

We should note that zero is always an element of the spectrum of the linear operator in a reaction diffusion system.

Generally, the elements of the spectrum of the linear operator in nonlinear PDEs are one of the three following cases [5];
1· If at least one of the elements of the spectrum is located on the right hand side of the complex plane, then the condition (1.21) will not be satisfied; thus, we have an unstable propagating wave.
2· If the elements of the spectrum are non-positive and there is a spectral gap between the negative elements and those which are located on the imaginary axis, then the stability can be determined.
3· If the elements of the spectrum are non-positive and can not be separated from the imaginary axis (no spectral gap) then there is no generic method known to determine the stability.

As zero is always an element of the spectrum of the linear operator of reaction diffusion system due to translational invariance [42], then there is no chance to obtain case 1. In fact, the elements of the spectrum of the linear operator in a reaction diffusion system as in (1.25) are likely to be reflected by case 2.

However, in our work, as we will see in chapters 3 and 4, we have not investigated the stability of the wave solution by studying the spectrum of the linear operator. Instead of that, we have used direct numerical simulation to investigate the stability of the travelling wave.

1.8 Dynamical Instability and Numerical Instability

The numerical simulation of system of PDEs can be subjected to instability. The instability in the numerical solution might occur due to the instability of the numerical scheme or due to dynamical instability.

As seen in the previous section, dynamical stability depends on the parameters. Also, it relates to the stability of the solution as time evolves. On the other hand, the numerical stability is independent on the parameters in the system. Moreover, it mentions to the stability of the numerical scheme [51].

Sometimes, it is difficult to distinguish between the type of the instability as the solution grow exponentially in both types of these instabilities. At the same time, computing the dynamical stability condition in nonlinear systems is not that easy. Moreover, the condition of having a stable numerical scheme for nonlinear PDEs is not possible to be found in some cases.

Here is an indication of one way which can be applied to distinguish the type of the instability. This method is observing the behaviours of the numerical solution for different discretisation steps. If the instability behaviour does not change, then this is an indication that the system is dynamically unstable. If the instability appearance is diminished or increased after changing the discretisation steps, then this is an indication that the instability is related to the numerical scheme.

This thesis consists of five chapters. After revising the area that this thesis is working on as shown in the introduction, we introduce in Chapter 2 a quartic polynomial for reaction cross-diffusion system that has an exact analytical solution. In this chapter we discuss the possibilities to make this system generalised for Fisher-KPP and ZFK-Nagumo models. In this system we have different four cases that depend on the values of the quartic polynomial. In Chapter 3 we provide the numerical simulation for all those four cases. Also, we have demonstrated whether the instability, that we have faced, is dynamical or numerical instability. In Chapter 4 we deal with the reaction cross-diffusion system that has no analytical solution yet known. We use numerical continuation software a lot in this chapter. We have found a new stable propagating pulse for this system. Also we have provided some features of this system as we vary the parameters. Discussion of the results and further works are shown in Chapter 5.

CHAPTER 2

REACTION CROSS-DIFFUSION MODEL WITH AN EXACT ANALYTICAL SOLUTION

2.1 Problem Formulation

An analytical solution for propagating wave in the reaction diffusion system with FHN cubic nonlinearity has not yet been found, in systems with cross-diffusion.

Tyson and Keener [59] have considered a generic N-shaped function rather than a cubic FHN to analyse features of reaction in a self-diffusion system. In a similar manner, Biktashev and Tsyganov [9] have considered a piece-wise linear polynomial function as a kinetic term in a reaction cross-diffusion system to make the problem analytically solvable. In this chapter we intend to do similar to what have been done in the previous works. We aspire to find new exact analytical solution for reaction cross-diffusion system by replacing the cubic nonlinearity with continuous polynomial function.

First, we will explain briefly the analytical approach to the reaction cross-diffusion system in [9]; then, we will introduce a new exact analytical solution. The generalisation

of the reaction cross-diffusion system is

$$\begin{aligned} u_t &= f(u) - v + D_v v_{xx}\,, \\ v_t &= \epsilon(u - v) - D_u u_{xx}\,, \end{aligned} \tag{2.1}$$

where $f(u)$ in an N-shaped function, D_u and D_v are positive and ϵ is a small parameter.

The direct numerical simulation of (2.1) with a no-flux boundary condition shows existence of solution in the form of a propagating pulse wave. The width of the pulse

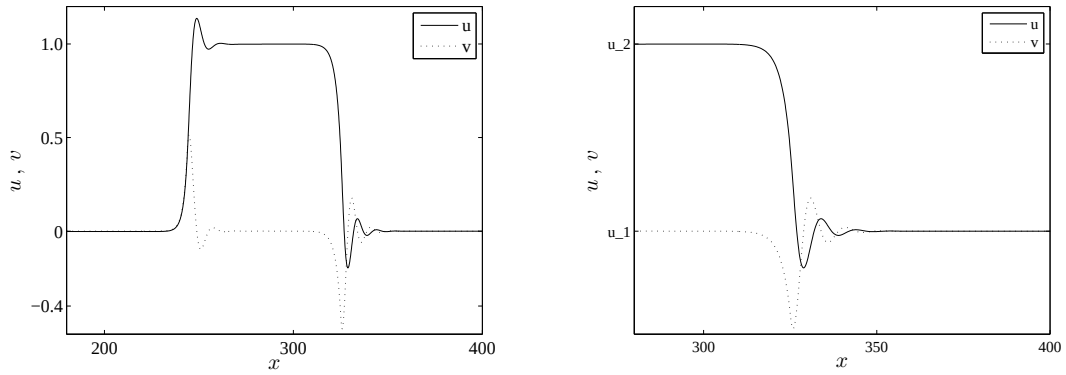

Figure 2.1: Left: Numerically, the reaction cross-diffusion system (2.1) exhibits a propagating pulse with $f(u) = u(u-0.3)(1-u)$ and the values of parameters are $\epsilon = 0.001, D_u = 5$ and $D_v = 0.5$. Right: At small distance and time, the front of the pulse of reaction cross-diffusion system with a cubic nonlinearity approach to two asymptotic states (u_1, v_1) and (u_2, v_2).

in the system (2.1) is inversely proportional to ϵ. This means that the wave front and the wave back of the pulse going apart from each other by letting $\epsilon \to 0$, as deduced from the numerical simulation in [9]. The front and back of this pulse at finite times and distances show the connection between two distinct points (u_1, v_1) and (u_2, v_2), see figure 2.1.

2.1.1 Wave Solution for Reaction cross-diffusion System

By considering $\epsilon \to 0$, the system (2.1) turns into

$$\begin{aligned} u_t &= f(u) - v + D_v v_{xx}\,, \\ v_t &= -D_u u_{xx}\,. \end{aligned} \tag{2.2}$$

Consequently, for $\epsilon \to 0$, there are equilibria, which satisfy

$$f(u_j) = v_j, \qquad j = \{1,2\}. \tag{2.3}$$

The equilibria (u_1, v_1) and (u_2, v_2) coincide with the asymptotic states of the wave front and the wave back.

We consider the propagating wave front solution of (2.3)

$$u(x,t) = \hat{u}(\xi), \qquad v(x,t) = \hat{v}(\xi), \tag{2.4}$$

where $\xi = x - ct$ and $c > 0$.

By substituting the wave solution (2.4) in (2.2) we obtain

$$D_v \frac{d^2\hat{v}}{d\xi^2} + c\frac{d\hat{u}}{d\xi} + f(\hat{u}) - \hat{v} = 0, \tag{2.5}$$

$$-D_u \frac{d^2\hat{u}}{d\xi^2} + c\frac{d\hat{v}}{d\xi} = 0. \tag{2.6}$$

As the front is an asymptotically approaching distinct steady states, we have

$$\hat{u}(\xi \to \pm\infty) = u_{1,2} \quad , \quad \hat{v}(\xi \to \pm\infty) = v_{1,2}, \tag{2.7}$$

$$\frac{d\hat{u}}{d\xi}(\xi \to \pm\infty) = \frac{d\hat{v}}{d\xi}(\xi \to \pm\infty) = 0. \tag{2.8}$$

Integrating (2.6) with respect to ξ yields

$$v_\star = \hat{v} - \frac{D_u}{c}\hat{u}'. \tag{2.9}$$

By using the limits as shown in (2.7) we obtain the following. When $(\xi \to \pm\infty)$, equation (2.9) satisfies $v_\star = v_{1,2}$ and then equation (2.5) turns into

$$f(u_{1,2}) - v_\star = 0 \Rightarrow f(u_{1,2}) = v_{1,2}. \tag{2.10}$$

As we see here u_1 and u_2 are two roots of function $f(u) - v_\star$.

Now, removing $\hat{v}$ from (2.5) as follows: from equation (2.6) we have

$$c\frac{d\hat{v}}{d\xi} = D_u \frac{d^2\hat{u}}{d\xi^2} \;\Rightarrow\; \hat{v}'' = \frac{D_u}{c}\hat{u}'''. \tag{2.11}$$

Substituting this value of $\hat{v}''$ in (2.5) yields

$$\frac{D_v D_u}{c}\hat{u}''' + c\hat{u}' + f(\hat{u}) - \hat{v} = 0\,.$$

Multiplying this equation by c and then using (2.9) gives:

$$D_v D_u \hat{u}''' + \left(c^2 - D_u\right)\hat{u}' + c(f(\hat{u}) - v_\star) = 0, \qquad \hat{u}(\pm\infty) = u_{1,2}\,. \tag{2.12}$$

This differential equation is deduced by applying the wave variable on the reaction cross-diffusion system (2.2). That is, we start with a reaction diffusion system with two equations and end up with one differential equation. This reduction in dimensionality is a significant feature of the reaction cross-diffusion system that is impossible to obtain if self-diffusion terms are there.

2.1.2 Piecewise Linear Function

Biktashev and Tsyganov [9] consider a piecewise linear function that is a caricature of cubic FHN. This piecewise linear function is given as

$$f(\hat{u}) = \gamma(-\hat{u} + \Theta(\hat{u} - a))\,, \tag{2.13}$$

where $\gamma > 0$, $a \in (0,1)$ and $\Theta()$ is a Heaviside step function. The plot of this function is shown in figure 2.2.

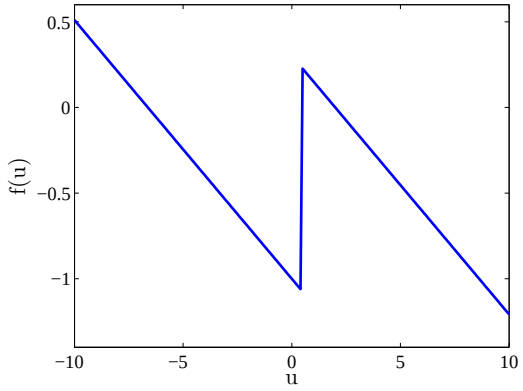

Figure 2.2: The shape of the piecewise linear function (2.13) that is considered in [9] as a caricature of cubic FHN.

The fronts that are obtained from the piecewise linear function is oscillatory fronts (see figure 2.3) that are similar to the fronts of the wave solution for a general N-shaped function. In the next section, instead of a piecewise linear function, we will consider a

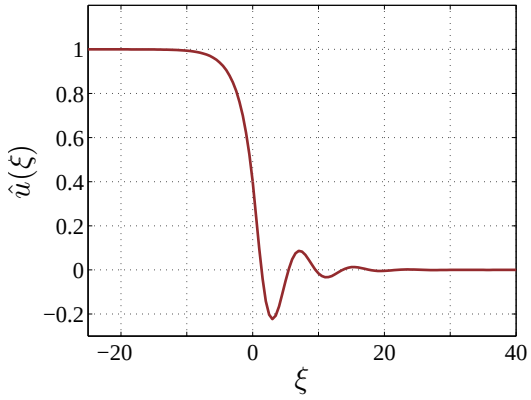

Figure 2.3: The profile of the front wave that is obtained by considering the piecewise linear function $f(u)$.

polynomial function for $f(\hat{u})$ in the differential equation (2.12).

2.2 Polynomial Function in Reaction cross-diffusion System

Previously, we showed in detail how the problem is formulated. At the end of that formulation, we obtained the following differential equation

$$D_v D_u \hat{u}''' + \left(c^2 - D_u\right)\hat{u}' + c(f(\hat{u}) - v_\star) = 0, \qquad \hat{u}(\pm\infty) = u_{1,2}\,, \tag{2.14}$$

where $\hat{u}(\xi)$ is the wave solution of the reaction cross-diffusion system (2.2).
Here, we aim to find, explicitly, a continuous polynomial function that can be chosen for $f(\hat{u})$ which makes the differential equation (2.14) analytically solvable.

Let us now find a suitable degree of this polynomial function $f(\hat{u})$ and find corresponding solution $\hat{u}(\xi)$.
Equation (2.14) can be written as:

$$A\hat{u}''' + B\hat{u}' = f(\hat{u}) - v_\star, \qquad \text{where} \quad A = -\frac{D_u D_v}{c} \quad and \quad B = \frac{D_u - c^2}{c} \tag{2.15}$$

We apply a reduction of order substitution:

$$\frac{d\hat{u}}{d\xi} = y(\hat{u}). \tag{2.16}$$

From (2.16), the differential equation (2.15) is written as follows

$$\begin{aligned} A\left(yy'^2 + y^2y''\right) + By &= f(\hat{u}) - v_\star \\ \Rightarrow y\left\{A(y'^2 + yy'') + B\right\} &= f(\hat{u}) - v_\star . \end{aligned} \tag{2.17}$$

We assume that function $f(\hat{u})$ is a polynomial function. We can ensure that, $y(\hat{u})$ is also a polynomial function.

To find the possible degree of those polynomials $y(\hat{u})$ and $f(\hat{u})$ that makes the problem analytically solvable, let $y \in P_n$ where P_n is a set of polynomials of degree n. Thus, $y' \in P_{n-1}$ and $y'' \in P_{n-2}$.
From (2.17), we have

$$f(\hat{u}) - v_\star = y\left\{A(y'^2 + yy'') + B\right\} \in P_{3n-2} \tag{2.18}$$

If $n = 1$ then $f(\hat{u}) - v_\star$ is linear, which is not of interest in current case.
If $n = 2$, then the polynomial function $f(\hat{u})$ is found to be quartic. This quartic polynomial is comparable to cubic FHN if it has at least three simple roots. Therefore, $n = 2$ is the smallest suitable choice. Consequently, $y \in P_2$, which is a quadratic function.

2.2.1 Solution in Hyperbolic Tangent Form

The reaction cross-diffusion system with quartic polynomial is an abstract problem, i.e. it has not yet been applied to a real world problem. Biktashev and Tsyganov [9] compared the front and back of the pulse, that obtained from a reaction cross-diffusion system with the FHN model, with the fronts that were obtained analytically from reaction cross-diffusion system with piece-wise linear reaction term. Here, we will attempt to write the solution in hyperbolic tangent form as a step toward comparing our analytical solution with other known solutions.

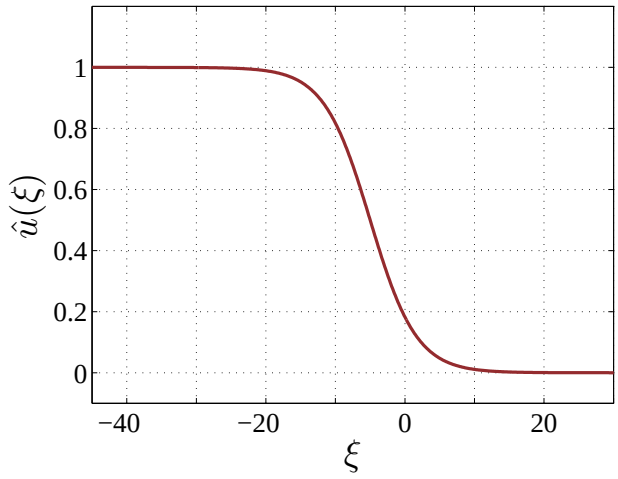

Figure 2.4: The plot of formula (2.20) shows that the solution $\hat{u}(\xi)$ is similar to the shape of hyperbolic tangent function. The values in this plot are $g = 1; h = 0; k = 0.3$ and $C = 5$.

Previously, we found that, in (2.17), the smallest suitable degree of the polynomial function $f(\hat{u})$ is four whereas $y(\hat{u})$ is a quadratic function. The formula of $y(\hat{u})$ is inspired by the exact solution of ZFK-Nagumo, which is shown in details in the Appendix, Section 6.1. The travelling wave differential equation for ZFK-Nagumo can be solved analytically by a reduction of order. By chance, the reduction of order in ZFK-Nagumo leads to variable $y(\hat{u})$ as quadratic also. The formula of quadratic function $y(\hat{u})$ is better to be presented as a factorised quadratic function, such as

$$y(\hat{u}) = k(\hat{u} - g)(\hat{u} - h), \tag{2.19}$$

where $\hat{u} = \hat{u}(\xi)$.

Then, from the relation that presented in (2.16), we integrate (2.19) to obtain the solution $\hat{u}(\xi)$. So, by integrating (2.19) with respect to ξ, we obtain

$$\hat{u}(\xi) = \frac{g + h\mathrm{e}^{\chi}}{1 + \mathrm{e}^{\chi}}, \qquad \chi = k(\xi + C)(g - h), \tag{2.20}$$

where C is an arbitrary constant. Indeed, formula (2.20) gives a similar plot to the hyperbolic tangent function that presents the front wave, (see figure 2.4).

Moreover, we see that the resting states ahead and behind the front wave coincide with the roots of quadratic function $y(\hat{u})$. This is the reason behind writing $y(\hat{u})$ in factorised form, which is to make the pre-front and the post-front states easily defined.

Once $\hat{u}(\xi)$ is known, from (2.9), we can compute the formula of $\hat{v}(\xi)$, which is

$$\hat{v}(\xi) = v_\star + \frac{D_u}{c}\hat{u}'. \tag{2.21}$$

Obviously, the profile of component $\hat{v}$ does not represent the wave front but a pulse. By applying condition (2.8) in (2.21), we obtain

$$\hat{v}(\xi \to \pm\infty) = v_\star + \frac{D_u}{c}\hat{u}'(\xi \to \pm\infty) = v_\star .$$

2.2.2 Correspondent Polynomial Function to the Solution

Previously, we assumed the solution of (2.17) where we had the front wave. In this section, we will attempt to find the corresponding polynomial function $f(\hat{u})$, as well as the expression of the parameters A, B and $v_\star$ that satisfy (2.17).
To achieve this, we substitute (2.19) in (2.17), which gives

$$k(\hat{u}-g)(\hat{u}-h)\{A\left(k^2(2\hat{u}-g-h)^2 + 2k^2(\hat{u}-g)(\hat{u}-h)\right) + B\} = f(\hat{u}) - v_\star . \tag{2.22}$$

Without loss of generality, the quartic polynomial $f(\hat{u})$ can be given in the following form:

$$f(\hat{u}) = \sigma(\hat{u}-u_0)(\hat{u}-u_1)(\hat{u}-u_2)(\hat{u}-u_3); \quad u_i \in \mathbb{R} \quad , i = 0,1,2,3 , \tag{2.23}$$

where $\sigma = +1$ or -1.
By substituting (2.23) in (2.22), we obtain

$$\begin{aligned} &k(\hat{u}-g)(\hat{u}-h)\{A\left(k^2(2\hat{u}-g-h)^2 + 2k^2(\hat{u}-g)(\hat{u}-h)\right) + B\} \\ &= \sigma(\hat{u}-u_0)(\hat{u}-u_1)(\hat{u}-u_2)(\hat{u}-u_3) - v_\star . \end{aligned} \tag{2.24}$$

Equating like terms in equation (2.24) cascades to the following system

Coefficient of $\hat{u}^4$:

$$\frac{6k^3D_uD_v}{c} = -\sigma\,.$$

Coefficient of $\hat{u}^3$:

$$\frac{12k^3D_uD_v(g+h)}{c} = -\sigma(u_0+u_1+u_2+u_3)\,.$$

Coefficient of $\hat{u}^2$:

$$\frac{k^3D_uD_v(7g^2+22gh+7h^2)}{c} + \frac{k(c^2-D_u)}{c} = -\sigma(u_0u_1+u_0u_2+u_0u_3+u_1u_2+u_1u_3+u_2u_3)\,.$$

Coefficient of $\hat{u}^1$:

$$\frac{k^3D_uD_v(g+h)(g^2+10gh+h^2)}{c} - \frac{k(g+h)(-c^2+D_u)}{c}$$
$$= -\sigma(u_0u_1u_2+u_0u_1u_3+u_0u_2u_3+u_1u_2u_3)\,.$$

Coefficient of $\hat{u}^0$:

$$\frac{k^3ghD_uD_v(g^2+4gh+h^2)}{c} + \frac{gkh(c^2-D_u)}{c} = -\sigma(u_0u_1u_2u_3-v_\star)\,. \tag{2.25}$$

This system is underdetermined as it is composed of 5 equations and 11 unknowns. Consequently, to solve the system, we need to assign 6 of the parameters as free, then 5 parameters will be dependent on those free parameters.

In our case, we restrict ourselves to the following, the free parameters have to be real numbers that also produce real dependent parameters. Moreover, to control easily the position of the resting states of solution (2.20), it is wise to assign variables g and h as free variables.

2.3 Stability of the Roots of f(u) in the Reaction Cross-diffusion System

Before describing the solution of (2.25), we discuss what sort of solutions we would like to have. We have seen that the exact solution has the form of front wave. This front wave has two distinct rest states. It is important to investigate the stability of those resting states as it affects the behaviour of the solution.

The pre-front state of the wave in Fisher-KPP equation is unstable, while the post-front state is stable. In ZFK-Nagumo, both resting states are stable but there is one unstable root between them. In this section, we compute the equation by which we can investigate the stability of the equilibrium in the reaction cross-diffusion system with a quartic polynomial.

By considering the quartic polynomial function (2.23) in the nonlinear system (2.2), we then have four equilibria points. We can study the stability of those equilibria by linearising the nonlinear PDE about the equilibria.
System (2.2) can be written in matrix form, as follows

$$\omega_t = F(\omega) + \underline{D}\omega_{xx}, \tag{2.26}$$

where

$$\omega = \begin{bmatrix} u \\ v \end{bmatrix}, \quad F(\omega) = \begin{bmatrix} f(u,v) \\ 0 \end{bmatrix}, \quad \text{and } \underline{D} = \begin{bmatrix} 0 & D_v \\ -D_u & 0 \end{bmatrix}.$$

Assume $\omega^* = [u^*, v^*]^T$ is an equilibrium point for the system (2.26) , i.e. $F(\omega^*) = 0$. We can find the stability of the equilibrium point after adding a perturbation term. Let

$$\omega = \tilde{\omega} + \omega^*, \tag{2.27}$$

for small $\tilde{\omega}$. Applying (2.27) in (2.26) yields

$$\tilde{\omega}_t + \omega_t^* = F(\tilde{\omega} + \omega^*) + \underline{D}\tilde{\omega}_{xx} + \underline{D}\omega_{xx}^*. \tag{2.28}$$

Linearising the nonlinear term $F(\tilde{\omega}+\omega^*)$ gives

$$\tilde{\omega}_t + \omega_t^* = F(\omega^*) + F'(\omega^*)\tilde{\omega} + \underline{D}\tilde{\omega}_{xx} + \underline{D}\omega_{xx}^* . \tag{2.29}$$

Note that, the term $\left(\omega_t^* = F(\omega^*) + \underline{D}\omega_{xx}^*\right)$ vanishes as it corresponds with the solution at the equilibrium point. Consequently, equation (2.29) becomes

$$\tilde{\omega}_t = F'(\omega^*)\tilde{\omega} + \underline{D}\tilde{\omega}_{xx} . \tag{2.30}$$

Equation (2.30) is linear homogeneous. Thus, by separation of variables, particular solutions for (2.30) can be written as

$$\tilde{\omega}(x,t) = Ce^{ikx}e^{\lambda t} \tag{2.31}$$

$$\Rightarrow \begin{bmatrix} \tilde{u} \\ \tilde{v} \end{bmatrix} = \begin{bmatrix} C_1 e^{ikx}e^{\lambda t} \\ C_2 e^{ikx}e^{\lambda t} \end{bmatrix} . \tag{2.32}$$

By substituting (2.32) in (2.30), we get the following system

$$\begin{aligned} \lambda C_1 e^{ikx}e^{\lambda t} &= f'(u^*,v^*)C_1 e^{ikx}e^{\lambda t} - k^2 D_v C_2 e^{ikx}e^{\lambda t} , \\ \lambda C_2 e^{ikx}e^{\lambda t} &= k^2 D_u C_1 e^{ikx}e^{\lambda t} , \end{aligned} \tag{2.33}$$

which can be rearranged to be

$$\lambda \begin{bmatrix} C_1 \\ C_2 \end{bmatrix} = \begin{bmatrix} f'(u^*,v^*) & -k^2 D_v \\ k^2 D_u & 0 \end{bmatrix} \begin{bmatrix} C_1 \\ C_2 \end{bmatrix} . \tag{2.34}$$

This is an eigenvalue equation. By characteristic polynomial, we have

$$\begin{vmatrix} f'(u^*,v^*) - \lambda & -k^2 D_v \\ k^2 D_u & -\lambda \end{vmatrix} = 0 ,$$

$$\Rightarrow \quad \lambda^2 - \lambda f'(u^*,v^*) + k^4 D_u D_v = 0 . \tag{2.35}$$

We end up with

$$\lambda = \tfrac{1}{2}\left(f'(u^*,v^*) \pm \sqrt{(f'(u^*,v^*))^2 - 4k^4 D_u D_v} \right) . \tag{2.36}$$

From equation (2.31), we see that, if $\Re\mathfrak{e}(\lambda) < 0$, then the perturbation term $\tilde{\omega}(x,t)$ decays exponentially. This means the perturbed solution as shown in (2.27) about equilibrium point (u^*, v^*) will converge exponentially to equilibrium point (u^*, v^*). In this case, we say that this equilibrium point is stable. If $\Re\mathfrak{e}(\lambda) > 0$, then perturbation $\tilde{\omega}(x,t)$ increases exponentially. In this case, we say that this equilibrium point is unstable.

From (2.36) we conclude that, if $f'(u^*, v^*)$ is positive, then $\Re\mathfrak{e}(\lambda) > 0$. So ,in this case (u^*, v^*) is unstable. If $f'(u^*, v^*)$ is negative then from (2.36) we have: $\Re\mathfrak{e}(\lambda) < 0$ for all k.

2.4 Possibilities of Generalising ZFK-Nagumo or Fisher-KPP by the Quartic Polynomial

We have not found any studies of the reaction cross-diffusion system with quartic nonlinearity in literature. There is no application for such a system in a real world problem.

Here, we want to see if we can make the reaction cross-diffusion system with quartic polynomial to look like generalizations, in one sense or another, of other well-known models. We shall say that we "imitate" those models. The models that we want to imitate are Fisher-KPP and ZFK-Nagumo. Those models are presented as follows:

$$
\begin{aligned}
u_t &= u_{xx} + f(u), \\
f(u) &= u(1-u), && \text{Fisher-KPP} \\
f(u) &= u(u-a)(1-u), \quad a \in (0,1), && \text{ZFK-Nagumo}
\end{aligned}
$$

The plot of the reaction term for both models is presented in figures 2.5.

The solution for each exhibits a front propagating wave that has the following property

$$
\hat{u}(\xi) \longrightarrow \begin{cases} 1 & \xi \to -\infty, \\ 0 & \xi \to +\infty. \end{cases} \tag{2.37}
$$

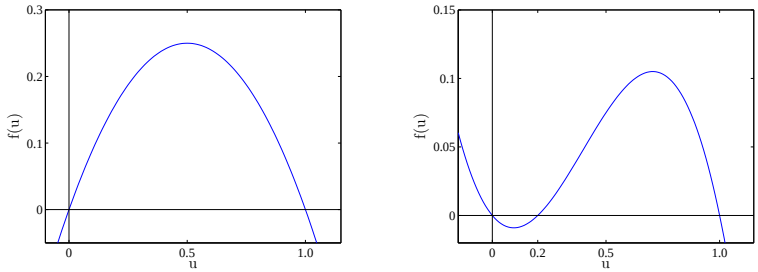

(a) Fisher-KPP (b) ZFK-Nagumo

Figure 2.5: (a) The shape of the kinetic term in Fisher-KPP model. (b) The shape of the kinetic term in ZFK-Nagumo model.

This property can be achieved also using the solution in our system by letting $g = 0$ and $h = 1$ in (2.20).

We found in the previous section that the sign of the eigenvalues of equilibrium depends on the sign of the derivative of the quartic polynomial at the equilibrium point. To imitate the Fisher-KPP wave front, our system requires that the quartic polynomial has an unstable pre-front and a stable post-front. To imitate the ZFK-Nagumo wave front, our system requires that the quartic polynomial has a stable pre-front and a stable post-front and an unstable root between them.

However, the possibility of imitating Fisher-KPP and/or ZFK-Nagumo front waves from the reaction cross-diffusion system with quartic polynomial will be deduced from the following proposition.

Proposition 1. *The reaction cross-diffusion system*

$$\hat{u}_t = f(\hat{u}) - v + D_v v_{xx}\,,$$
$$v_t = -D_u \hat{u}_{xx}\,,$$

where the kinetic term $f(\hat{u}) - v$ *is the quartic polynomial as defined in the right hand side of* (2.24)*, has the travelling wave front solution shown in* (2.20) *where the resting states of the front are either the inner roots of the quartic polynomial* $f(\hat{u}) - v$ *or the outer roots of the quartic polynomial.*

Proof. :

From equation (2.20) we find that the resting states of the front of this system coincide with $(\hat{u} = g)$ and $(\hat{u} = h)$. By studying the slope of the quartic polynomial at those resting states, we obtain from equation (2.24) that

$$\left.\frac{d\big(f(\hat{u})-v_\star\big)}{d\hat{u}}\right|_{\hat{u}=g} = \sigma(g-h)k\Big(Ak^2(g-h)^2+B\Big),$$

$$\left.\frac{d\big(f(\hat{u})-v_\star\big)}{d\hat{u}}\right|_{\hat{u}=h} = \sigma(h-g)k\Big(Ak^2(g-h)^2+B\Big).$$

Clearly, the sign of the slope at $\hat{u} = g$ and $\hat{u} = h$ is different, so they are either adjacent roots or the outer roots of the quartic polynomial.

Furthermore, for the case in which the resting states are adjacent roots of the quartic polynomial $f(u)-v$, this means that they are the inner roots of the quartic. This is deduced from the formula for the roots of the quartic. Let the roots corresponding to the resting state be $\hat{u} = \{g,h\}$. Then from (2.24) and by satisfying the system (2.25), we find the roots of the quartic polynomial that are $\hat{u} = \{g,h\}$, which coincide with the resting states, while the other two roots are given by the following formula:

$$\hat{u}_{1,2} = \frac{1}{2}(g+h) \pm \frac{1}{6}\sqrt{3\big(Ak(g-h)^2 - \frac{2B}{k}\big)}.$$

The center of symmetry for the above formula is $\frac{1}{2}(g+h)$, which means either $\hat{u}_{1,2} \notin (g,h)$ or $\hat{u}_{1,2} \in (g,h)$. □

From Proposition 1, we conclude that of the resting states of the front wave solution, only one can be stable but not both. Consequently, it is impossible to imitate ZFK-Nagumo but there is a chance to imitate Fisher-KPP front wave by reaction cross-diffusion system with the quartic polynomial.

2.5 Choice of Signs to Imitate Fisher-KPP

We have shown that there is a possibility to imitate Fisher-KPP front wave, regarding to the stability of the ahead and behind of the front, by reaction cross-diffusion system

with quartic polynomial nonlinearity. In this section, we will proceed further according to that how we can imitate Fisher-KPP wave.

Firstly, we want ensure the formula (2.20) satisfies the boundary condition of Fisher-KPP front wave, which is:

$$\hat{u}(\xi) \longrightarrow \begin{cases} 1 & \xi \to -\infty, \\ 0 & \xi \to +\infty. \end{cases} \tag{2.38}$$

This condition can be satisfied by making a proper choice of the parameters. Previously, from (2.25) we found that it has to be assigned six free parameters to ensure the system (2.25) has a unique solution. We choose k, g and h as free parameters. The other free parameters will be appointed later.

Specifying k, g and h as free variables makes it easier to achieve the property (2.38). Having done this, then we have different choices that ensure the solution (2.20) satisfies the property (2.38). Table 2.1 exhibits those possibilities;

Assumptions				Results		
	g	h	k	χ	$u(\xi)_{\xi\to+\infty}$	$u(\xi)_{\xi\to-\infty}$
I	1	0	(+)	$\nearrow$	$h=0$	$g=1$
II	1	0	(−)	$\searrow$	$g=1$	$h=0$
III	0	1	(+)	$\searrow$	$g=0$	$h=1$
IV	0	1	(−)	$\nearrow$	$h=1$	$g=0$

Table 2.1: Examining different cases to find which assumption can produce a wave front similar to Fisher-KPP. The symbols ($\nearrow$) and ($\searrow$) mean increasing and decreasing function of ξ, respectively.

Clearly, assumptions (I) and (III) are of interest. In both assumptions equation (2.19) becomes

$$\begin{aligned} y(\hat{u}) &= k\hat{u}(\hat{u}-1), \qquad k>0 \\ \text{So, } y'(\hat{u}) &= 2k(\hat{u}-1), \qquad y''(\hat{u}) = 2k \end{aligned} \tag{2.39}$$

The quartic polynomial function $f(\hat{u})$ is initially suggested in (2.23) with two different values; $\sigma = \{-1, 1\}$.

We have found that from equating the coefficient of $\hat{u}^4$ as shown in (2.25) that,

$$6k^3 D_u D_v = -\sigma c \tag{2.40}$$

If $\sigma = +1$ then the solution (2.20) will not satisfy the condition (2.38) for the following reason. As D_u, D_v and c are positive parameters, then equation (2.40) implicates that $k < 0$, which is inconsistent with (2.39).

So, we apply the negative value of $\sigma = -1$ for the quartic, which gives

$$f(\hat{u}) = -(\hat{u} - u_0)(\hat{u} - u_1)(\hat{u} - u_2)(\hat{u} - u_3); \quad u_i \in \mathbb{R} \quad , i = 0,1,2,3\,. \tag{2.41}$$

By substituting (2.39) and (2.41) in (2.17), we get

$$k\hat{u}(\hat{u}-1)\Big\{A\big(k^2(2\hat{u}-1)^2 + 2k^2\hat{u}(\hat{u}-1)\big) + B\Big\} = -(\hat{u} - u_0)(\hat{u} - u_1)(\hat{u} - u_2)(\hat{u} - u_3) - v_\star\,, \tag{2.42}$$

where $A = \frac{-D_u D_v}{c}$ and $B = \frac{D_u - c^2}{c}$.

Combining like terms of $\hat{u}$ in the expression (2.42) yields to the following system

$$\frac{6k^3 D_u D_v}{c} = 1\,, \tag{2.43}$$

$$\frac{12k^3 D_u D_v}{c} = u_0 + u_1 + u_2 + u_3\,, \tag{2.44}$$

$$\frac{6k^3 D_u D_v}{c} + \frac{k^3 D_u D_v}{c} - k\frac{-c^2 + D_u}{c} = u_0u_1 + u_0u_2 + u_0u_3 + u_1u_2 + u_1u_3 + u_2u_3\,, \tag{2.45}$$

$$\frac{k^3 D_u D_v}{c} - k\frac{-c^2 + D_u}{c} = u_0u_1u_2 + u_0u_1u_3 + u_0u_2u_3 + u_1u_2u_3\,, \tag{2.46}$$

$$u_0u_1u_2u_3 = -v_\star\,. \tag{2.47}$$

Previously, we let variables g, h and k be free. However, we still need to assign arbitrary values to three more parameters.

We choose D_u, D_v and u_0 as free variables. Consequently, the rest of the variables will be dependent on those free parameters. We have obtained that the values of the

parameters are given as follows

$$c = 6k^3 D_u D_v\,, \tag{2.48}$$

$$u_3 = 1 - u_0 \quad , \quad u_3 = \tfrac{1}{2} \pm \tfrac{1}{6}\sqrt{36(\rho - u_0^2 + u_0) + 3}\,, \tag{2.49}$$

$$u_2 = 1 - \tfrac{1}{2}(u_0 + u_3) + \tfrac{1}{6}\sqrt{-27u_0^2 - 18u_0u_3 - 27u_3^2 + 36\rho + 36u_0 + 36u_3 - 6}\,, \tag{2.50}$$

$$u_1 = 2 - u_0 - u_2 - u_3\,, \tag{2.51}$$

$$v_\star = -u_0u_1u_2u_3\,, \tag{2.52}$$

where

$$\rho = \frac{k(D_u - c^2)}{c}\,. \tag{2.53}$$

As long as we do not link system (2.2) with the full system (2.1) (which we do not intend to do here), we can, without loss of generality, set $u_0 = 0$. This facilitates the problem as we then have $v_\star = 0$ and $u_3 = 1$. Consequently, by this choice, the roots u_0 and u_3 coincide with the resting states of the fronts and the quartic polynomial is simplified as follows

$$f(u) = -u(u-1)(u-u_1)(u-u_2)\,, \tag{2.54}$$

where u_1 and u_2 turn into

$$u_1 = \tfrac{1}{2} - \tfrac{1}{6}\sqrt{3 + 36\rho}\,, \tag{2.55}$$

$$u_2 = \tfrac{1}{2} + \tfrac{1}{6}\sqrt{3 + 36\rho}\,. \tag{2.56}$$

We expect that, in principle, if the quartic polynomial is substituted into the system (2.2) , i.e.

$$\begin{aligned} u_t &= -u(u-1)(u-u_1)(u-u_2) - v + D_v v_{xx}\,, \\ v_t &= -D_u u_{xx}\,, \end{aligned} \tag{2.57}$$

then the solution of (2.57) is a front wave that resembles the front wave in Fisher-KPP with respects to the stability of the ahead and behind of the front. Moreover, the speed of the propagating front wave solution of the system (2.57) that is given by the formula (2.48) depends on the parameters. In other words, unlike Fihser-KPP propagating front,

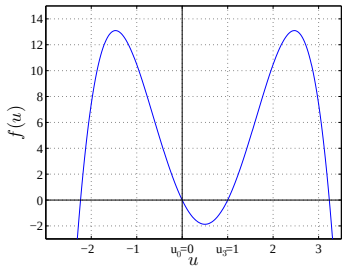

Figure 2.6: The shape of the kinetic in the quartic polynomial (case when $u = 0$ and $u = 1$ are inner roots). The values of other roots are $u_1 = -2.2362$ and $u_2 = 3.2362$.

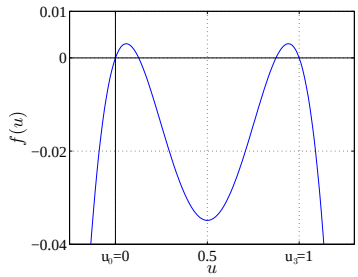

Figure 2.7: The shape of the kinetic in the quartic polynomial (case when $u = 0$ and $u = 1$ are outer roots). The values of other roots are $u_1 = 0.1265$ and $u_2 = 0.8735$.

here we have discrete not continuous values of speed. Consequently, the solution of (2.57) is a front wave that resembles the front wave in ZFK-Nagumo with respects to the discrete speed.

The choices of values of the given parameters change the values of the roots u_1 and u_2, which leads to one of the following cases. If $u_{1,2} \notin (0,1)$, then the resting states of the front, u_0 and u_3 , are the *inner roots* of the quartic polynomial (see figure 2.6). If $u_{1,2} \in (0,1)$, then we have that the resting states of the front are the *outer roots* of the quartic polynomial (see figure 2.7). Obviously, having inner roots or outer roots can be controlled by the formulae (2.55) and (2.56), by which we obtain the following conditions

- Condition to make u_0 and u_3 outer roots $\rho \in (-\infty, \frac{1}{6})$ (2.58)
- Condition to make u_0 and u_3 inner roots $\rho \in (\frac{1}{6}, +\infty)$ (2.59)

In fact the case when $\rho \in (-\infty, \frac{1}{6})$ the positions of u_1 and u_2 will give three different

cases depends on the value of ρ. These cases are summarised as follows

$$(a) \quad \rho \in (-\infty, -\tfrac{1}{12}), \tag{2.60}$$

$$(b) \quad \rho \in (-\tfrac{1}{12}, \tfrac{1}{6}), \tag{2.61}$$

$$(c) \quad \rho = \tfrac{-1}{12}. \tag{2.62}$$

For (a) the roots u_1 and u_2 are complex roots. For case (b) the roots u_1 and u_2 are distinct real roots. For case (c), then $u_1 = u_2$. However, those cases will be discussed in more details in the following chapter.

In the next chapter we will show that in the PDE, the behaviour of the solution in inner roots case is not same as the behaviour of the solution in outer roots case.

2.6 Chapter Summary

In the beginning of this chapter, we replaced the cubic nonlinearity of the FHN model in two components reaction cross-diffusion system by a general function. Then, we focused on the front wave solution that caused the disappearance of the kinetic term of the second equation of the system. The dimensionality of the system could then be reduced to one equation. After that we introduced the wave solution with appropriate boundary conditions.

At that time, the general function was considered to be a continuous polynomial. Relying on this consideration, we found, analytically, the corresponding solution and the values of the dependent parameters. After that, we discussed the possibility of imitating Fisher-KPP and ZFK-Nagumo front waves using our system. We introduced a proposition with proof that it is impossible to have front wave with stable pre-front and post-front states as in ZFK-Nagumo.

In this chapter, we introduced the travelling wave front solution analytically for the reaction cross-diffusion system with quartic polynomial. The analytical solution we introduced in this chapter does not have the features of Fisher-KPP front wave nor features of ZFK-Nagumo front wave in full. In other words, the analytical solution did

not have discrete speed and stable pre-front and post-front at the same time as ZFK-Nagumo front wave has. Furthermore, it did not have continuous speed and stable pre-front and unstable post-front at the same time as Fisher-KPP front wave has.

In fact, the analytical solution for this problem can resemble the Fisher-KPP front wave in that the existence of unstable post-front and stable pre-front. Also this front wave solution can resemble ZFK-Nagumo front wave in that both have discrete speed.

However, the analytical wave solution that we have found presents a monotonic wave front which is inconsistent with the existence of an oscillatory fronts that are observed in numerical solutions of the reaction cross-diffusion systems.

CHAPTER 3

NUMERICAL SIMULATION

3.1 Introduction

The analytical wave solution of a reaction cross-diffusion system with quartic polynomial has been discussed in the previous chapter. This chapter will be allocated for numerical simulation. The numerical simulation will be applied to investigate all the possibilities of imitating Fisher-KPP front wave by reaction cross-diffusion system with quartic polynomial. Moreover, we will investigate the stability of the analytical travelling wave solution numerically.

Although we have already found the analytical solution, numerical solution is still desirable. The problems in the reality are subject to disturbances, that may not be reflected by analytical solution. In fact, the numerical solution could be considered as perturbed solution for the travelling wave solution. Roughly speaking, the discretisation of the space and time in the numerical simulation has an influence on the behaviour of the solution that could be interpreted as a disturbance. Consequently, by applying the analytical solution that we have found as an initial condition in numerical simulation, one could make a conclusion about the stability of this travelling wave front. This conclusion is described as follows; if the numerical solution matches the analytical solution then

we say the travelling wave is stable. This is one motivation to numerically simulate the analytical solution, that is presented in the previous chapter.

This chapter has been arranged as follows, we start with problem formulation and describing the scheme that will be used in this simulation. Also, we give the cases that could be derived from the system as well as the stability of the post-front and pre-front resting state and how they match Fisher-KPP front wave, all these are shown in the first section.

In the second section we consider the case when the resting states coincide with the inner roots of the quartic polynomial. We show appropriate choices of free parameters that give this case and the result of the simulation for this case. The third to the fifth sections are devoted for outer roots case, double roots and complex conjugate roots. In each of those sections we show the condition of the appropriate choices of the parameters and the results of the numerical simulation. After that we discuss the instability of the numerical solution in all those four cases. In the last section, we give a brief summary about the results in this chapter.

3.2 Numerical Scheme for the Simulations

3.2.1 Problem Formulation for The Simulation

The problem which will be numerically simulated is the reaction cross-diffusion system where the kinetic term is quartic polynomial, that has the form

$$\begin{aligned} u_t &= f(u,v) + D_v v_{xx}\,, \\ v_t &= -D_u u_{xx}\,, \end{aligned} \qquad -a \le x \le b\,,\ t \ge 0\,, \tag{3.1}$$

where $f(u,v)$ is a quartic polynomial that is simplified in (2.54) to be

$$f(u,v) = -u(u-1)(u-u_1)(u-u_2) - v\,, \tag{3.2}$$

where u_1 and u_2 are dependent parameters that were given in (2.55) and (2.56).
We applied no-flux boundary condition whereas the initial condition is taken from the

analytical solution, as shown in (2.20) and (2.21), that is

$$u(x,0) = \hat{u}(\xi) \quad , \quad v(x,0) = \hat{v}(\xi)\,,$$
$$u_x(-a,t) = u_x(b,t) = 0 \quad , \quad v_x(-a,t) = v_x(b,t) = 0\,.$$

An example of the profile of the initial condition for case $(a = b = 20)$ is shown in figure 3.1.

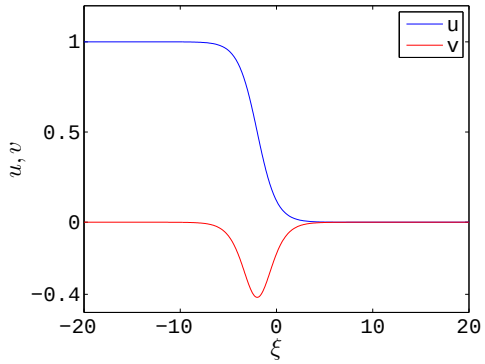

Figure 3.1: An example of the front wave profile that will be applied as an initial condition of the simulations in this chapter. This front wave is obtained by setting $g = 0, h = 1, k = 1$ and the arbitrary constant $C = 2$.

3.2.2 Finite Difference Scheme To Simulate The Problem

The method that we have used to simulate the problem numerically, is a fully explicit scheme. We used first order time step for time derivative and second order central difference for space derivative. First we will introduce space discretisation steps that are defined as follows

$$\Delta x = \frac{L}{N}, \qquad \text{where } L = a + b \text{ and } N \in \mathbb{Z}^+\,,$$
$$\Delta t = \frac{T}{M}, \qquad \text{where } T \in \mathbb{R}^+ \text{ and } M \in \mathbb{Z}^+\,.$$

This defines the grid points (x_j, t_m) , such that

$$x_j = -a + (j-1)\Delta x, \qquad j = \{1,2,\cdots,N+1\}\,,$$
$$t_m = m\Delta t, \qquad m = \{0,1,2,\cdots,M\}\,.$$

So, by applying explicit finite difference scheme with this discretisation on (3.1), the solution is computing by the following formula

$$\begin{aligned} \frac{u_j^{n+1}-u_j^n}{\Delta t} &= f(u_j^n, v_j^n) + D_v \frac{v_{j-1}^n - 2v_j^n + v_{j+1}^n}{\Delta x^2}, \\ \frac{v_j^{n+1}-v_j^n}{\Delta t} &= -D_u \frac{u_{j-1}^n - 2u_j^n + u_{j+1}^n}{\Delta x^2}, \end{aligned} \tag{3.3}$$

where $u_j^n = u(x_j, t_n)$ and $v_j^n = v(x_j, t_n)$, while the formula of the solution at the boundary points $(-a,t)$ and (b,t), is given as follows

$$\begin{aligned} \frac{u_j^{n+1}-u_j^n}{\Delta t} &= f(u_j^n, v_j^n) + D_v \frac{2v_J^n - 2v_j^n}{\Delta x^2}, \\ \frac{v_j^{n+1}-v_j^n}{\Delta t} &= -D_u \frac{2u_J^n - 2u_j^n}{\Delta x^2}, \end{aligned}$$

where the subscript $J = j+1$ at the point $(-a,t)$ where $j=1$ and $J = j-1$ at the point (b,t) where $j = N+1$.

The discretisation steps that are used in the numerical simulation are $\Delta x = 0.15$ and $\Delta t = 4 \times 10^{-6}$ unless otherwise stated. The choice of the discretization steps is motivated by the stability and accuracy analysis of the scheme, which is presented later, on pages (80-82).

Operator splitting method is applicable for this problem, that is applying explicit scheme on nonlinear term and implicit scheme on linear cross-diffusion terms. We avoid this method as in this problem it takes too much time to completely implement. In fact, the existence of quartic polynomial function requires small discretisation steps. This small steps give big size matrices for implicit scheme that leads to time-consuming, especially for this problem as we will simulate different cases as shown in the following sections.

3.2.3 The Cases inside the System

We have shown previously that, according to the relation between the resting states of the front wave and the quartic polynomial we have only two cases. Those cases are called inner roots case and outer roots case. The conditions to have one of the two cases are presented in (2.58) and (2.59).

We proved that there are no more cases in regards to the relation between the resting states of the front wave and the roots of the quartic polynomial, as presented in proposition 1.

We have found that the outer roots case could be presented in three different situations depending on the values of u_1 and u_2 which are depending on the value of ρ as clarified in the end of section 2.5.

Indeed, changing the values of u_1 and u_2 will not affect the position of the resting states of the front wave but their stabilities might be affected.

In the end, in the numerical simulation we will consider, separately, the following cases;

- $u_1, u_2 \notin (0,1)$ which represents 'inner roots case',
- $u_1, u_2 \in (0,1)$ and $u_1 \neq u_2$ which represents 'outer roots case',
- $u_1 = u_2$ which represents 'double roots case',
- $\{u_1, u_2\} \in \mathbb{C} \setminus \mathbb{R}$ which represents 'complex roots case'.

In this classification, 'double roots case' and 'complex roots case' are special cases of outer roots case, so we keep term 'outer roots case' for distinct roots case $u_1 \neq u_2$ and distinguish the special cases by other names.

By expanding ρ we see that the condition to have one of those cases depend on the choices of the free parameters k, D_u and D_v. For each case we show the result of the simulation for two different choices of the free parameters as a way to prove the behaviour of the solution will not be changed significantly for different values of free parameters. Also, we would be sure that there is no numerical artifact.

In the next sections, we will show the condition of choices of the free parameters for each case as well as the results of the simulation. Later, we will investigate the stability of the front waves solution for each case by direct numerical simulation.

3.2.4 Stability of The Resting States

The stability of the resting states of the front in each of the four cases will be provided here. Formerly, we have linearised the system (3.1) for general function $f(u)$ about the

equilibrium and derived the formula of the eigenvalues (2.36). Substituting the quartic polynomial function (3.2) into the function of the eigenvalue yields that, the eigenvalue of the equilibrium $u = u_0 = 0$ is given by

$$\lambda = \frac{1}{2}\big(u_1 u_2 \pm \sqrt{(u_1 u_2)^2 - 4k^4 D_u D_v}\big), \tag{3.4}$$

while the eigenvalue of the equilibrium $u = u_1 = 1$ is given by

$$\lambda = \frac{1}{2}\big(-(1-u_1)(1-u_2) \pm \sqrt{(-(1-u_1)(1-u_2))^2 - 4k^4 D_u D_v}\big). \tag{3.5}$$

In fact, the values of u_1 and u_2 are to be considered important in the simulation as they play a role in the stability of the reaction cross-diffusion system (3.1) at the equilibria $u = \{0, 1\}$, the resting states of the wave front. From the formulae (3.4) and (3.5) it suffice to study the sign of the term $(u_1 u_2)$ and $(1-u_1)(1-u_2)$ to make a judgement about the stability of the post-front $u = 1$ and the pre-front $u = 0$, respectively.

In the inner roots case, the two roots u_1 and u_2 have distinct signs. To be precise, $u_1 < 0$ and $u_2 > 1$.
So, from (3.4) we have that

$$u_1 u_2 < 0,$$

then $\mathfrak{Re}(\lambda) < 0$ at the equilibrium $u = 0$. And from (3.5) we have that

$$-(1-u_1)(1-u_2) > 0,$$

then $\mathfrak{Re}(\lambda) > 0$ at the equilibrium $u = 1$. Therefore, in the inner roots case the pre-front $u = 0$ is stable and the post-front $u = 1$ is unstable. In other words, in inner roots case it is usually the unstable state invades the stable state. The similarity between Fisher-KPP and inner roots case is that both systems have two consecutive roots of $f(u)$ that coincide with the resting states of a wave front. The difference between them is that the pre-front in Fisher-KPP is unstable and the post-front is stable, while in inner roots case the pre-front is stable and the post-front is unstable.

In the outer roots case, the roots u_1 and u_2 are positive and less than one.
By applying this fact in (3.4) we have that

$$u_1 u_2 > 0$$

then $\mathfrak{Re}(\lambda) > 0$, therefore the equilibrium $u = 0$ is unstable.
And from (3.5) we have that

$$-(1-u_1)(1-u_2) < 0$$

then $\mathfrak{Re}(\lambda) < 0$, therefore the equilibrium $u = 1$ is stable.
Indeed, in this case, the stability of the resting states of the front is matching the behaviour of the stability of the front in Fisher-KPP, that is there is an invasion of stable states into unstable states. The difference is that, there are two equilibria $\{u_1, u_2\}$ located between the equilibria $\{u_0, u_3\}$, which are the resting states of the front. In Fisher-KPP model there is no root between $u = 0$ and $u = 1$.

In double roots case, $u_1 = u_2$ are positive and less than one. So, the stability of the resting states of the front is similar to the stability of the resting states of the front in outer roots case.

In complex roots case, the roots u_1 and u_2 are a complex conjugate pair, where the real part is equal $\frac{1}{2}$ as deduced from the formulae (2.55) and (2.56). By substituting those complex number in (3.4) we found

$$u_1 u_2 > 0$$

that means the equilibrium $u = 0$ is unstable. And from (3.5) we found

$$-(1-u_1)(1-u_2) < 0$$

so, the equilibrium $u = 0$ is stable.

The table 3.1 sums up the results of the stability of the resting states of the front of each case and how it matches the stability of Fisher-KPP model. In the next section we will show the result of the numerical simulation for each case, separately.

Choice of roots	Pre-front	Post-front	Matching with Fisher-KPP
Inner	stable	unstable	x
Outer	unstable	stable	✓
Double	unstable	stable	✓
Complex	unstable	stable	✓

Table 3.1: The stability of the resting states in the front wave depends on the choice of the roots of the quartic polynomial.

3.3 Resting States of The Front are Inner Roots of The Quartic

3.3.1 Choices of The parameters in The Inner Roots Case

Firstly, we need to pick appropriate values of the free parameters to satisfy that the inner roots of the quartic polynomial coincide with the resting states of the wave front. To achieve that, we should make our choices for the free parameters depend on the condition (2.59). In order to facilitate the use of this condition, we will express this condition in terms of the free parameters. So, by substituting (2.48) into (2.53) we obtain

$$\rho = \frac{-36D_uD_v^2k^6+1}{6k^2D_v}. \tag{3.6}$$

Substituting (3.6) into the condition (2.59) yields

$$\frac{1}{6} < \frac{-36D_uD_v^2k^6+1}{6k^2D_v},$$

which could be simplified to be as follows

$$1 > k^2D_v(1+36k^4D_uD_v). \tag{3.7}$$

The method we have followed to make the choices of free parameters is that, we fixed one parameter and plot the inequality for the other two parameters. We choose parameter k to be fixed as it appears with large power. Before choosing values of the free parameters we should note that all of them have to be positive. Of course, one could pick values of the free parameters without plotting but then one needs to examine whether

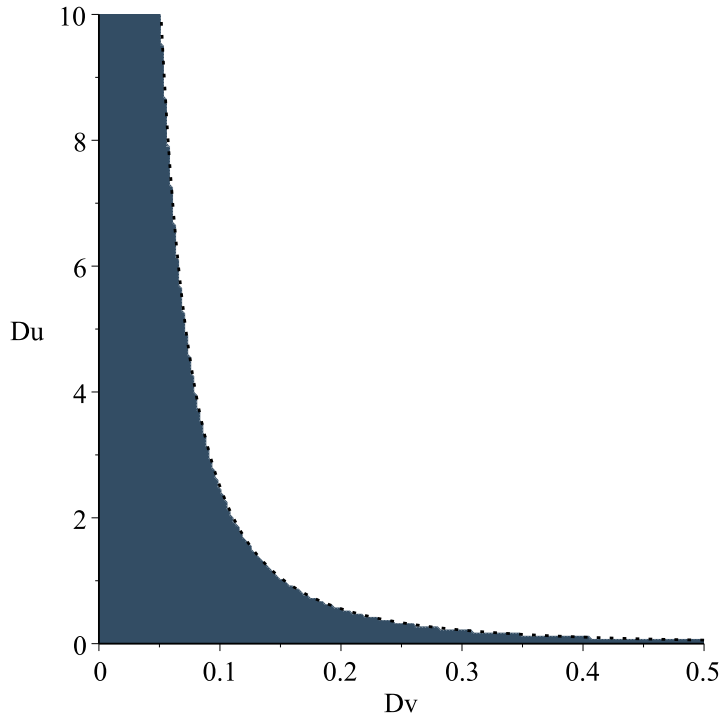

Figure 3.2: The plot of inequality (3.7) where we fix $k = 1$. Picking values for D_u and D_v from the shaded area yields the inner root case i.e. the resting states of the front are adjacent roots of the quartic. This shaded area increase as we let $k \to 0$.

the choice satisfies the condition or not for every change of choice we make. So the plot will ease choosing proper values of free parameters. For instance, we fixed $k = 1$ in (3.7) and then we plot the area from which to pick values of free parameters D_u and D_v that guarantees that the roots of the quartic polynomial satisfy (3.7), see figure 3.2. An example to the correspondent quartic polynomial in this case is shown in figure 3.3.

3.3.2 The Result of Simulation The Inner Roots Case

Previously, we showed that in the inner roots case the post-front state is unstable whereas the pre-front state is stable. So, in this case, the post front state will not remain in its level and attracting the pre-front state as in Fisher-KPP. In fact, in this case we suppose that the post-front state will be attracted by a stable equilibrium. Moreover, unlike Fisher-KPP, in inner roots case the unstable post-front state $u = 1$ will invade into the stable pre-front state $u = 0$.

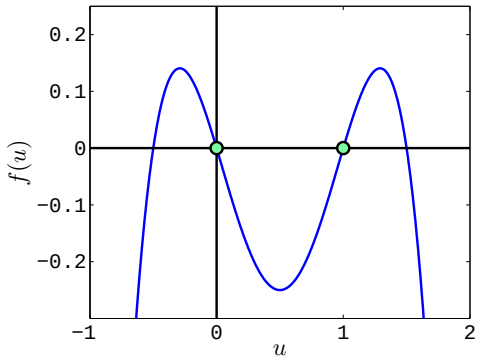

Figure 3.3: The shape of the quartic polynomial where the roots $u = 0$ and $u = 1$ are inner roots. The free parameters are $D_u = 1.25, D_v = 0.1$ and $k = 1$, which give $u_1 = -0.5$ and $u_1 = 1.5$.

Although we know the inner roots case does not reflect Fisher-KPP, it is still worth it to see what is going to happen in that case as well as to comprehend all the possible cases in reaction cross-diffusion system with the quartic polynomial with real roots.

The shape of the quartic polynomial that we used in the first simulation is presented in figure 3.3. As seen in this figure, the roots $u_0 = 0$ and $u_3 = 1$, that coincide with the resting states of the front, are surrounded by two roots $u_1 = -0.5$ and $u_2 = 1.5$. By (2.36) we found that the equilibrium u_2 is stable as the eigenvalue of this equilibrium is found $\Re\mathfrak{e}(\lambda) = -1.5 < 0$. So, the post-front, that coincides with $u_3 = 1$, is surrounded by two stable equilibria $u_0 = 0$, that corresponds to pre-front, and $u_2 = 1.5$. Thus in this case we expect the post-front state u_3 will be attracted by either u_0 or u_2. The result of the numerical solution in this case is presented in figures 3.4.

Interestingly, we have seen in the numerical simulation that the post-front state is attracted by both stable equilibria. Precisely, the post-front state is pulled by $u_2 = 1.5$ first. Then after a period of time the post-front state is pulled by the other stable equilibrium $u_0 = 0$. Actually, the preceding part of the post-front state, that is connecting to the front, is pulled by stable equilibrium u_2 while the latter part of the post-front state, that is connecting to the boundary, is pulled by another stable equilibrium u_0. This movement of the post front forms a bounded plateau.

We re-simulate the propagating front in case, the resting states are inner roots, with a different choice of parameters that is $D_u = 3.0$, $D_v = 0.5$ and $k = 0.5$. By this choice,

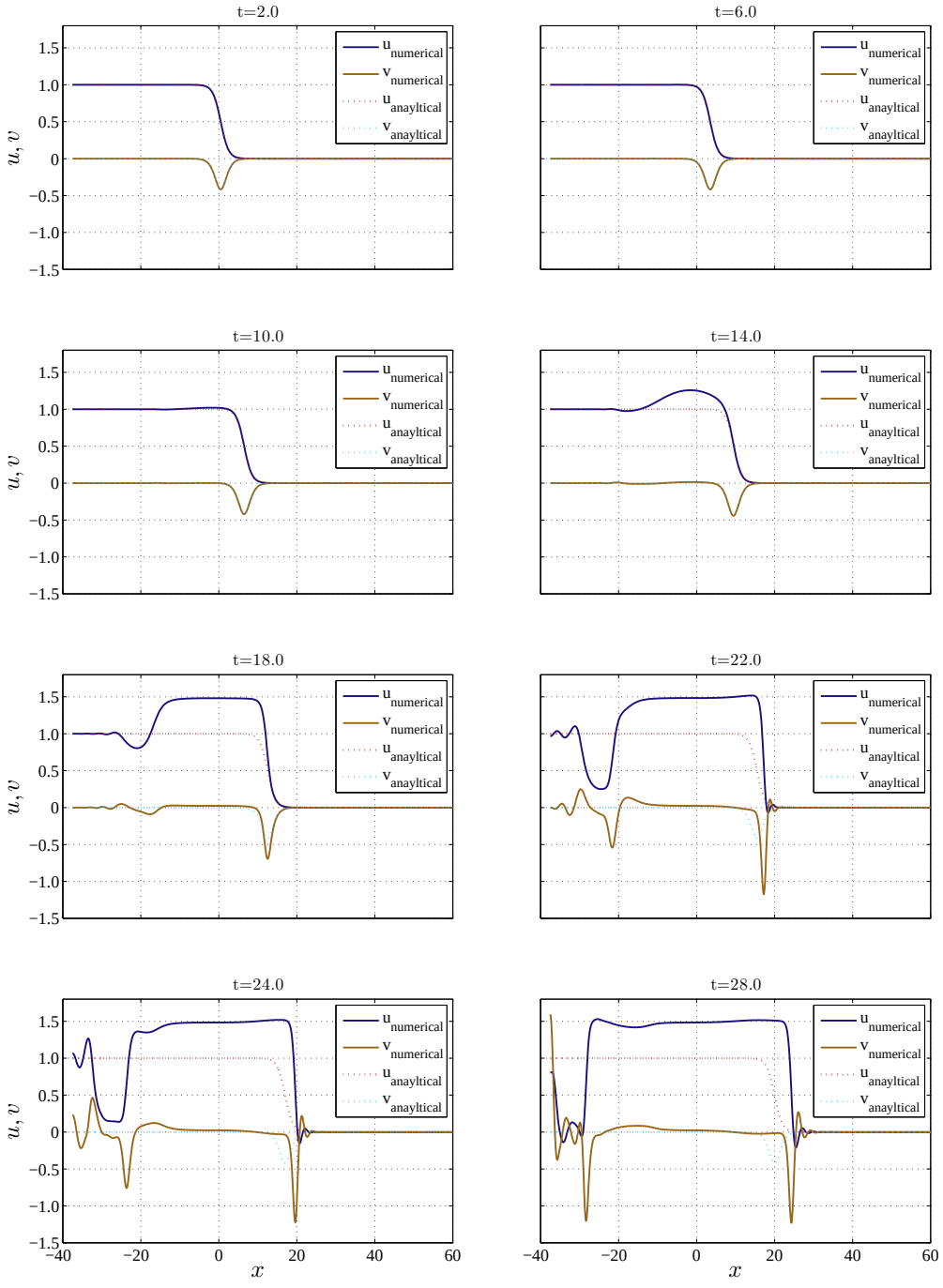

Figure 3.4: The numerical simulation of reaction cross-diffusion system with quartic polynomial where the resting states of the front coincides with the **inner roots** of the quartic. The values of parameters in this simulations are $(D_u = 1.25), (D_v = 0.1)$ and $(k = 1)$.

the quartic polynomial still has $u_0 = 0$ and $u_3 = 1$ whereas the values of the other roots become $u_1 = -0.424$ and $u_2 = 1.424$.

The result of applying this choice of parameters in the simulation is shown in figure 3.5. We see that, with this choice of values of free parameters, the propagating wave front behaves as we expected. Unlike the propagating front in figure 3.4, the pre-front state is attracted only by the equilibrium u_2 and there is no evidence of the affect of the equilibrium $u_0 = 0$, so there is no bounded plateau formed in this case. However, the numerical simulation shows that the wave front in inner roots case is not a stable propagating front.

3.4 Resting States of The Front are Outer Roots of The Quartic

3.4.1 Choices of The parameters in The Outer Roots Case

We will now consider the case when there are other two roots $\{u_1, u_2\} \in (0,1)$ of the quartic polynomial that are real and distinct. As consequence, $u_0 = 0$ and $u_3 = 1$ are outer roots of the quartic polynomial. The other situations of outer roots case, when $\{u_1, u_2\} \in (0,1)$ are real and equal (double roots case) or when they are a complex conjugate pair will be considered in separate sections.

Previously, we showed the condition (2.61) which makes our choices of the free parameters give real distinct u_1 and u_2 as well as let $\{u_1, u_2\} \in (0,1)$. From (3.6) and (2.61) we obtain that

$$-\frac{1}{12} < \frac{-36D_u D_v^2 k^6 + 1}{6k^2 D_v} < \frac{1}{6} \quad \Rightarrow \quad -\tfrac{1}{2}k^2 D_v < -36D_u D_v^2 k^6 + 1 < k^2 D_v \,,$$

which could be simplified to

$$0 < -72k^6 D_u D_v^2 + 2 + k^2 D_v < 3k^2 D_v \,. \tag{3.8}$$

Similar to what we have done in section 3.3.1, we will fix k and then plot the inequality

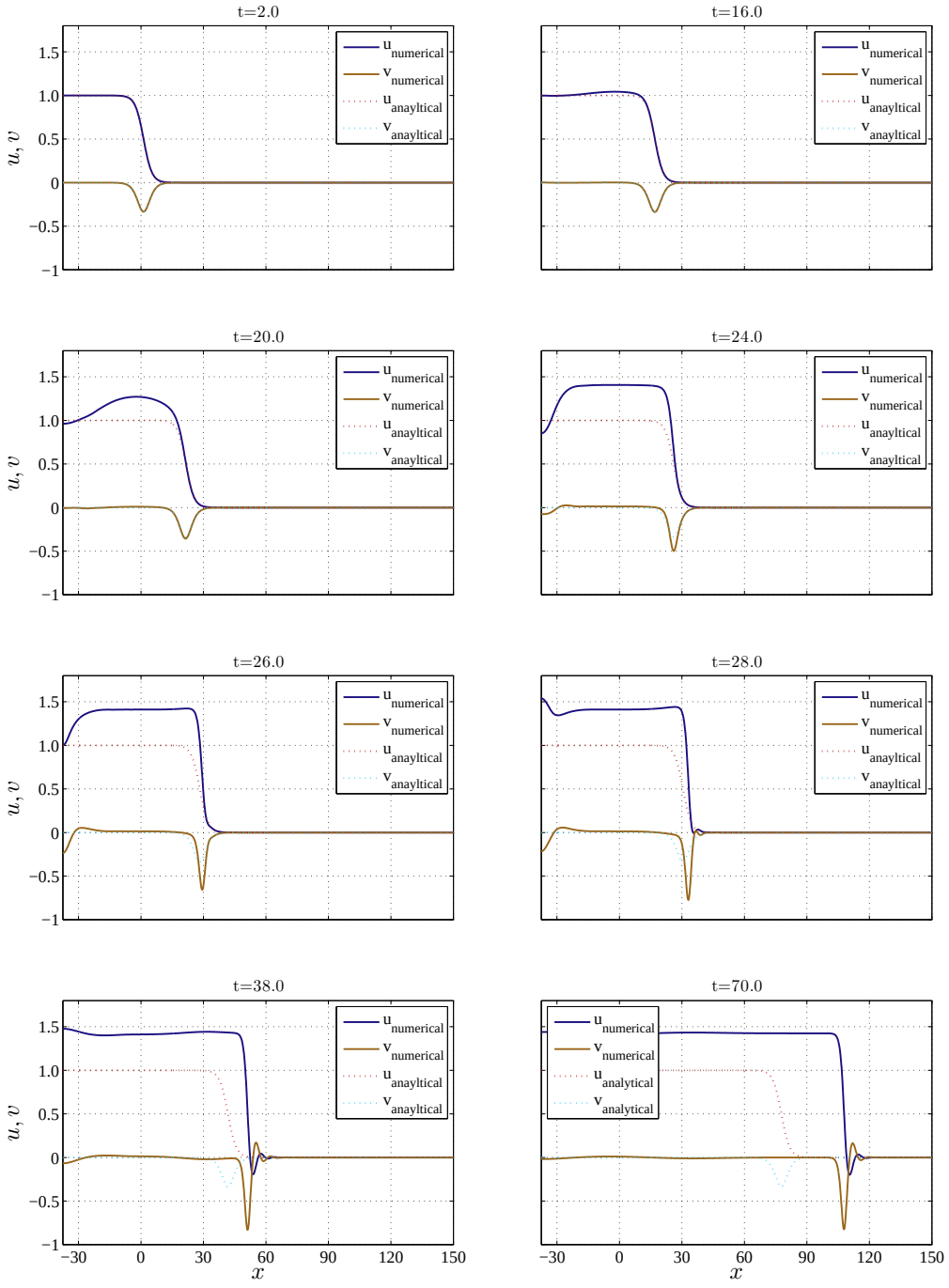

Figure 3.5: The numerical simulation of reaction cross-diffusion system with quartic polynomial where the resting states of the front coincide with the **inner roots** of the quartic. The values of parameters in these simulations are $D_u = 3.0, D_v = 0.5$ and $k = 0.5$.

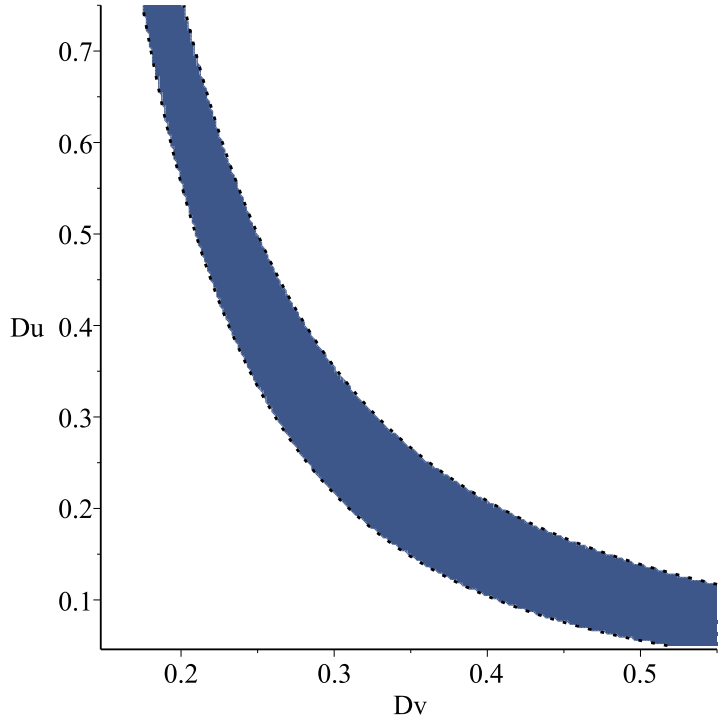

Figure 3.6: The plot of inequality (3.8) where we fix $k = 1$. Picking values for D_u and D_v from the shaded area yields the outer root case i.e. there are two roots of the quartic between the resting states of the front. This shaded area increase as we let $k \to \infty$.

(3.8). For this case the values of D_u and D_v could be chosen from the shaded area in the figure 3.6. An example to the correspondent quartic polynomial is shown in figure 3.7.

3.4.2 The Result of Simulation The Outer Roots Case

From the table 3.1, we showed that the stability of the resting states of the front in the outer roots case is matching the stability of the front in Fisher-KPP. The difference is that, there are two equilibria $\{u_1, u_2\}$ located between the equilibria $\{u_0, u_3\}$, that coincide with the resting states of the front.

In this simulation we used the quartic polynomial that is presented in figure 3.7. The result of the simulation is given in figure 3.8. In this figure we see that the front wave in outer roots case propagates with fixed shape remaining close to the analytical front wave for a period of time.

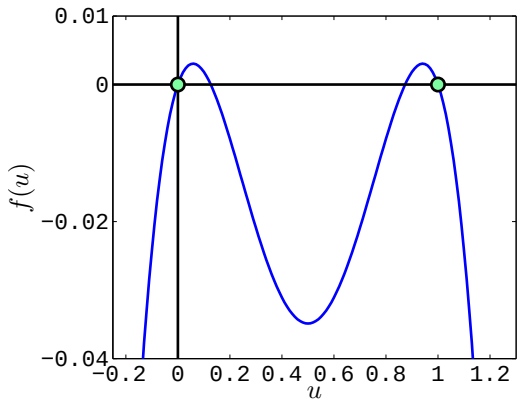

Figure 3.7: The shape of the quartic polynomial function with parameters $k = 1$. Parameters D_u and D_v are chosen from the shaded area in 3.6, precisely $D_u = 0.2$ and $D_v = 0.35$. By this choice, the resting states of the wave front $u = \{0, 1\}$ are outer roots of the quartic while $u_1 = 0.1265$ and $u_2 = 0.8735$.

As the time evolves, there are oscillations appearing in the onset of the front in the numerical front wave. This oscillation grows as time evolves. Due to growth of the oscillation, the numerical solution is destroyed after a period of time. In our case the numerical solution can not be seen after $t = 112$.

We re-simulate the wave front for outer roots case with a different choice of the free parameters. The result is shown in figure 3.9. From this result we see that, the behaviour of this propagating wave in general does not change when we change the values of parameters.

3.5 Resting States of The Front and Double Roots of The Quartic

One of the advantages of the quartic polynomial as a kinetic term in reaction diffusion system is that we could have the case where the resting states of the front coincide with the real roots of the quartic polynomial while the other two roots are double roots or even complex conjugate. This cannot be obtained if the kinetic term is quadratic polynomial as in Fisher-KPP nor if the kinetic term is cubic polynomial as in ZFK-Nagumo.

In this section we will consider the double root case. First we will show the condition

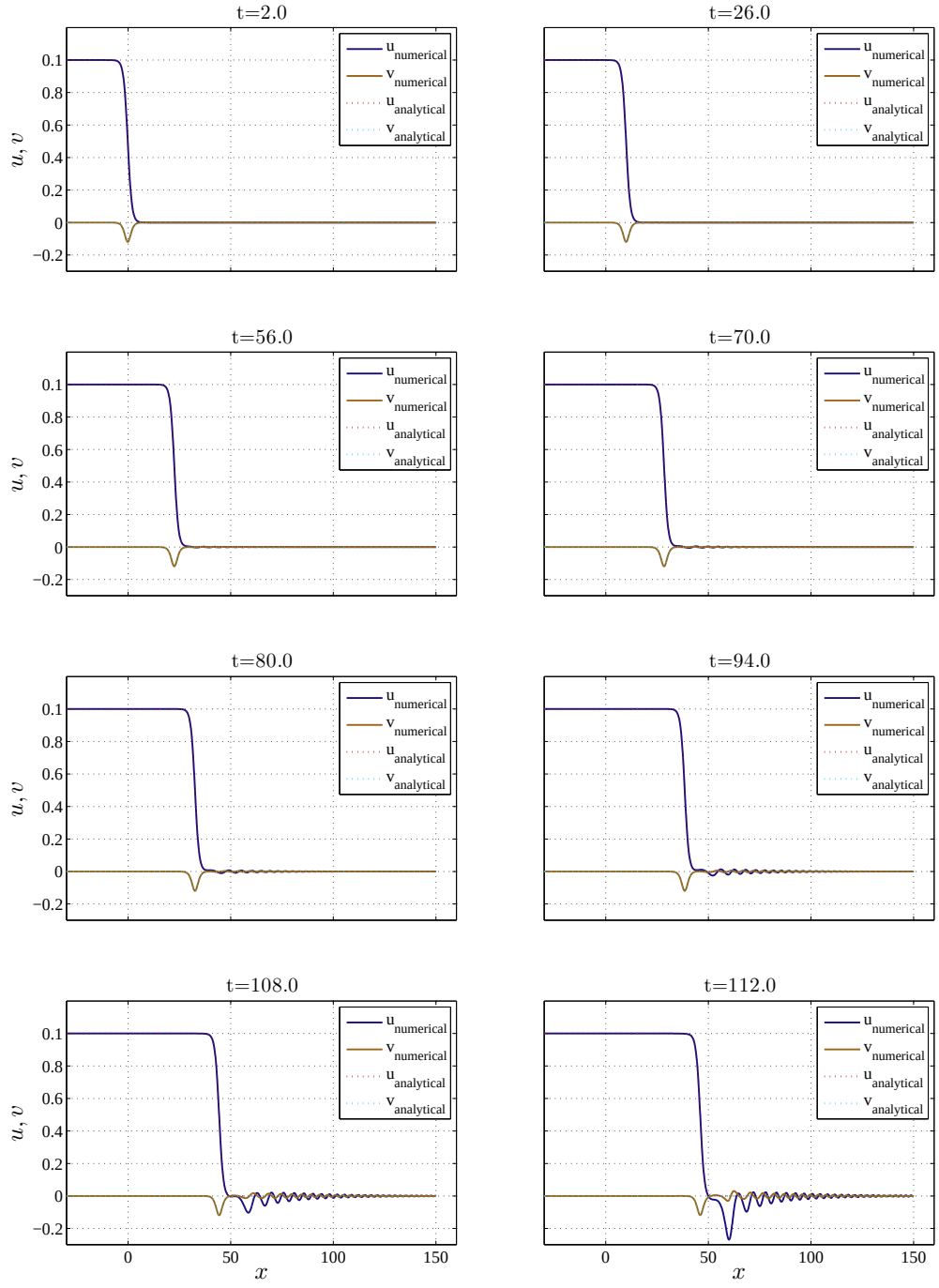

Figure 3.8: The numerical solution of the system (3.1) where the resting states of the front are **outer roots** of quartic polynomial. The values of free parameters are $D_u = 0.2, D_v = 0.35$ and $k = 1$.

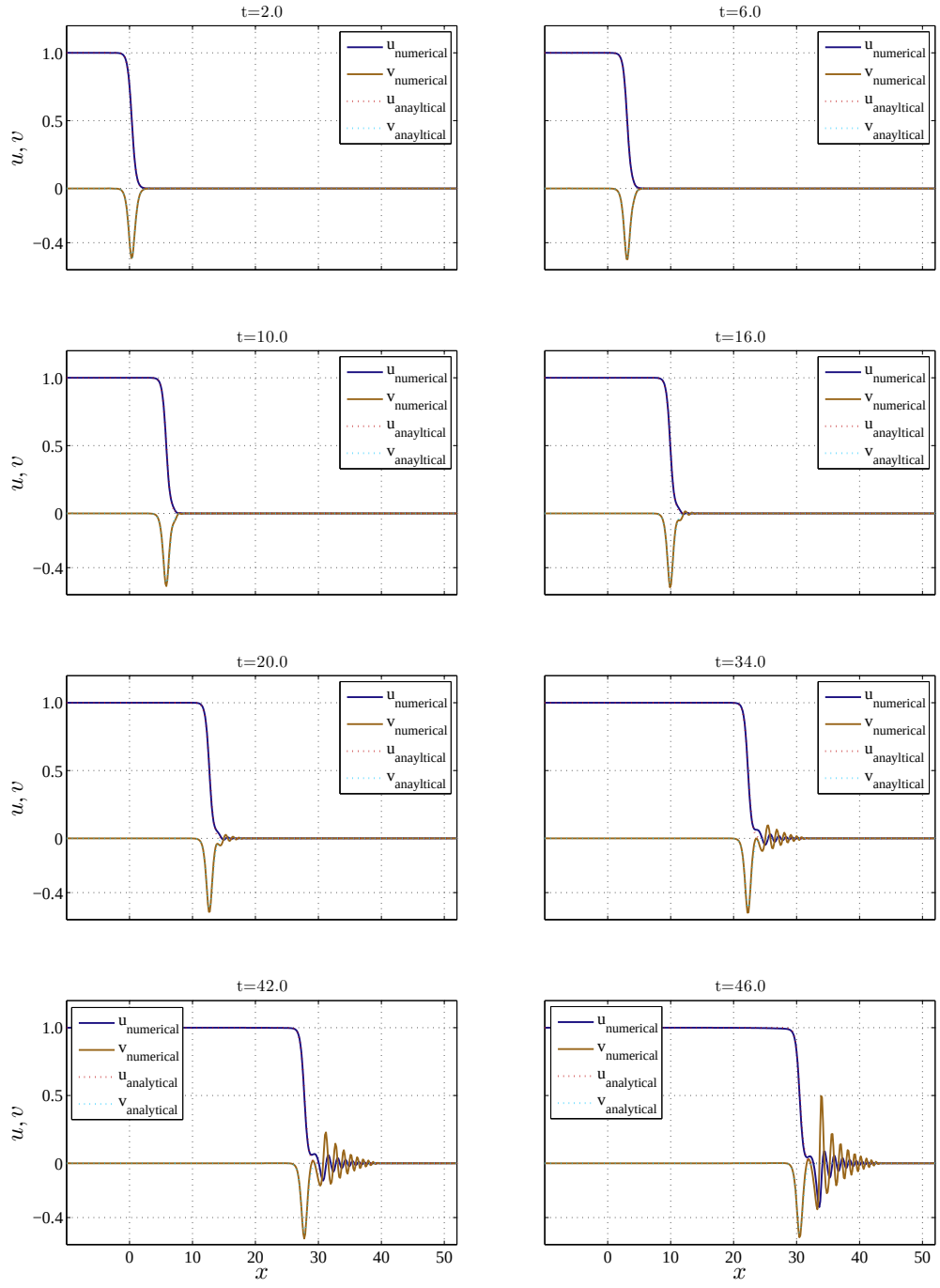

Figure 3.9: Another numerical simulation of the system (3.1) where the resting states of the front are **outer roots** of quartic polynomial with different choice of parameters. The values of free parameters are $D_u = 0.47, D_v = 0.009$ and $k = 3$.

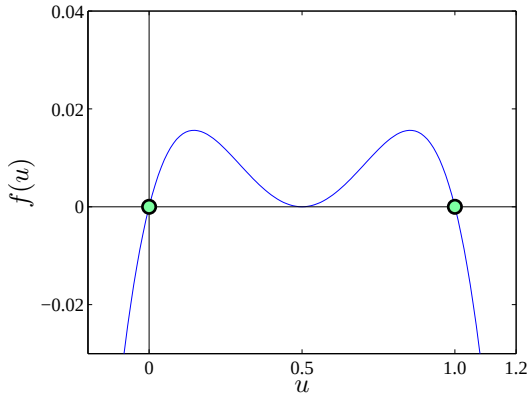

Figure 3.10: The profile of the quartic polynomial with double roots case. The values of the parameters are $k = 1$ and $D_v = 0.1$ where D_u is given in the formula (3.9).

of free parameters that gives this case and then we will show the result of the numerical simulation.

3.5.1 Choices of The parameters in The Double Roots Case

In this case we will seek the suitable choices of the free parameters that make the other two roots; u_1 and u_2 are double root of the quartic polynomial, i.e $(u_1 = u_2)$.

The condition is revealed formerly in (2.62), that is

$$\rho = \frac{-1}{12}.$$

By substituting (3.6) into the above equation we obtain the following equation

$$\frac{-36D_u^2D_v^2k^6 + D_u}{k^2D_uD_v} + \frac{1}{12} = 0.$$

If the parameters k and D_v are let to be free then

$$D_u = \frac{1}{72}\frac{D_vk^2 + 2}{D_v^2k^6}. \tag{3.9}$$

This is the condition to have double roots case. That is the parameter D_u is no longer a free. The shape of the quartic polynomial with double roots is shown in figure 3.10.

3.5.2 The Result of Simulation The Double Roots Case

We have shown previously the behaviour of the resting states of the front in the double roots case is same as the outer roots case. The difference between double roots case and outer roots case is the following, the stability of the equilibrium which is $(u = u_1 = u_2 = 1/2)$. By (2.36) we found that, the equilibrium $u = 1/2$ is not hyperbolic, i.e.

$$\lambda \in i\mathbb{R}.$$

We have substituted the quartic polynomial in figure 3.10 in the system of reaction cross-diffusion (3.1). The numerical simulation is presented in figures 3.11. From this figure we see that the propagating wave front behaves similarly to the wave front in outer roots case. In other words, the numerical propagating wave remains close to the analytical wave for a period of time. Then an oscillation appears in the onset of the front. After that the oscillation grows as the time evolves, which causes the numerical solution to break up. In this simulation the numerical solution breaks up at $(t = 54)$.

Another numerical simulation for the double roots case, with other choice of free parameter is shown in figure 3.12. The instability still exists even when we choose different values of free parameters. The difference between the results in the figure 3.11 and results in figure 3.12 is the time of appearance of the oscillation but in general both fronts are unstable.

3.6 Resting States of The Front and Complex Roots of The Quartic

In this section we consider the case when the quartic polynomial has a complex conjugate roots pair. As a result there are two equilibria only. These equilibria correspond with the post-front and pre-front.

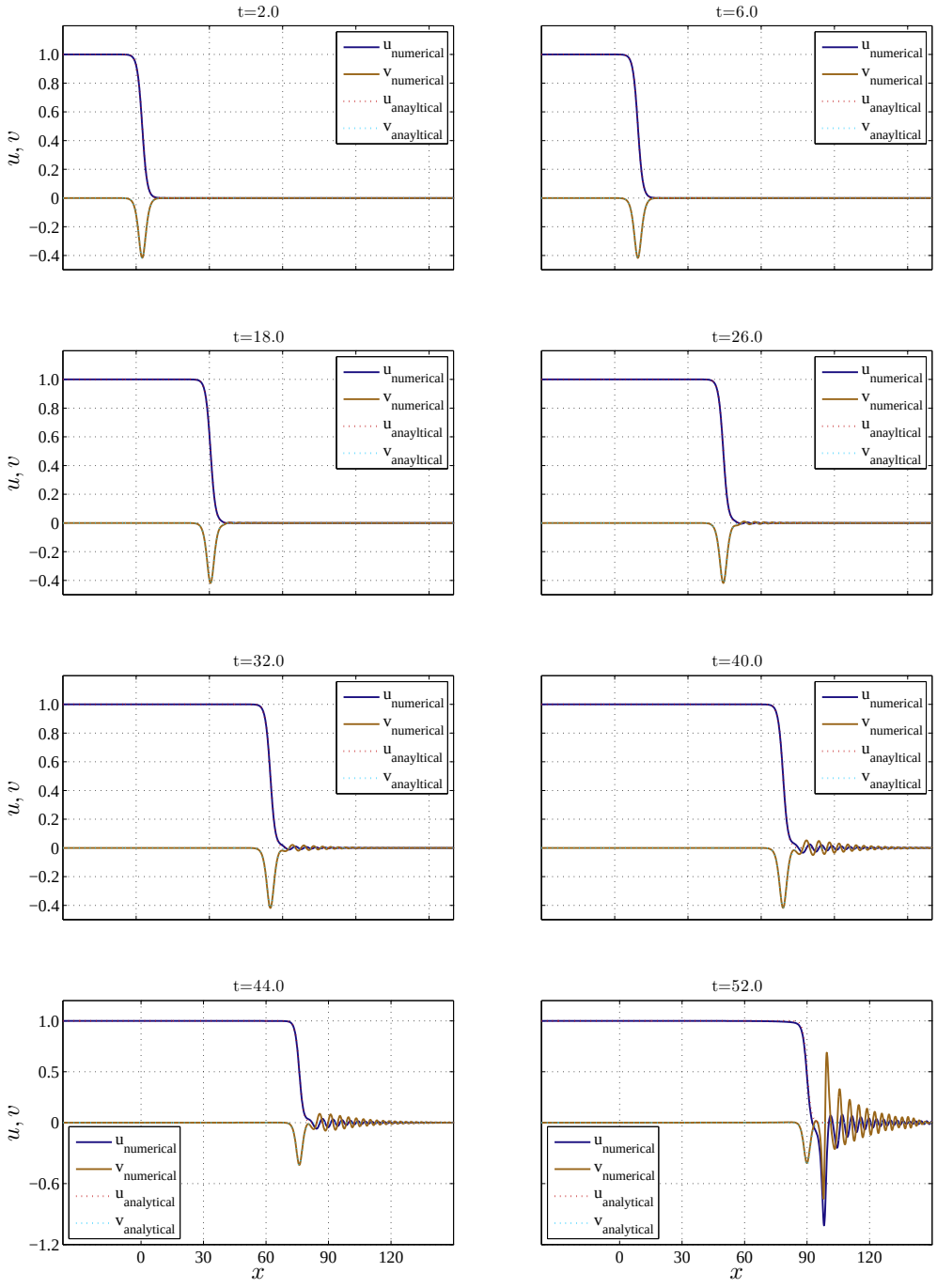

Figure 3.11: The numerical simulation of reaction cross-diffusion system with quartic polynomial where there are **double roots** and the resting states are simple roots. The values of parameters in these simulations are $D_v = 0.1$ and $k = 1$ where D_u is given in the formula (3.9).

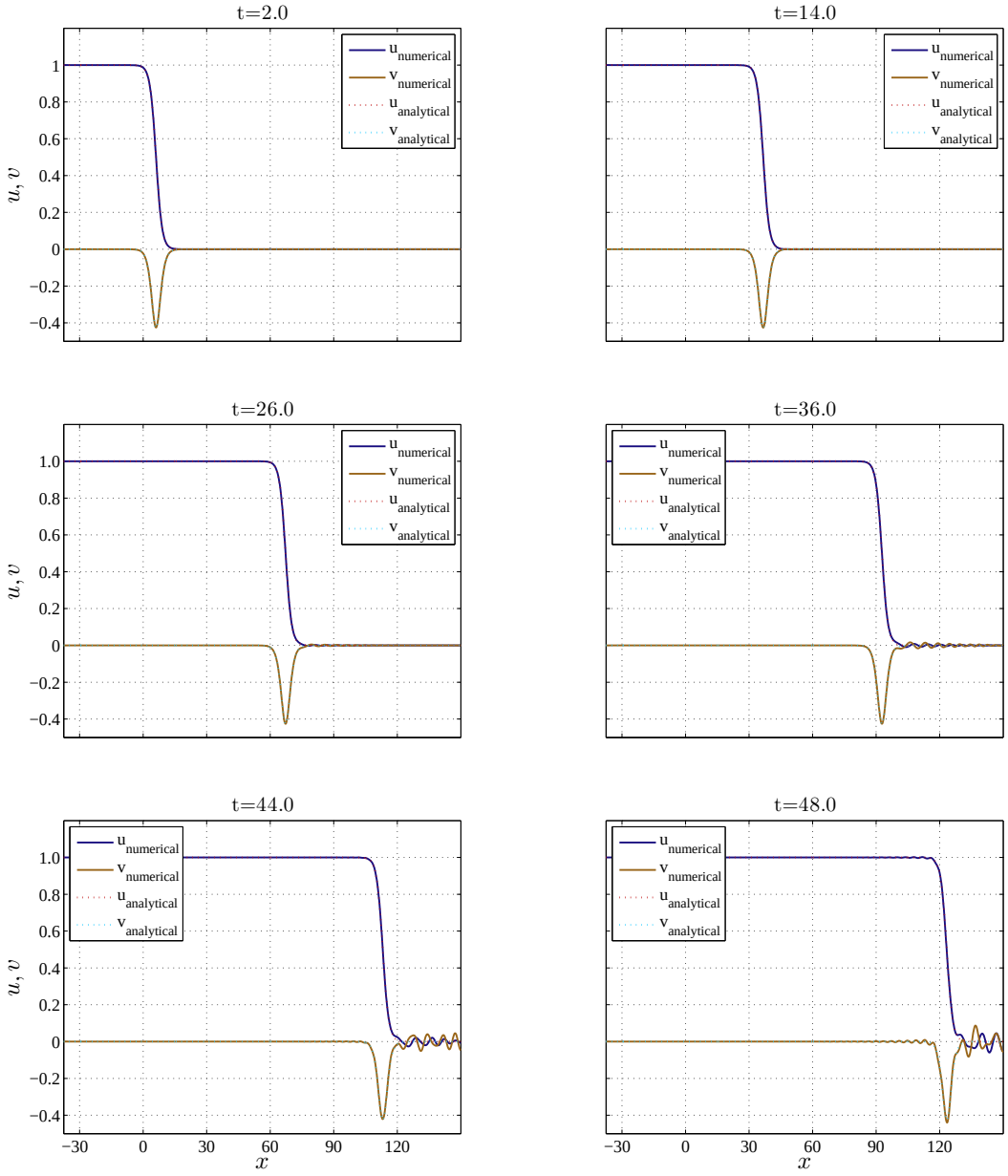

Figure 3.12: The numerical simulation of reaction cross-diffusion system with quartic polynomial where there are **double roots** and the resting states are simple roots. The values of parameters in this simulations are $D_v = 0.2$ and $k = 0.7$ where D_u is given in the formula (3.9).

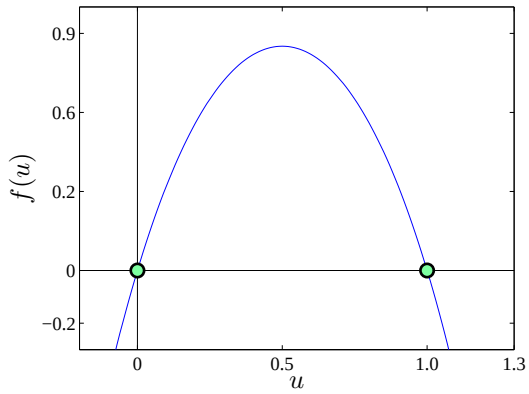

Figure 3.13: The shape of the quartic polynomial with two complex conjugate roots. In this case there are two equilibria $u = 0$ and $u = 1$. The values of free parameters are $k = 1, D_u = 0.4$ and $D_v = 1.5$.

3.6.1 Choices of The parameters in The Complex Conjugate Roots Case

The choices of given parameters that give complex conjugate roots of the quartic polynomial is shown in (2.60). This condition is could be expressed as follows

$$\rho < -\tfrac{1}{12},$$

By substituting (3.6) into the above inequality one could obtain the condition in terms of the free parameters, that is

$$k^2 D_v - 72 D_u D_v^2 k^6 + 2 < 0.$$

The shape of the quartic polynomial in this case is shown in figure 3.13.
The face of the shape of the quartic polynomial is similar to the kinetic polynomial that is used in Fisher-KPP model. In the following section we will investigate whether the propagating front wave in this case is stable as the front wave in Fisher-KPP or not.

3.6.2 The Result of Simulation The Complex Roots Case

We used the polynomial in 3.13 in the simulation. The result is shown in figure 3.14. From this result we observe that the instability occurs earlier than all previous cases

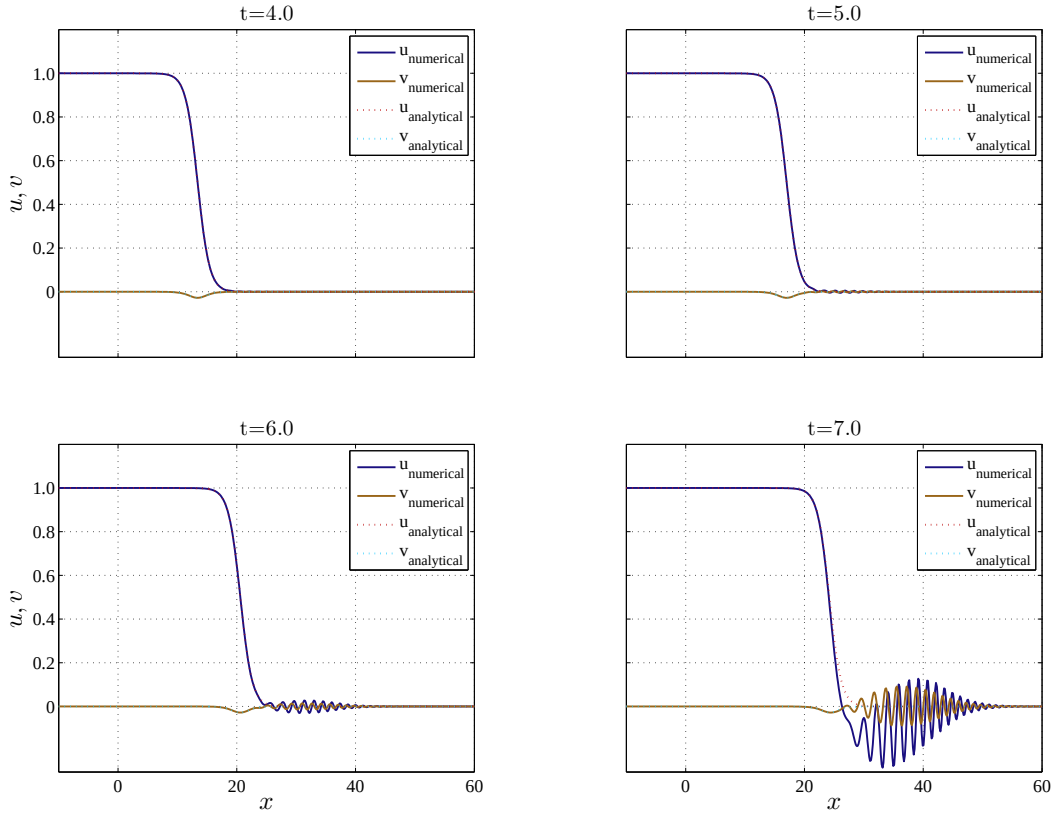

Figure 3.14: The numerical simulation of reaction cross-diffusion system with quartic polynomial where there are two **complex conjugate roots**. The values of parameters in these simulations are $D_u = 0.4, D_v = 1.5$ and $k = 1$. The instability make the numerical solution run away at $t = 8$.

(inner roots case, outer roots case and double roots case). Moreover, the numerical front does not last as long as those front waves in the other cases.

We show the simulation for other choice of free parameters in figure 3.15. Generally, there is no significant difference between the propagating front waves in figure 3.14 and those in figure 3.15. We observe only one different that the propagating front waves in 3.15 lasts longer than the propagating front waves in 3.14.

3.7 The instability of the solution

In the previous sections we have shown the results of direct numerical simulation on reaction cross-diffusion system (3.1) where the initial condition is an exact analytical

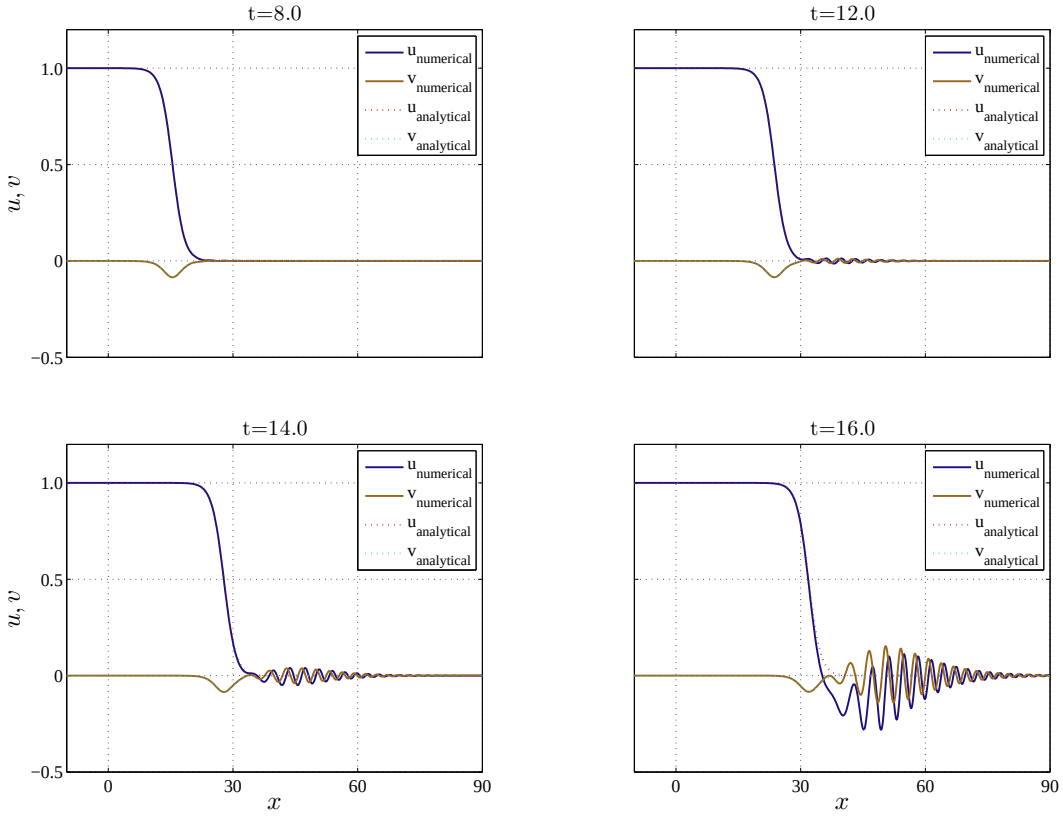

Figure 3.15: The numerical simulation of reaction cross-diffusion system with quartic polynomial with case of **complex conjugate roots** with other choice of the free parameters. The values of parameters in this simulation are $D_u = 1.0, D_v = 1.0$ and $k = 0.7$. The instability make the numerical solution run away at $t = 18$.

wave solution. This analytical solution presents a monotonic wave front.

We have considered different four cases dependent on the different positions of the roots of the quartic polynomial. There are oscillations which appear in the onset of the wave front in all those different four cases. This oscillation grows as time evolves, which obviously means the propagating wave front is not stable. This oscillation has occurred due to either dynamical instability or numerical instability.

One can tell whether the instability is numerical or dynamical describes as follows. If we have numerical instability then the oscillation could be reduced or even vanished by changing the discretisation steps. While in dynamical instability the behaviour of the solution will not be affected by refining the discretisation steps.

In order to investigate the reason behind the instability we will study the stability of

the numerical scheme that we have applied. By removing the kinetic terms from system (3.1), we obtain the following

$$\begin{aligned} u_t &= D_v v_{xx}, \\ v_t &= -D_u u_{xx}. \end{aligned} \tag{3.10}$$

We have applied fully explicit scheme in our simulation, that gives

$$\begin{aligned} u_j^{n+1} &= u_j^n + \delta_1 v_{j-1}^n - 2\delta_1 v_j^n + \delta_1 v_{j+1}^n, \\ v_j^{n+1} &= v_j^n + \delta_2 u_{j-1}^n - 2\delta_2 u_j^n + \delta_2 u_{j+1}^n, \end{aligned} \tag{3.11}$$

where

$$\delta_1 = \frac{D_v \Delta t}{\Delta x^2} \quad , \quad \delta_2 = -\frac{D_u \Delta t}{\Delta x^2}. \tag{3.12}$$

Let $\hat{u}_j^n$ and $\hat{v}_j^n$ are the errors, i.e.

$$\hat{u}_j^n = \tilde{u}_j^n - u_j^n \quad , \quad \hat{v}_j^n = \tilde{v}_j^n - v_j^n, \tag{3.13}$$

where $\tilde{u}_j^n$ and $\tilde{v}_j^n$ are the exact solution for the difference equations in the system (3.11). By using (3.13) in the system (3.11) we obtain

$$\begin{aligned} \hat{u}_j^{n+1} &= \hat{u}_j^n + \delta_1 \hat{v}_{j-1}^n - 2\delta_1 \hat{v}_j^n + \delta_1 \hat{v}_{j+1}^n, \\ \hat{v}_j^{n+1} &= \hat{v}_j^n + \delta_2 \hat{u}_{j-1}^n - 2\delta_2 \hat{u}_j^n + \delta_2 \hat{u}_{j+1}^n. \end{aligned} \tag{3.14}$$

By Fourier method we introduce

$$\hat{u}_j^n = A_1 \rho_q^n e^{iqx_j} \quad , \quad \hat{v}_j^n = A_2 \rho_q^n e^{iqx_j} \qquad \forall q \in \mathbb{R}, \tag{3.15}$$

and the scheme is stable if

$$|\rho_q| \leq 1. \tag{3.16}$$

Substituting (3.15) into (3.14) yields

$$\rho_q \underline{A} = \underline{M}\,\underline{A}, \tag{3.17}$$

where

$$\underline{A} = \begin{bmatrix} A_1 \\ A_2 \end{bmatrix} \quad , \quad \underline{M} = \begin{bmatrix} 1 & \delta_1 e^{-iq\Delta x} - 2\delta_1 + \delta_1 e^{iq\Delta x} \\ \delta_2 e^{-iq\Delta x} - 2\delta_2 + \delta_2 e^{iq\Delta x} & 1 \end{bmatrix}. \tag{3.18}$$

Note that

$$\delta_k(e^{-iq\Delta x} - 2 + e^{iq\Delta x}) = \delta_k(e^{-iq\Delta x/2} - e^{iq\Delta x/2})^2 = -4\delta_k \sin^2(\tfrac{q\Delta x}{2}), \tag{3.19}$$

where $k = \{1,2\}$. Now by computing

$$\det|\underline{M} - I\rho_q| = 0, \tag{3.20}$$

we end up with

$$|\rho| = \sqrt{1 + \tfrac{16\Delta t^2 D_u D_v}{\Delta x^4} \sin^4(\tfrac{q\Delta x}{2})}, \tag{3.21}$$

which means that the numerical scheme is unstable as the condition (3.16) will not be satisfied.

However, we have checked the growth rate that happens due to the instability of the numerical scheme. We have found the formula of time interval for the numerical solution $\left(T_{\text{inst}}\right)$ to grow from *machine epsilon* that is $u = 1 \times 10^{-15}$ to a noticeable value $u = 0.01$ due to the instability which is given as follows

$$T_{\text{inst}} = \frac{\ln\left|\frac{0.01}{1 \times 10^{-15}}\right| \Delta x^4}{8\Delta t D_u D_v}. \tag{3.22}$$

By substituting all the values of parameters that we have used in our simulation we see that, T_{inst} is very big comparing to the time when the numerical waves are broken up $\left(T_{\text{break}}\right)$. The table 3.2 clarifies more by numbers.

This big difference between T_{break} and T_{inst} indicates that the instability which happened in the simulation is dynamical instability.

In order to do further confirmation about the existence of dynamical instability in our simulation, we re-simulate the results once with smaller discretisation steps and once with bigger discetisation steps. We have found that the behaviour of the solution does not change even after we refine the discretisation. In other words, once the oscillations appear, we have found the growth rate of the oscillation is the same in all different discretisation steps. For example, in outer roots case we see that the rate of growth is not affected by refining the discretisation steps, see figure 3.16.

case	T_{inst}	T_{break}
Inner roots	3788.5	30
Inner roots	315.7	70
Outer roots	6765.1	112
Outer roots	11950	46
Double roots	1626.6	52
Double roots	3099.7	48
Complex roots	789.26	7
Complex roots	473.55	16

Table 3.2: Comparison between the time when the numerical solution is run away $\left(T_{\text{break}}\right)$ and the time interval when the solution grow from $u = 1 \times 10^{-15}$ to $u = 0.01$ $\left(T_{\text{inst}}\right)$.

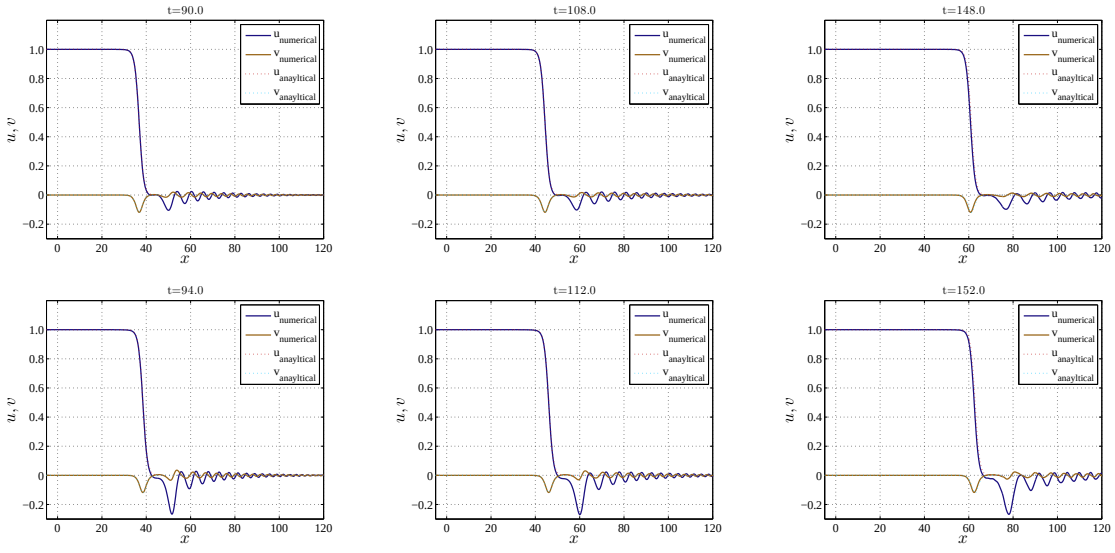

(a) (b) (c)

Figure 3.16: The dynamical instability appears for **outer roots case**. The behaviour of the solution does not change even after the steps are refined. The values of parameters are $k = 1, D_u = 0.2$ and $D_v = 0.35$. The discretisation is (a) $(\Delta x = 0.25, \Delta t = 4 \times 10^{-5})$, (b) $(\Delta x = 0.15, \Delta t = 4 \times 10^{-6})$; (c) $(\Delta x = 0.05, \Delta t = 1 \times 10^{-7})$.

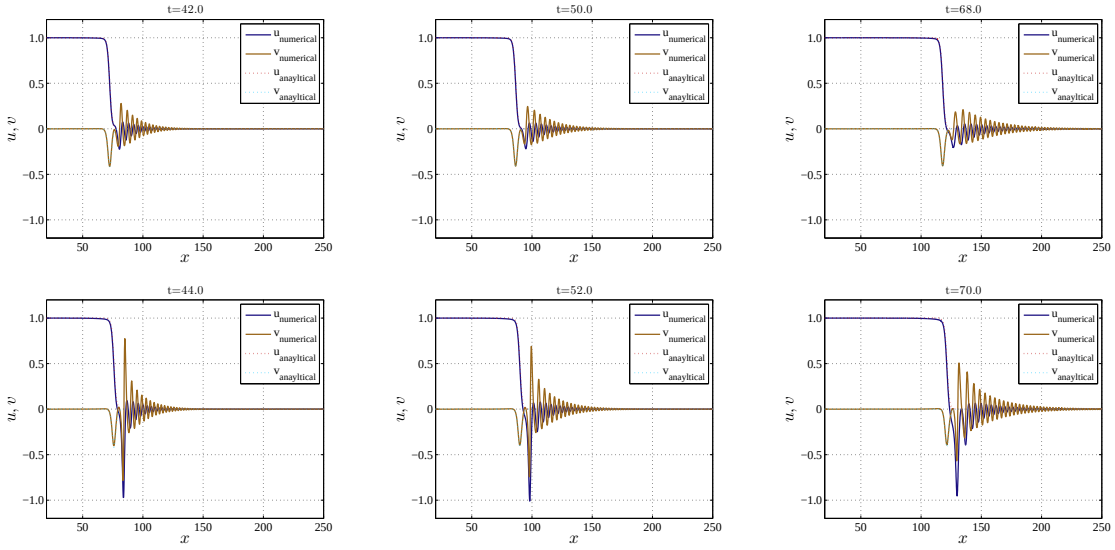

(a) (b) (c)

Figure 3.17: The dynamical instability appears for **double roots case**. Each column represents the front wave for different discretisation steps. The behaviour of the solution does not change even if the steps are refined. The values of parameters are $k = 1$ and $D_v = 0.1$. The discretisation is (a) $(\Delta x = 0.25, \Delta t = 4 \times 10^{-5})$, (b) $(\Delta x = 0.15, \Delta t = 4 \times 10^{-6})$; (c) $(\Delta x = 0.05, \Delta t = 1 \times 10^{-7})$.

The same thing happened in double roots case and complex roots case. Different size of discretisation steps affects the time of the appearance of the instability. But then the rates of growth of the oscillation are similar for all different discretisation steps, see figures (3.17), (3.18).

For the inner roots case, we have seen in the numerical simulation the invasion of unstable state into stable state as we have unstable post-front and stable pre-front, that led to different behaviour which did not appear in other cases. In inner roots case the instability appears, at first, as change in the level of u of the post-front of the wave. So, to study the instability in this case we compare the growth rate of the change of the level of the post-front with different discretisation steps. The result is shown in figure 3.19. In this case we have seen that the time of the birth of instability is different due to different discretisation steps. But then the growth rate of the change of the level of the post-front is similar even after refining the discretisation steps. As time evolves, a bounded plateau appears and back for the propagating wave is formed. By focusing on the front wave of these waves we see that the discretisation does not affect the behaviour

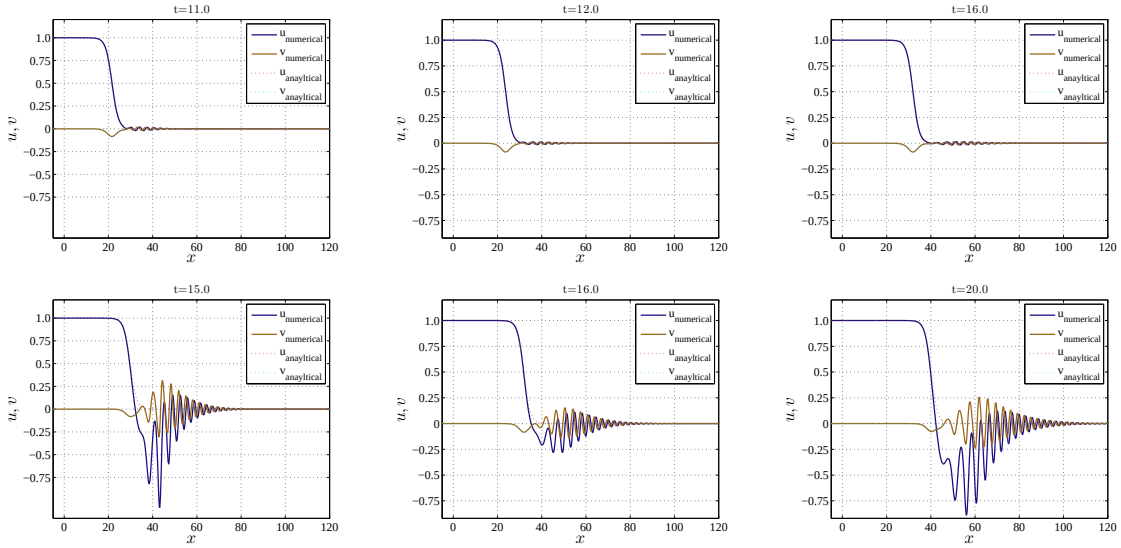

(a) (b) (c)

Figure 3.18: The dynamical instability appears for **complex roots case**. Each column represents the front wave for different discretisation steps. The behaviour of the solution does not change even if the steps are refined. The values of parameters are $k = 1$, $D_u = 1.25$ and $D_v = 0.1$. The discretisation is (a) $(\Delta x = 0.25, \Delta t = 4 \times 10^{-5})$, (b) $(\Delta x = 0.15, \Delta t = 4 \times 10^{-6})$; (c) $(\Delta x = 0.05, \Delta t = 1 \times 10^{-7})$.

of propagating front. This is proving that the system is dynamically unstable.

Our results are comparable to propagating wave in Fisher-KPP as follows. In Fisher-KPP model, if $c < 2$, then there is no stable propagating wave front. The proof could be found in [38]. At the same time, when $c < 2$, the eigenvalues of equilibria are not located on the real axis.

In our results, for outer roots and double roots cases we have found that, our choices of the free parameters in the simulations yielded that equilibria $u = 0$ and $u = 1$ are spiral source and spiral sink, i.e. the eigenvalues have no zero imaginary parts. This can be concluded by substituting the values of the parameters, that we have chosen, into (3.4) and (3.5).

However, depending on the analytical analysis of the stability of stationary solution as shown in section 1.7, what we have obtained is an indication of the spectrum of linear operator $\mathscr{L}$ of the system (3.1) with the values of parameters that we have applied in the numerical simulation has at least one element with positive real part, where $\mathscr{L}$ is

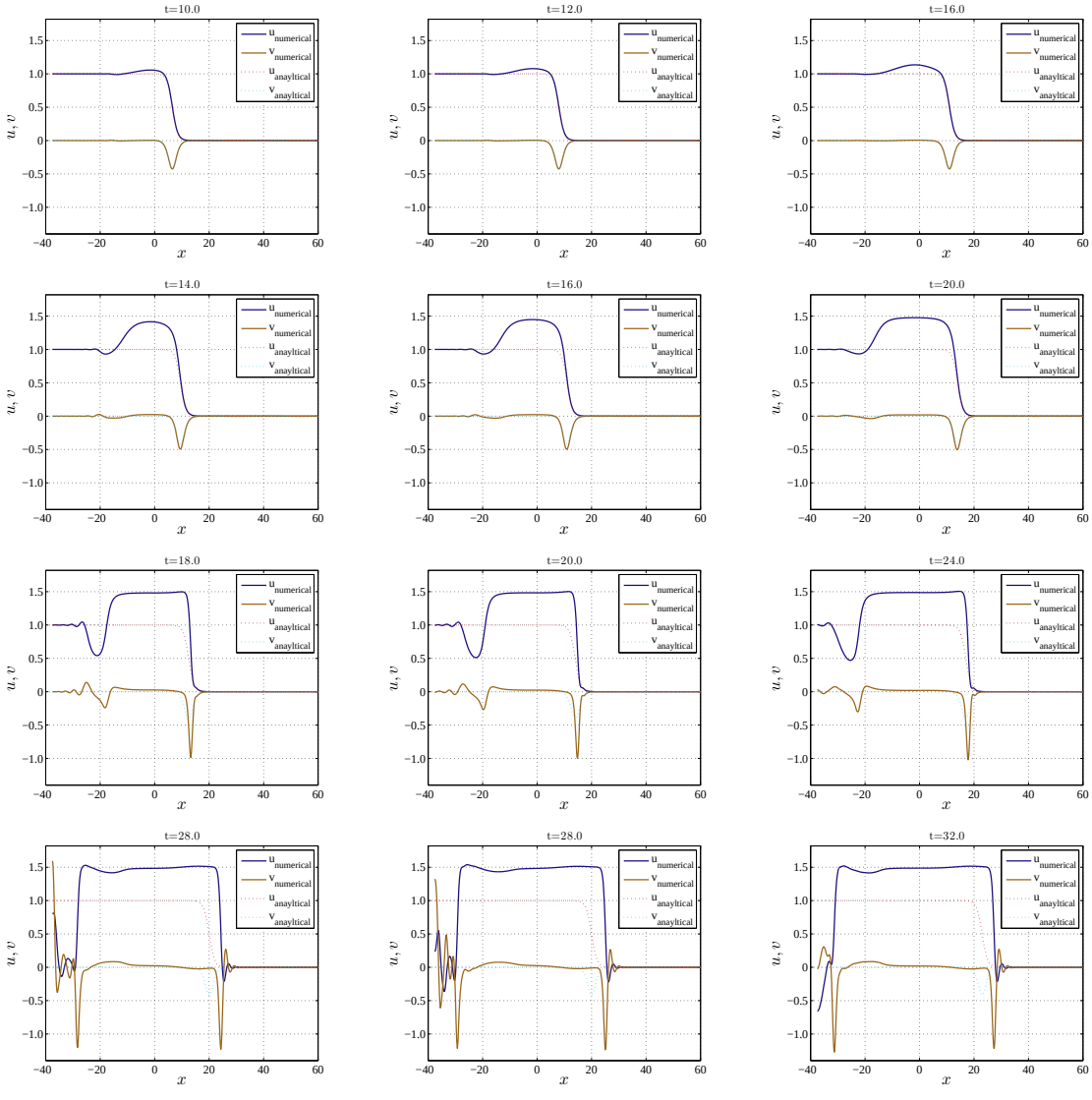

Figure 3.19: The dynamical instability appears for **inner roots case**. Each column represents the front wave for different discretisation steps. The behaviour of the solution does not change even the steps are refined. The values of parameters are $k = 1$, $D_u = 1.25$ and $D_v = 0.1$. The discretisation is **(a)** $(\Delta x = 0.25, \Delta t = 4 \times 10^{-5})$, **(b)** $(\Delta x = 0.15, \Delta t = 4 \times 10^{-6})$; **(c)** $(\Delta x = 0.05, \Delta t = 1 \times 10^{-7})$.

the linear operator of the system around the stationary solution.

3.8 Chapter Summary

In this chapter we have provided the direct numerical simulation of the reaction cross-diffusion system with quartic polynomial. The initial condition that is used in all the simulation was taken from the exact analytical solution while the boundary condition is Neumann boundary condition.

As we have seen in chapter 2, we have four different cases to simulate; inner roots case, outer roots case, double roots case and complex roots case. We simulated each case two times with two different choices of parameters.

According to the stability of the resting states of the wave front, we have shown that outer roots, double roots and complex roots cases present the invasion of stable state into unstable state, which are a feature of Fisher-KPP front wave. The numerical simulation of all these three cases have similar behaviour. This behaviour is that the numerical front wave is propagating close to the analytical front wave for a period of time. Then an oscillation appears in the onset of the front. This oscillation grows as time evolves leading to breaking up of the numerical solution.

In the inner roots case, we have shown that usually there is an invasion of unstable state into stable state. The post-front in inner roots case is attracted by one of two distinct stable equilibria. We have shown the case when the post front is attracted by only one of the stable equilibrium. For another choices of the free parameters we have shown the case when the post-front is attracted by two stable equilibria, first it is attracted by the stable equilibrium $u = 1.5$ and later the post-front is attracted by the stable equilibrium $u = 0$. So, in this case we see a finite length plateau has formed.

However, the front propagating in all cases are subjected to dynamical instability. This fact was demonstrated by direct numerical simulation, that is, we have simulated each case with three different discretisation steps. In this proof we have shown that in all cases the growth rate of the appearance of the instability is not affected by refining

the discretisation steps.

As presented in section 1.7, the dynamical instability could be analysed aiming to find the regions of parameters that give stable propagating wave solution. We have not provided this analysis in this work. In any case, the inner roots case does not present stable propagating front as the resting state of the post-front is unstable.

CHAPTER 4

CONTINUATION OF CROSS REACTION DIFFUSION SYSTEM WITH FITZHUGH-NAGUMO-TYPE NONLINEARITY

4.1 Introduction

Previously in chapter 2 we focused on the front wave which is resulting from a modified reaction cross-diffusion system with FHN model. Those modifications are as follows: replacing cubic FHN function with a general N-shaped function and considering fronts rather than pulses by letting the linear kinetic term of the second component approach zero. The reason behind these modifications is to simplify the original problem to make it analytically solvable. In this section we will consider the original problem, which is reaction cross-diffusion system with cubic kinetics

$$\begin{aligned} u_t &= f(u,v) + D_{uv} v_{xx}\,, \\ v_t &= g(u,v) - D_{vu} u_{xx}\,, \end{aligned} \tag{4.1}$$

where

$$f(u,v) = u(u-a)(1-u) - k_1 v \quad , \quad g(u,v) = \epsilon u\,. \tag{4.2}$$

So, in this section we will deal with a system which has no analytical solution known yet.

This system has been analysed by direct numerical simulation with Neumann boundary-initial value problem [55]. Here in this section we will consider a periodic boundary value problem of the system (4.1).

After computing periodic travelling wave PTW we will proceed to compare our results with other stable solitary pulse, which is obtained by direct numerical simulation [55]. This could be done by increasing the period of PTW. For a large period, PTW will have the appearance of the solitary pulse.

Also, after we consider the stability of the PTWs, we analyse some bifurcation in the system. All these elements, depend on varying the parameters in the system and study the qualitative change of the behaviour of the system. Due to the absence of the analytical solution, we will use numerical continuation software. The software that is used in this work is AUTO-07P [17].

The sections in this chapter are arranged as follows. Before entering to periodic boundary problem and applying the continuation method we will show in the first section some properties of the cross-diffusion system with FHN kinetics. In this section we will compute the speed of the stable solitary wave and show the types of the propagating waves in the system. Also, we will determine the speed of the propagating pulses and the eigenvalues of the equilibrium. In the second section we will describe the system that we will study by continuation. In this section we will present the steps that are followed in the continuation as well as the resulting PTWs with large period. In the third section we will compare one of the PTWs to the stable solitary pulse which is found in [55]. The fourth section is dedicated to the proof of stability of the propagating pulses that will be done by direct numerical simulation. In the fifth section we will show the continuation in the parametric plane (a, c) as well as the corresponding pulses profiles. In the last section we will give a brief summary of the work in this chapter.

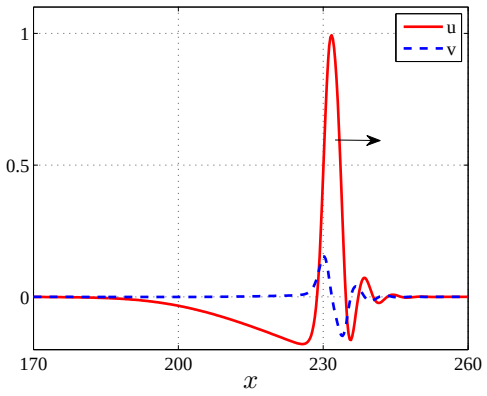

Figure 4.1: The profile of the stable propagating pulse in (4.1) with FHN cubic nonlinearity in (4.2) . The values of parameters are shown in (4.3).

4.2 Features of the System

Before proceeding to the numerical continuation, we will show some features of the solutions of the system (4.1). We will start with the stable propagating waves that is found by Tsyganov and Biktashev [55] using finite difference method. The values of parameters that yield the stable propagating pulse are, e.g.

$$D_{uv} = D_{vu} = 1 \quad , \quad k_1 = 10 \quad , \quad \epsilon = 0.01 \quad , \quad a = 0.22 \,. \tag{4.3}$$

The profile of this stable pulse is shown in figure 4.1. In the following section we will pass through the features of the system.

4.2.1 The Speed of Stable Propagating Pulse

The first feature that will be investigated is the speed of the stable propagating wave that has been found in [55]. We will compute this speed via continuation of PTW, for comparison. As we mentioned formerly, PTW with large period has the solitary wave's appearance.

In fact, the speed of the stable pulse with values of parameters that equal to (4.3) is presented in [55] in a figure, which do not enable us to know the speed with good precision. Thus, we will recompute the speed of this stable propagating pulse aiming to find good approximation to it.

The way of computing the speed of this stable wave is summarised as follows, first we re-simulate the problem in [55] using exactly the numerical method and the initial and boundary conditions that have been used in that paper. Then we specify a value, say u^*, on the propagating wave pulse of u-component. The choice of the value u^* should be above the oscillation front of the propagating pulse. Also, u^* should not be equal to the maximum point of u-component because the maximum point of the numerical simulated pulse may not be located exactly on the summit of the pulse due to the discretisation. Thus, in our computation we choose $u^* = 0.5$. This value $u^* = 0.5$ might happen in both the front and back of the pulse or due to the discretisation there is no such value u^* equals exactly 0.5. We focus on the front of the pulses and if there is no value $u^* = 0.5$ we then take the nearest two points that surrounded u^*. Then we apply linear interpolation in order to get a better approximation to the position of the point with $u = u^*$.

Of course, the recording of position and time will not be carried out until the pulse has fixed shape and speed. Meaning that, as we know the propagating wave requires a period of time to evolve to its fixed shape and constant speed, see figure 4.2.

Having specified u^* and waited until the pulse takes its fixed shape, we then record the position, say x^* that corresponds to point u^* , i.e. (x^*, u^*) for a period of time. With this recording of time and position we easily compute the speed. To get better approximation of the speed, we fit what we have recorded by linear least square method to the model

$$x^* = ct + \beta,$$

where x^* corresponds to the position and t corresponds to time. Obviously dx/dt gives the value of the speed. This recording of time and position and the linear fitting is shown in figure 4.3.

We have found that the speed of the stable propagating pulse that is found in [55] is

$$c = 3.3255 \tag{4.4}$$

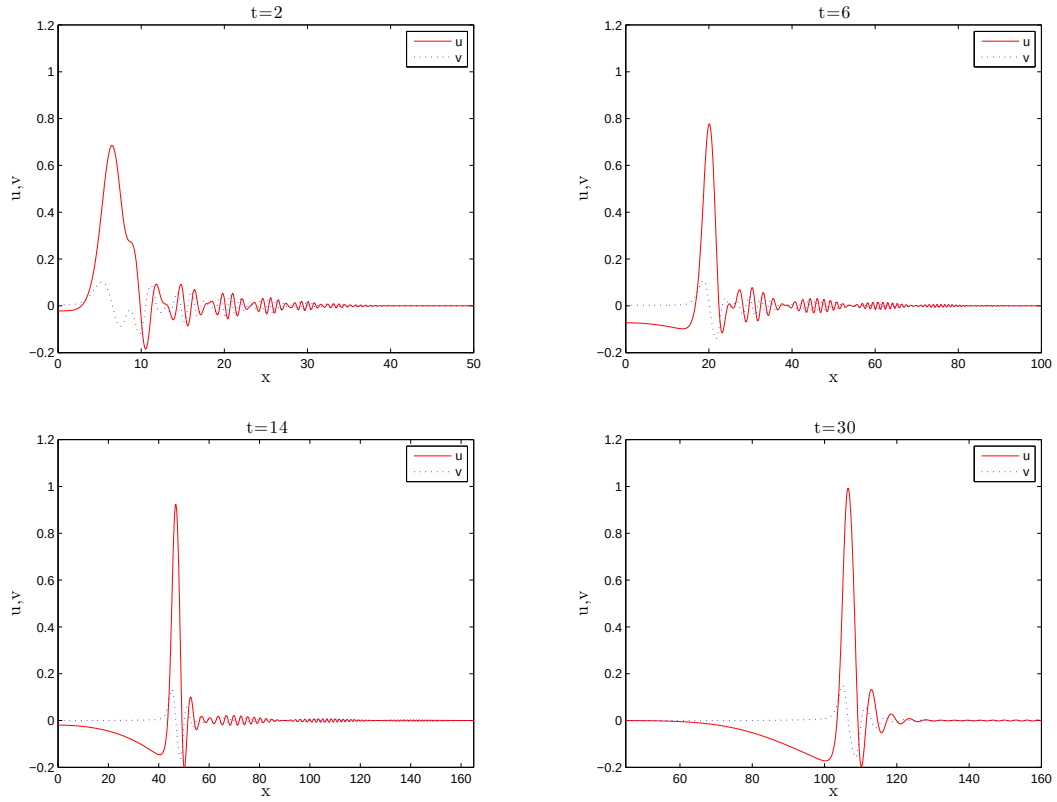

Figure 4.2: Direct numuerical simulation of system (4.1) where the values of parameters are given in (4.3). The initial condition is Heaviside step function while the boundary condition is Neumann boundary condition. At the beginning of the simulation the profile has no fixed shape. The computation of the speed started at $t = 30$ when the pulse takes its fixed shape.

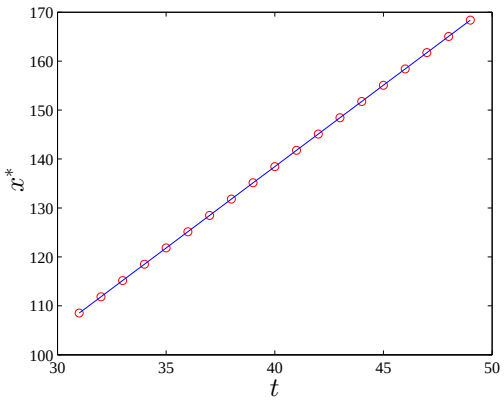

Figure 4.3: Recording of position of x^* versus time. The red circles represent the points (x^*, t^*), where x^* is the recorded position of u^* at time t^*. The blue line is the linear fit produced by least square method.

4.2.2 Types of Propagating Waves in The System

The propagating pulse of the reaction cross-diffusion system with FHN (4.1) takes different behaviours depending on the values of parameters. The propagating pulse has been studied for some ranges of parameters a and ϵ in [55], from where we summed some of those behaviours as follows;

- (SFR) single fixed shape reflecting, that represents stable propagating pulse.
- (SER) single envelope reflecting, that represents a wave that has no fixed shape. So, (SER) represents unstable propagating pulse.
- (SIR) the values of parameters a and ϵ are coming between those values which correspond to SFR and SER.

There are other behaviours provided in [55] such as multi-envelope propagating pulses. However, we neglect those behaviours as we will not consider them in our analysis in this chapter.

4.2.3 Linearisation about the equilibrium

Linearising a nonlinear system about the equilibrium is a useful step that is deepening our realisation about how the type of equilibrium effects the solution of the system. For instance, we could see the relation between the eigenvalues and the different types of propagating waves in the system. Here we linearise the stationary solution system (4.1) about the equilibrium. So, first we introduce the wave variable

$$\eta = x - ct \tag{4.5}$$

on the system (4.1) then we get the following

$$\begin{aligned} f(u,v) + D_{uv} v_{\eta\eta} + c u_\eta = 0\,, \\ g(u,v) - D_{vu} u_{\eta\eta} + c v_\eta = 0\,, \end{aligned} \tag{4.6}$$

To linearise the nonlinear terms about the equilibrium (u_0, v_0), we introduce

$$u = \tilde{u} + u_0 \quad , \quad v = \tilde{v} + v_0 \quad \text{where } \tilde{u}, \tilde{v} \ll 1\,,$$

by which we end up with the following quartic equation

$$D_{uv}D_{vu}\,\lambda^4 + (c^2 - \epsilon D_{uv} - D_{vu}\,k_1)\lambda^2 - a\,c\,\lambda + \epsilon\,k_1 = 0\,, \tag{4.7}$$

where λ is the eigenvalue of the equilibrium (u_0, v_0).

When the values of parameters are equal to (4.3) then the characteristic polynomial (4.7) becomes

$$\lambda^4 + (c^2 - 10.01)\lambda^2 - 0.22c\lambda + 0.10 = 0\,. \tag{4.8}$$

For $c = 3.3255$, which is approximate to speed for propagating wave as presented in section 4.2.1, the roots of (4.8) are

$$\lambda_1 = 0.19\,,\ \lambda_2 = 0.39\,,\ \lambda_{3,4} = -0.294 \pm 1.11i\,, \tag{4.9}$$

that agrees with the resulted pulse as shown in figure 4.1, that is the pulse has monotonic tail and oscillatory front. The monotonic tail in the corresponding pulse wave in figure 4.1 occurs due to the positive real eigenvalues while the oscillation in the front of the pulse occurs due to the complex eigenvalues with negative real parts.

Furthermore, the positive real part of the eigenvalue corresponds to the back of the pulse as the system is triggered to make an excursion in the excitable system. While the negative real part corresponds to the front of the pulse that make the excursion end to the position where it was launched. This excursion draws a trace which we call pulse wave.

We plot the solution of (4.8) for chosen values of c (see figure 4.4(e)-(f)). The circles present the intersection between the speed of the stable propagating wave with real and imaginary parts of the eigenvalues. We see from these results the proximity of the speed of stable propagating pulse to the point where the two positive real values are merged. To investigate if the proximity is inherent property for the stable propagating waves in the system, we will consider other values of parameters a and ϵ and corresponding values of c.

Here, we only take two values of ϵ that are ($\epsilon = 0.01$) and ($\epsilon = 0.015$) where a values are taken from the interval $[0.18, 0.25]$. Those values of a and the two values of ϵ will be

substituted in (4.7) while the parameter c will be computed by AUTO for each case. The steps of continuation the parameters are shown later in section 4.3.1 but here we bring the linearisation of the system about the equilibrium earlier as we want to introduce some features of the system before involving in the continuation of the parameters.

Indeed, one could examine more values but we choose those points as there are many different wave regimes appearing in this region as investigated in [55]. Also, it is costly to examine each values of a and ϵ that is considered in that bifurcation diagram.

The wave regimes for the system (4.1) are presented in parametric regions $(a,\epsilon)-$plane in [55]. So, by computing the speed for different values of a and ϵ and showing the corresponding eigenvalues, we then add some information on that bifurcation diagram.

For each value of a and ϵ we chose, two figures are plotted. One presents the positions of the real part of the eigenvalues of equilibrium versus the speed while the other one presents the position of the imaginary part of the eigenvalues of equilibrium versus the speed. Each real part and its corresponding imaginary part are plotted by the same colour. The result is shown in figures 4.4 and 4.5.

From these results we deduce that the proximity of c to the bifurcation point is a coincident not inherent property of stable propagating wave as could be deduced from 4.4(g)-(h).

To conclude, we have listed some of the features of reaction cross-diffusion system (4.1). Some of these features are found by direct numerical simulation as presented in [55]. The addition that we made is that we recomputed the speed of a stable travelling wave to get good approximation. Also, we linearised the system about the equilibrium and find the intersection between the eigenvalues and the speed. In the next section we will go further in this investigation of features of the system by applying numerical continuation with consideration of periodic boundary problems.

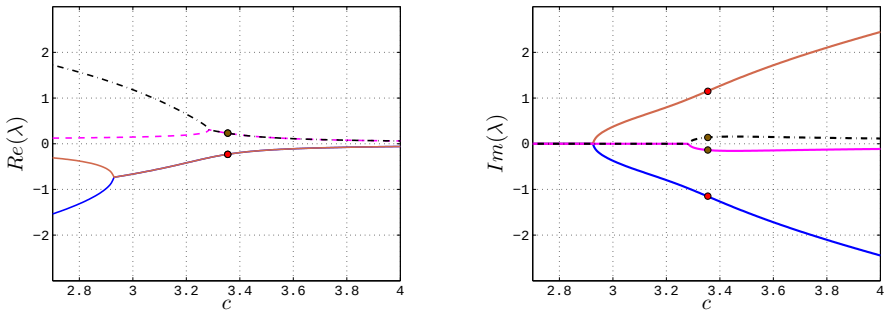

(a) $a = 0.18$ (SER)

(b) $a = 0.18$ (SER)

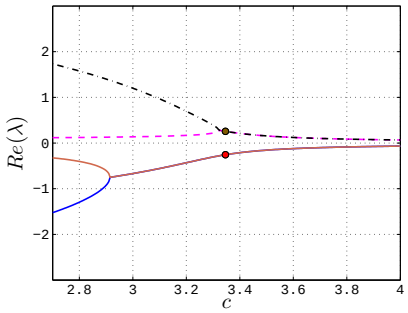

(c) $a = 0.20$ (SER)

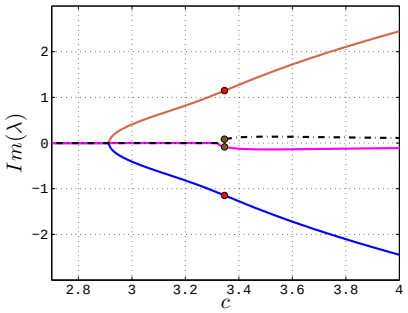

(d) $a = 0.20$ (SER)

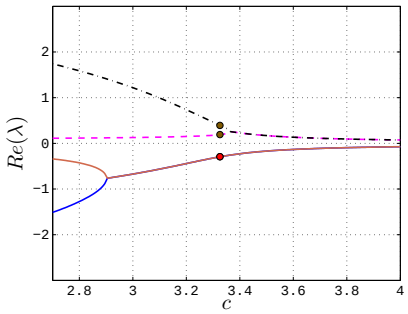

(e) $a = 0.22$ (SFR)

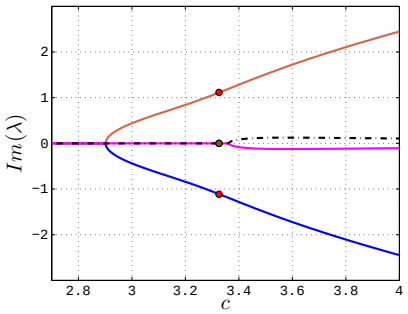

(f) $a = 0.22$ (SFR)

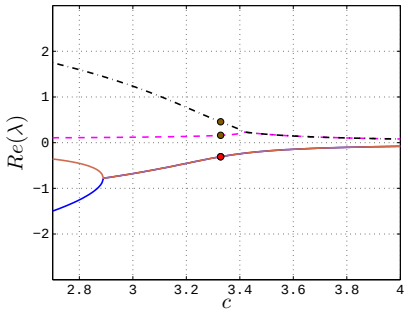

(g) $a = 0.24$ (SFR)

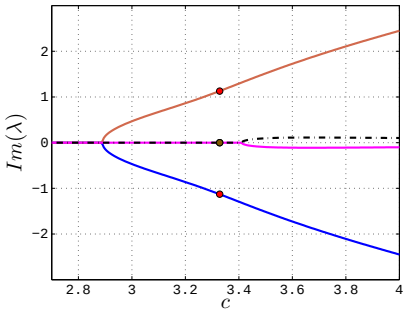

(h) $a = 0.24$ (SFR)

Figure 4.4: Bifurcation diagram shows the relation between the speed and eigenvalues for the linearisation about the equilibrium of the system (4.6) for $\epsilon = 0.01$. The circles show the eigenvalues that correspond to the speed of the propagating pulse. (SFR) stands for fixed-shape reflecting. (SER) stands for single envelope reflecting.

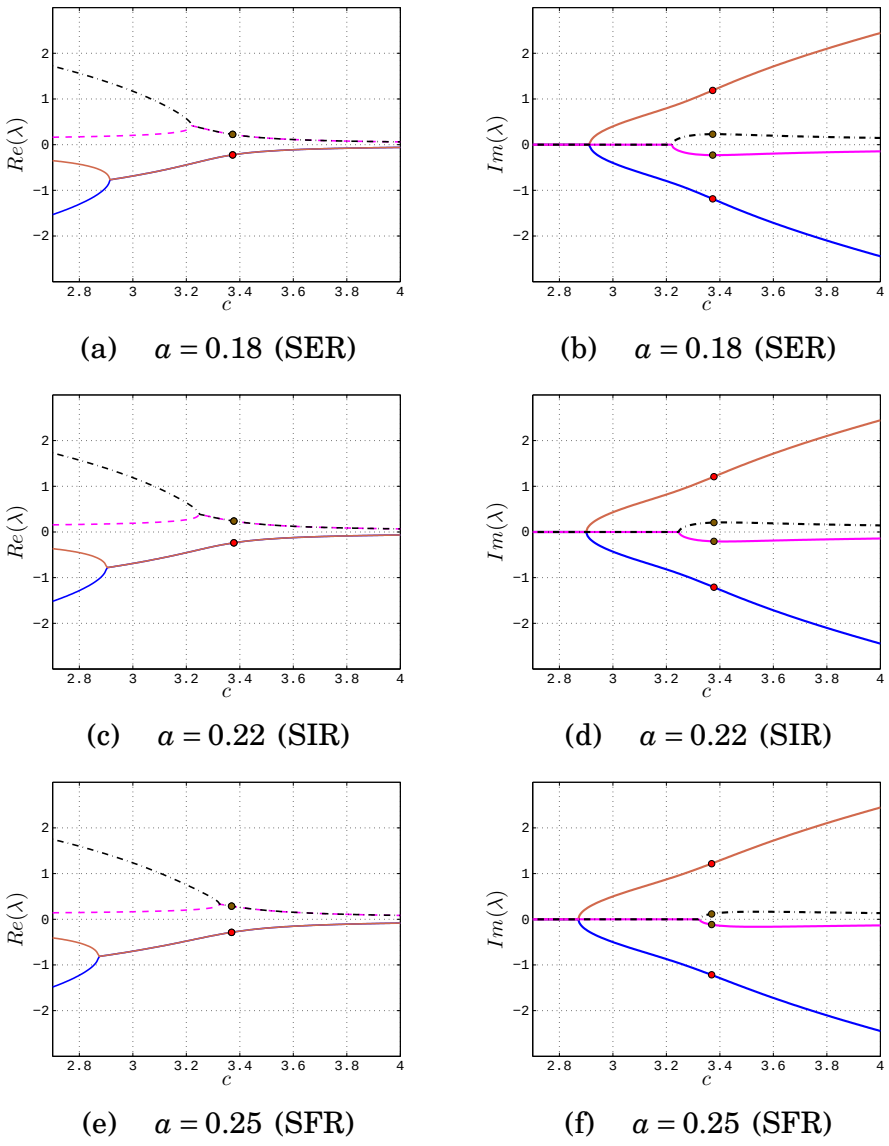

(a) $a = 0.18$ (SER) (b) $a = 0.18$ (SER)

(c) $a = 0.22$ (SIR) (d) $a = 0.22$ (SIR)

(e) $a = 0.25$ (SFR) (f) $a = 0.25$ (SFR)

Figure 4.5: Bifurcation diagram show the relation between the speed and eigenvalues for the linearisation about the equilibrium of the system (4.6) for $\epsilon = 0.015$. The circles shows the eigenvalues that correspond to the speed of the propagating pulse. (SFR) stands for fixed-shape reflecting. (SER) stands for single envelope reflecting. (SIR) ingle intermediate between SER and SFR.

4.3 Continuation The Equilibrium to Stable Pulse Wave

In this section we will find a family of PTW for the system (4.1). Moreover, we target the stable PTW that is identical to that solitary stable wave that is found in [55].

One of the similarities between PTW and travelling wave solutions is that they are function of single variable, which is called wave variable. Thus, the first step of computation PTW is applying wave variable on the reaction diffusion system. We will apply the wave variable

$$\xi = t - \frac{1}{c}x \tag{4.10}$$

on the system (4.1).

We have used wave variable in (4.10) instead of η as in (4.5) because it is more natural for AUTO. Another reason is that using wave variable η may lead to not interesting solution for large values of c. This point is described in the Appendix, Section 6.2.

Before starting the continuation we need to add parameter to the kinetic term in the activator component u as external stimuli. This parameter will be increased to move the equilibrium after that it will be decreased to zero. We have empirically observed that this external parameter can not be decreased to zero by AUTO. The reason behind this failure is beyond the scope of this study but it is worthy to be figured out. For that reason, we add the self diffusion terms to the system (4.1), such as follows

$$\begin{aligned} u_t &= f(u,v) + D_{uu}u_{xx} + D_{uv}v_{xx} \\ v_t &= g(u,v) + D_{vu}u_{xx} + D_{vv}v_{xx} \end{aligned} \tag{4.11}$$

where

$$f(u,v) = u(u-a)(1-u) - k_1 v + I_{ex} \tag{4.12}$$

$$g(u,v) = \epsilon(u - bv) \tag{4.13}$$

The continuation will be initiated on reaction *self* diffusion system and will end up with reaction *cross* diffusion system. This is conditional on success in continuing 'initial value' to 'target value' as clarified in the (initial/target) columns in the table 4.1.

Parameter	initial values	target values
c	10	
I_{ex}	0	0
a	0.13	0.22
k_1	1	10
b	2.7	0
D_{uu}	1	0
D_{vv}	0.001	0
D_{uv}	0	1
D_{vu}	0	-1
ϵ	0.003478	0.01

Table 4.1: The continuation will be started by continuing the equilibrium in (4.15) with the initial values aiming in the end of the continuation that we attained the target values. The initial value and target values columns show that we will start the continuation from the reaction self diffusion system and end with reaction cross-diffusion system. In the continuation we make D_{vu} and D_{uv} change simultaneously by setting $D_{vu} = -D_{uv}$ in the Fortran file.

The term I_{ex} is added to change this excitable system to be oscillatory system, as described in detail in [11]. Thus, some values of I_{ex} moves the equilibrium point of the system and makes it coexist with limit cycle. Also, we added a positive parameter b in order to incline the linear kinetic term. If the parameters I_{ex} and b are zero, then the kinetic terms (4.12) and (4.13) back to the original kinetic terms (4.2).

By applying the wave variable (4.10) on (4.11), the reaction diffusion system will be turned into a system of ordinary differential equations, that is

$$\begin{aligned} U_\xi &= f(U,V) + \frac{1}{c^2} D_{uu} U_{\xi\xi} + \frac{1}{c^2} D_{uv} V_{\xi\xi}\,, \\ V_\xi &= g(U,V) + \frac{1}{c^2} D_{vu} U_{\xi\xi} + \frac{1}{c^2} D_{vv} V_{\xi\xi}\,, \end{aligned} \tag{4.14}$$

where $U(\xi) = u(x,t)$ and $V(\xi) = v(x,t)$ correspond to the stationary wave solution where the periodic boundary condition we have is

$$U(\xi + P_t) = U(\xi) \quad , \quad V(\xi + P_t) = V(\xi)\,,$$

where P_t is the temporal period as the form of the wave variable is (4.10).

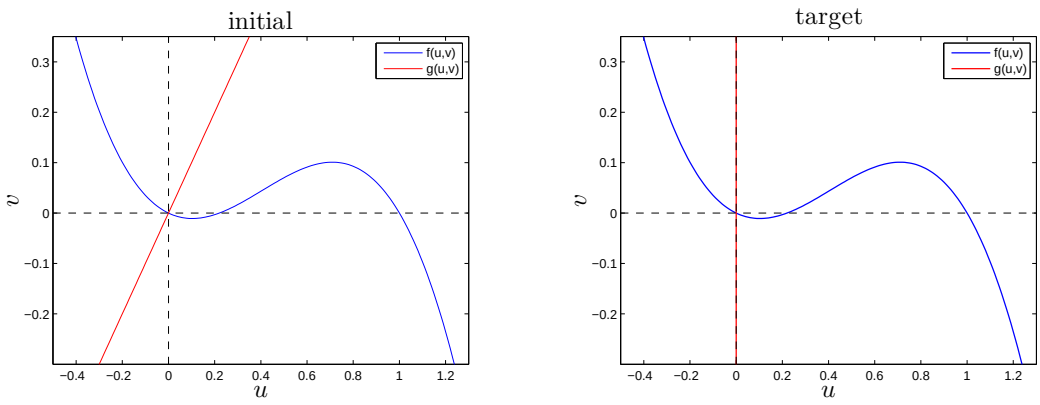

Figure 4.6: Null-clines of the reaction terms in the system (4.11) in the phase plane with initial values of the continuation (Left) and target values of the continuation (Right).

The system (4.14) cascades to the following four dimensional ODE system as follows

$$\begin{aligned} U_\xi &= W\,, \\ U_{\xi\xi} = W_\xi &= \frac{c^2}{\Delta}\{D_{vv}(W - f(U,V)) - D_{uv}(Z - g(U,V))\}\,, \\ V_\xi &= Z\,, \\ V_{\xi\xi} = Z_\xi &= \frac{c^2}{\Delta}\{D_{vu}(W - f(U,V)) - D_{uu}(Z - g(U,V))\}\,, \end{aligned} \tag{4.15}$$

where $\Delta = D_{uu}D_{vv} - D_{uv}D_{vu}$.

For each value of c we see that the equilibrium for the system (4.15) is

$$(U,V,W,Z) = (0,0,0,0)$$

Before starting the continuation we have checked the null-clines for the system for both initial and aim values. By sketching the null-clines we will know whether or not the system with 'initial value' is qualitatively different to the system with 'target value'. If it was, then it may be more difficult to pull the values of parameters from 'initial' to 'target' by continuation. As presented in the phase planes (4.6) there is only one equilibrium in both cases, which makes a promise that continuing the parameters values from 'initial value' to 'target value' will go well.

We also plot the corresponding wave profiles for initial values as it is shown in figure 4.7 while the profile of pulse that corresponds to target values is shown previously in

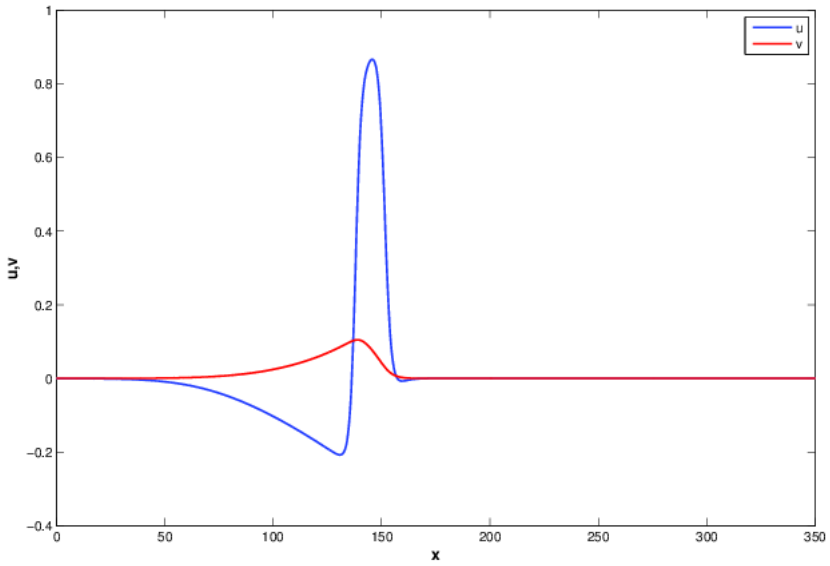

Figure 4.7: The shape of pulse for the system (4.11) with the initial values parameters. The wave is travelling to the right direction.

figure 4.1.

The parameter I_{ex} will be free when continuing the equilibrium aiming to find Hopf bifurcation point. As it is added to the cubic nonlinearity (4.12), it will shift the u nullcline vertically. As a consequence, as the parameter $b > 0$ then the intersection between null-clines of $f(u,v)$ and $g(u,v)$ see figure 4.6, which is the equilibrium, is moving and its behaviour is changing too.

The aim of this step is to grip a Hopf-point as we want to have a periodic solution through a limit cycle.

The existence of one parameter family of periodic solution for the system (4.14) is guaranteed by the theorem in Kopell and Howard [32]. The essence of that theorem is that, if the reaction terms $f(U,V), g(U,V)$ have an equilibrium with unstable focus, then the reaction diffusion system (4.14) has one parameter family of periodic solution growing from Hopf-point. Indeed, there is an unstable focus appears by $f(U,V), g(U,V)$ as explained in [22]. Obtaining PTW is a significant step in the continuation. Having successfully found PTW then we will go to the next step, that is continuing the values of parameters from initial to target values.

Step	Free Parameter(s)	Result
1. Increase I_{ex} to Hopf point	(I_{ex})	
2. Continue Hopf in $(T,c)-$ plane	(c , T)	
3. Continue I_{ex} to zero	(I_{ex} , c)	$I_{ex} = 9 \times 10^{-12}$
4. Increase T	(T , c)	$T = 1.025 \times 10^{3}$
5. Increase a	(a , c)	$a = 0.22$
6. Decrease b	(b , c)	$b = 2.4 \times 10^{-12}$
7. Increase D_{uv}	(D_{uv} , c)	$D_{uv} = 1$
8. Decrease D_{uu}	(D_{uu} , c)	$D_{uu} = 5.5 \times 10^{-10}$
9. Decrease D_{vv}	(D_{vv} , c)	$D_{vv} = -5.2 \times 10^{-8}$
10. Increase ϵ	(ϵ , c)	$\epsilon = 1.0004 \times 10^{-2}$
11. Increase k_1	(k_1 , c)	$k_1 = 10$

Table 4.2: Steps of the continuation that followed to continue the parameters from initial values to aim values. Parameter T denotes the temporal period.

The procedure of the continuation and the results are shown in the following section.

4.3.1 The Procedures of The Continuation

The steps that we have followed to continue those parameters from initial values to target values are described in the table 4.2. The first step is perturbing the equilibrium point. This step is fulfilled by increasing the parameter I_{ex}. So, for this step we free only one parameter. The result of this step is a Hopf point, giving birth of limit cycle. The resulted limit cycle has a small amplitude. Thus, we need to increase its period. To increase the period of the limit cycle, it is required to set one extra parameter to trace the limit cycle. Having found the limit cycle with reasonable period, then we can now take I_{ex} to zero. All the following steps are required two free parameters as we are continuing a limit cycle.

The order of the steps from (4-11) is based on trial and error. Furthermore, we should note that decreasing the parameters D_{uu} and D_{vv} to zero before increasing the parameter D_{uv} will lead to zero denominator as deduced from (4.15). However, we do some arrangement on the components of the results from AUTO. We will check the stability of the results from AUTO by direct numerical simulation as shown in section 4.5. In this case we will use the result as an initial condition when simulating system (4.1). The

results from AUTO is obtained from the stationary solution, that is solution to ordinary differential system depends only on one variable ξ. So, the first thing to arrange is to express the results from AUTO as a function of two variables x and t.

By AUTO we have a normalised independent variable such that $\bar{\xi} \in [0,1]$. We introduce

$$\xi = T\bar{\xi}, \qquad \xi \in [0,T], \tag{4.16}$$

where T is a temporal period that is already computed by AUTO. From (4.10) we elicit the formula of the variable x as follows

$$t - \frac{1}{c}x = T\bar{\xi} \quad \Rightarrow \quad x = -cT\bar{\xi}.$$

Now, from AUTO we obtain the following arrays

$$\Gamma = [x, u, v].$$

In our computation in AUTO we set the continuation step adaptive, so Γ contains irregular grid vectors. This is the second thing that we need to sort before applying the results from AUTO as an initial condition in the numerical simulation. To resolve this issue we need to interpolate points. Due to the oscillation that appears in the front in those pulses as seen in [55], we will apply *spline* interpolation that is provided in MATLAB. The interpolation gives the following arrays with regular grid

$$\Gamma = [\hat{x}, \hat{u}, \hat{v}]$$

The profile of the solution that is obtained by step 11 is shown in figure 4.8. We see that the PTW with large period is similar to that in figure 4.1 but with opposite direction of propagation. We will present later that the pulse wave in figure 4.8 is a stable pulse and it is identical to the solitary stable wave that is found in [55].

4.3.2 Continuation in $(T-c)-$Plane

After continuing the parameters to the target values we free the period and speed and fix all other parameters. We will compare the general behaviour of the result of this step to that in reaction self-diffusion system with FHN model.

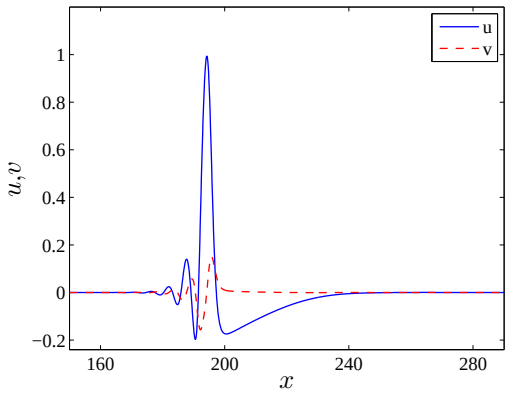

Figure 4.8: The profile of the PTW with large period (T = 1025) and the parameters are successfully continued to the target values. The wave is travelling to the left direction.

In reaction self-diffusion system with FHN model the continuation of period and speed generates another branch that forms a 'parabolic' curve in (P,c)-plane, where P denotes the spatial period. Upper branch of this 'parabolic' curve corresponds to a stable propagating pulse while lower branch corresponds to unstable propagating pulse. This fact could be found in e.g, [6] and in chapter 2 in [11].

The reaction self-diffusion system that is considered in [6] is

$$\begin{aligned} u_t &= u_{xx} + u(u-\beta)(1-u) - v\,, \\ v_t &= \gamma(\alpha u - v)\,, \end{aligned} \tag{4.17}$$

where $\gamma = 0.01$, $\alpha = 0.37$ and $\beta = 0.13$. In figure 4.9 we show the 'parabolic' curve in (P,c)-plane and corresponding stable pulse from upper branch and unstable pulse from the lower branch. The aim of this step is to investigate if this feature appears in reaction cross-diffusion system with FHN cubic nonlinearity.

To do this step we do further step after step 11, that is shown in the table 4.2, Section 4.3.1. This step is varying the parameters T and c in the continuation which is similar to step 4. By doing that, a 'parabolic' curve has been generated (see figure 4.10(a)). Each branch approaches different constant values of speed. The corresponding waves profiles are similar in the existence of oscillation front and monotonic tail. They are different in speed and the amplitude. The lower branch corresponds to slower propagating pulse wave that has a higher amplitude while the upper branch corresponds to faster

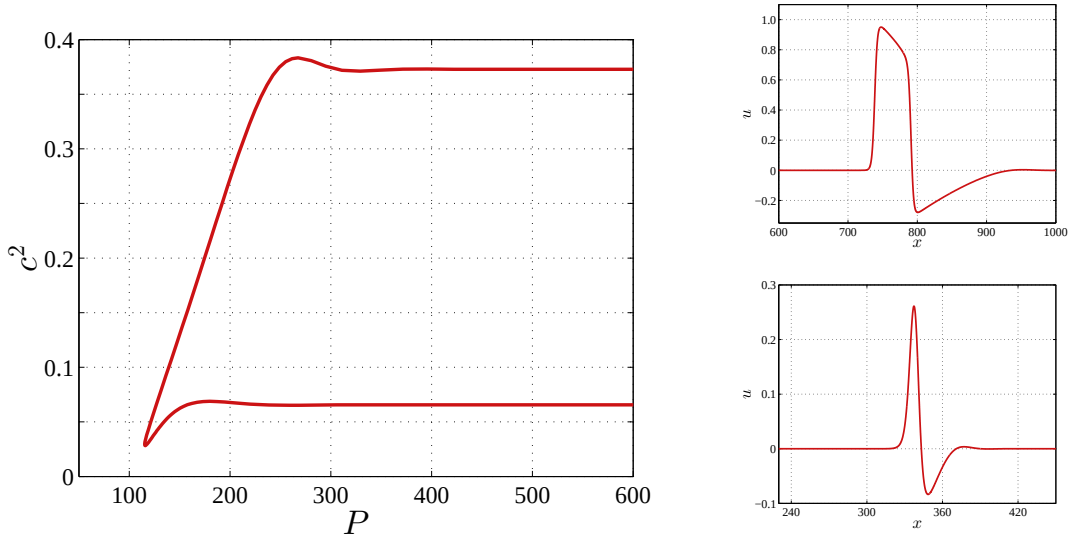

(a) (b)

Figure 4.9: (a) The 'parabolic' curve in $(P,c)-$plane in the reaction self-diffusion system (4.17). (b) Upper: is the stable pulse corresponds to the upper branch of the parabolic curve. Lower: is the unstable pulse corresponds to the lower branch of the parabolic curve

propagating pulse wave but has a lower amplitude, see figure 4.10(b).

However, the difference between the speed of the pulses in lower branch and those in upper branch in reaction cross-diffusion system is 0.036 which is very small compared that to the difference between the speed in reaction self-diffusion system which is 0.451.

The stability of the pulses in lower and upper branches in 4.10 will be investigated in the following section.

4.4 The Stability of The Pulses

We have obtained by the continuation in $(T,c)-$plane two pulses waves with different amplitudes. Those pulses, in large periods, are close to solitary pulses. This section and following section are dedicated to check the stability of those two pulses. We will check the stability by direct numerical simulation. Before that we will do comparison between the propagating waves in the lower branch and the stable solitary pulse that is found by direct numerical simulation in [55].

We will compare the profile of the pulse in the lower branch with a pulse from the

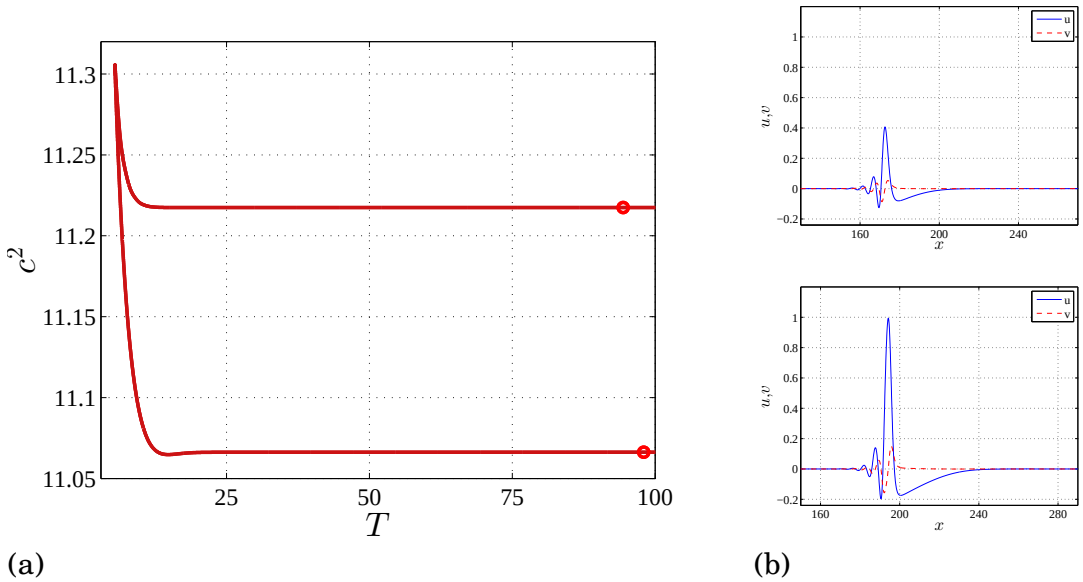

Figure 4.10: (a) The 'parabolic' curve in $(T, c)-$plane in the reaction cross-diffusion system (4.1) with the kinetic terms (4.2). (b) Upper: is the stable pulse corresponds to the upper branch of the parabolic curve. Lower: is the stable pulse corresponds to the lower branch of the parabolic curve

lower branch. Also, we will compare the speed of the stable pulse with the correspondent speed to the lower branch. If they are identical then this comparison gives an indication about the stability of PTW in the lower branch. However, this method is not applicable to be used for the upper branch as there is no stable pulse known beforehand.

Another way we will use to prove the stability of the propagating pulses is a direct numerical simulation. This way will be used to examine the stability of the pulses in the lower and upper branches too.

Firstly, we will show the results of the comparison between the pulses from the lower branch with the stable propagating pulse in [55]. Lastly we will apply a direct numerical simulation on the pulses from the lower and upper branch to check the stability of those propagating wave.

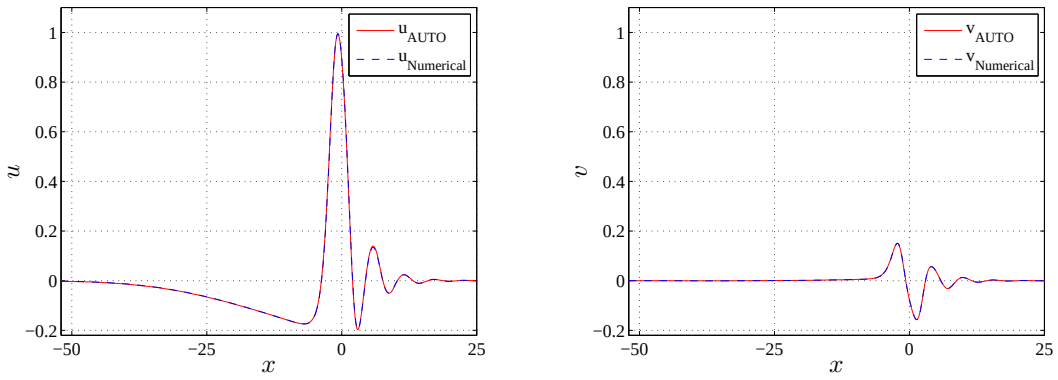

(a) (b)

Figure 4.11: Comparison of the profiles of simulated waves that is stable as shown in [55] with pulse wave that is taken from the lower branch in figure 4.10. (a): The comparison between u pulses, (b): comparison between v pulses. The waves are propagating from left to right.

4.4.1 Compare Speed and Profile of Stable Propagating Pulse with Lower Branch Pulse

Regarding the speed, we have found that the speed of the stable propagating wave is $c = 3.3255$ as shown in section 4.2.1. Also, the speed of the pulse in the lower branch is $c = 3.3266$, as computed by AUTO, see figure 4.10(a), which is very close to the speed of the stable propagating wave. This is the first evidence that the lower branch wave corresponds to the stable propagating wave.

To compare the profiles of stable propagating wave with a pulse from the lower branch we bring the pulse from the numerical simulation and that from the lower branch together to one place. Then we specify point u^*, as explained in section 4.2.1, on both the stable propagating wave and the wave pulse from the lower branch. Having specified u^* on each pulse, then we shift its corresponding points, say x^*, to make it in the position $x^* = 0$. Consequently, u^* in both profiles is pulled to be at $x = 0$. The result of this comparison is shown in figure 4.11. This figure shows the good agreement between both profiles. This is the second evidence that the lower branch corresponds to a stable pulse.

The third way to prove the stability of the pulse that corresponds to lower branch is

done by direct numerical simulation which will be discussed in the next section. Moreover, the direct numerical simulation will be the only way that we will use to investigate the stability of the pulse wave that corresponds to the upper branch.

4.5 Direct Numerical Simulation to Investigate The Stability

The stability of the propagating wave could be checked by perturbing the stationary solution and then observing the growth of the perturbation. There is analytical approach to study the stability of the propagating waves that is not in the scope of this study. However, we could investigate the stability of propagating waves by direct numerical simulation, which is less rigorous.

The direct numerical simulation will be used to investigate the stability as it was used in chapter 3 to investigate the stability of the propagating front of the reaction cross-diffusion system with quartic polynomial. So, we will solve numerically the system that is applied in this continuation work, which is (4.1) where the initial condition in this computation will be taken from (lower/upper) branch of the parabolic curve in figure 4.10. Then if the initial condition preserves its profile as the time evolves, then this is a sign of stability of the propagating wave.

4.5.1 The Scheme of the Numerical Method Used To Investigate The Stability

The reaction cross-diffusion system that we want to simulate is

$$\begin{aligned} u_t &= u(u-a)(1-u) - k_1 v + D_v v_{\hat{x}\hat{x}}\,, \\ v_t &= \epsilon(u - bv) - D_u u_{\hat{x}\hat{x}}\,, \end{aligned} \qquad 0 \le \hat{x} \le L\,. \tag{4.18}$$

where L varies according to the value of T that is computed by AUTO. The boundary condition is Neumann while the initial condition is

$$u(\hat{x},0) = \hat{u}_{1,2} \qquad , \qquad v(\hat{x},0) = \hat{v}_{1,2}\,,$$

where the profiles of $\hat{u}_{1,2}$ and $\hat{v}_{1,2}$ are shown in 4.10(b). The values of the parameters are equal to those we have obtained in the end of the continuation, that is

$$a = 0.22 \quad , \quad b = 0 \quad , \quad \epsilon = 0.01 \quad , \quad D_u = D_v = 1.0 \, .$$

The scheme that is used in this simulation is finite difference method, with operator splitting method [18]. We split each step to two sub-steps. In the first half step we apply fully explicit scheme on the kinetic terms and in the second half step we apply fully implicit scheme on the linear cross-diffusion terms, as describes in follows

$$\begin{aligned} u^{n+\frac{1}{2}} &= u^n + \Delta t u^n (u^n - a)(1 - u^n) - k_1 v^n \, , \\ v^{n+\frac{1}{2}} &= v^n + \epsilon \Delta t u^n \, , \end{aligned}$$

while the second half-step is a fully implicit step for the cross-diffusion terms, requiring solving the following linear system for u^{n+1} and v^{n+1}

$$\begin{aligned} u^{n+1} - u^{n+\frac{1}{2}} &= A v^{n+1} \, , \\ v^{n+1} - v^{n+\frac{1}{2}} &= B u^{n+1} \, , \end{aligned}$$

where

$$A = \begin{bmatrix} -2\rho & 2\rho & 0 & \cdots & \cdots & 0 \\ \rho & -2\rho & \rho & \ddots & & \vdots \\ 0 & \rho & -2\rho & \rho & \ddots & \vdots \\ \vdots & \ddots & \ddots & \ddots & \ddots & 0 \\ \vdots & \ddots & \ddots & \ddots & \ddots & \rho \\ 0 & \cdots & \cdots & \cdots & 2\rho & -2\rho \end{bmatrix} \qquad B = \begin{bmatrix} -2\gamma & 2\gamma & 0 & \cdots & \cdots & 0 \\ \gamma & -2\gamma & \gamma & \ddots & & \vdots \\ 0 & \gamma & -2\gamma & \gamma & \ddots & \vdots \\ \vdots & \ddots & \ddots & \ddots & \ddots & 0 \\ \vdots & \ddots & \ddots & \ddots & \ddots & \gamma \\ 0 & \cdots & \cdots & \cdots & 2\gamma & -2\gamma \end{bmatrix}$$

where $\left(\rho = \frac{\Delta t D_v}{\Delta x^2}\right)$ and $\left(\gamma = -\frac{\Delta t D_u}{\Delta x^2}\right)$. The discretisation steps in the simulation are $\Delta t = 5 \times 10^{-3}$ and $\Delta x = 0.1$.

The algorithm of this simulation is shown in the Appendix, Section 6.3.

The result of this simulation is shown in figure 4.12 when the initial condition is taken from the lower branch while the result when the initial condition is taken from the upper branch is shown in figure 4.13.

These results show that either initial condition gives a wave that propagates with a fixed shape. Those figures give the indication that the upper branch and lower branch

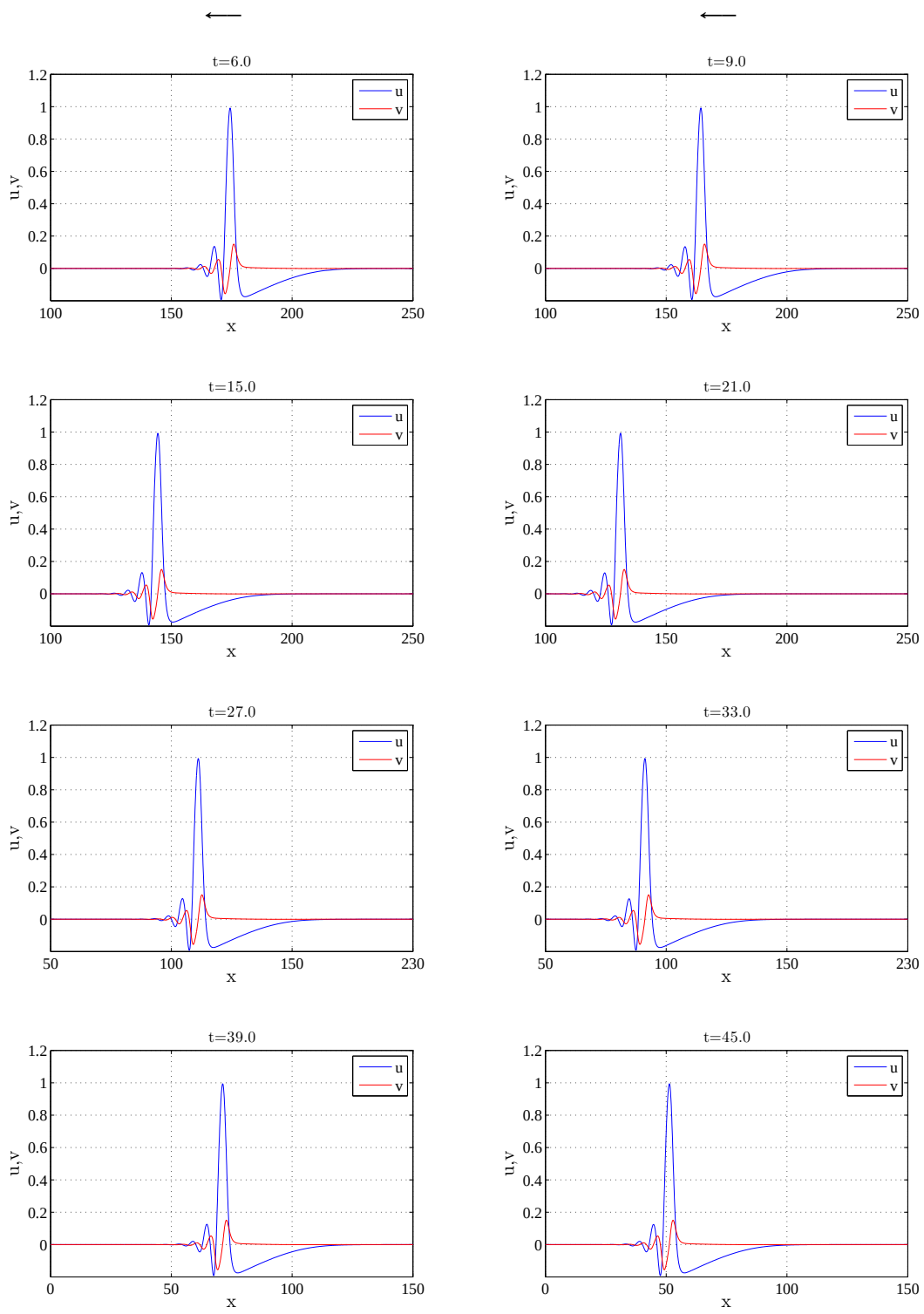

Figure 4.12: The results of FD solver for Reaction cross-diffusion system where the initial condition is taken from the lower branch in figure 4.10. The top arrows show the direction of propagation.

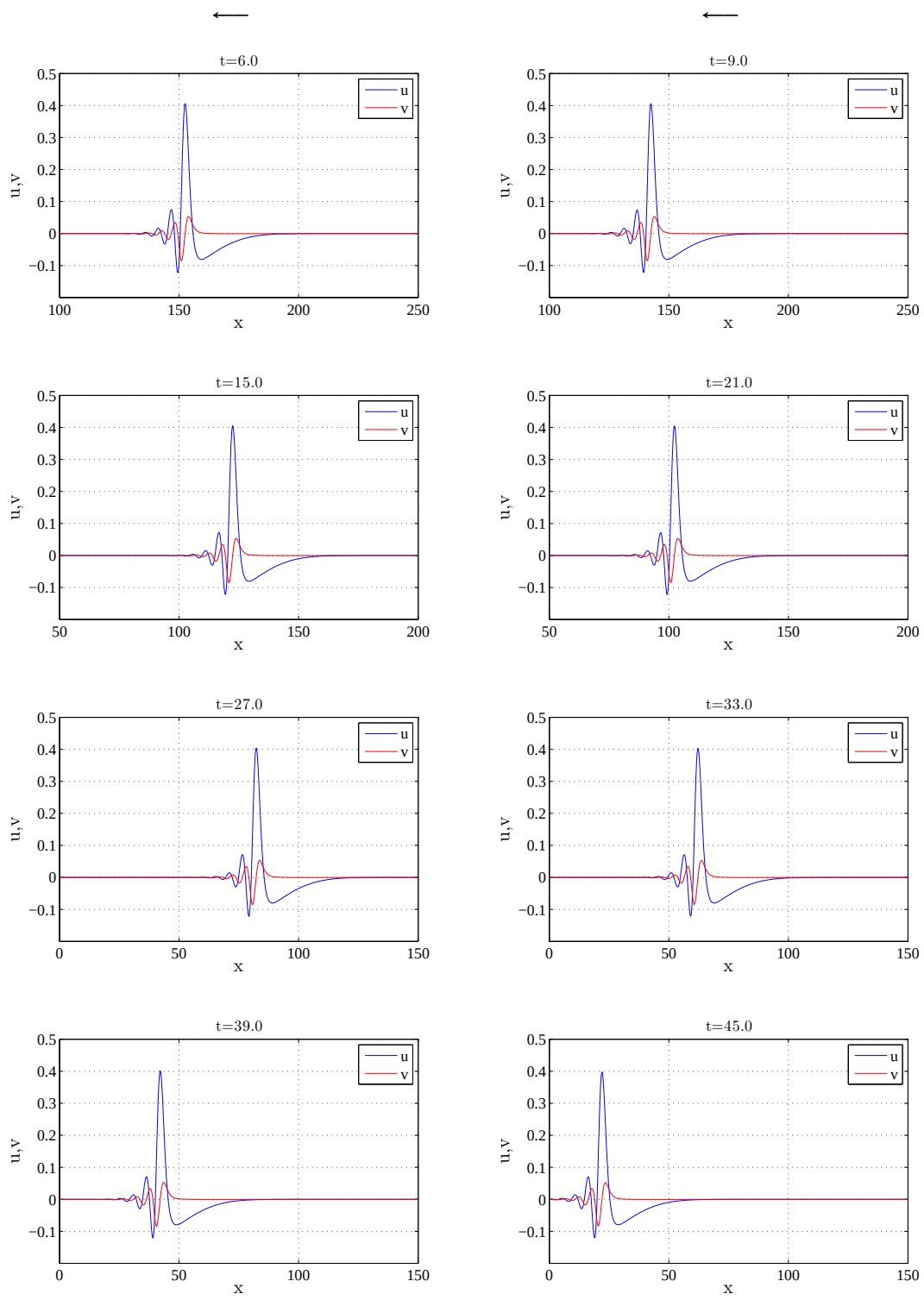

Figure 4.13: The results of FD solver for Reaction cross-diffusion system where the initial condition is taken from the upper branch in figure 4.10. The top arrows show the direction of propagation.

correspond to stable pulses. Furthermore, the lower branch is identical to the stable wave that is found in [55], that is because they are similar in the behaviour of the stability, there is no big difference between their speed and their profiles are corresponding as shown in section 4.4.1.

So, by reaction cross-diffusion system with FHN model we have 'parabolic' curve in (T,c)-plane both of its branches correspond to two different stable propagating pulses. This result is different from what is obtained in reaction self diffusion system with FHN model in that the upper branch corresponds to stable propagating pulses while the lower branch corresponds to unstable propagating pulses.

4.6 Varying Parameter a

Previously, we have shown the curve of continuation in $(T,c)-$plane, that gives a 'parabolic' curve where both branches give a stable pulse as this fact proven numerically. Those results are obtained by fixing all the parameters except T and c.

The parameter a plays a significant role in the behaviour of the propagating pulse. For smaller a the behaviour of the propagating pulse is changed from solitary to envelope or even to multi-envelope as shown in [55]. Thus, in this section we would see how far the curve in (T,c)-plane changes for various smaller values of a.

The procedure to do this step is that, we start to continue the stable pulse from the lower branch by fixing a large period. To be precise, this continuation will start from the red dot in the lower branch in figure 4.10(a).

First we decreased the values of a to the value of interest where the period is fixed and c is free. Then we fixed a and continue in $(T,c)-$plane. We have tried to do these steps starting with $a = 0.22$, then we decrease a by 0.02, such as $a = 0.20, 0.18, \cdots$. We can not reach $a = 0.10$ as we end up with 'no convergence' message that appears by AUTO, so we stopped at $a = 0.12$.
The resulting curves are shown in figure 4.14.

As a tends to zero, the shape of (T,c) curve becomes more complex. Furthermore,

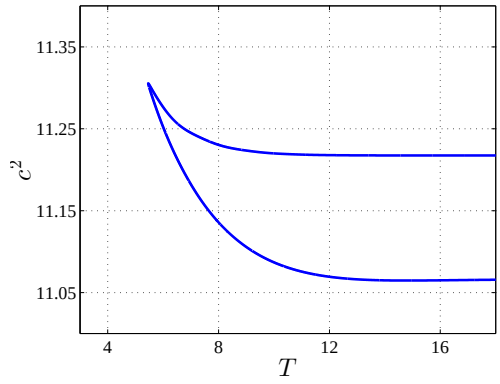

(a) $a = 0.22$

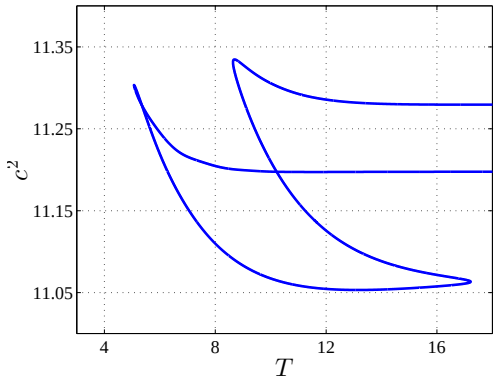

(b) $a = 0.20$

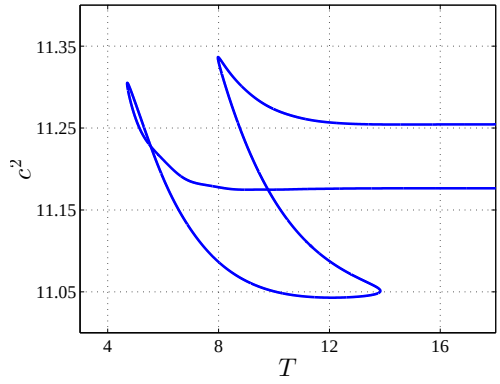

(c) $a = 0.18$

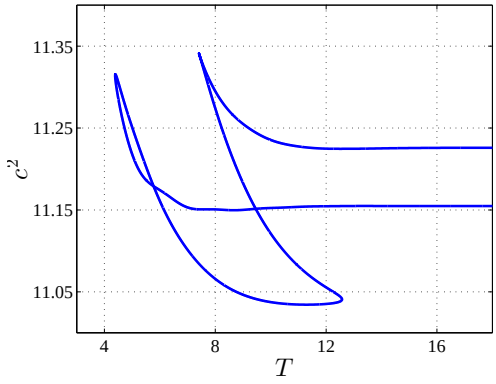

(d) $a = 0.16$

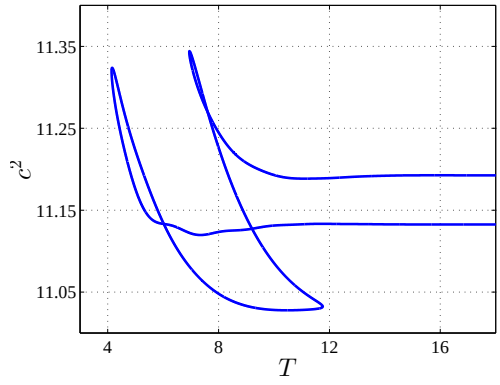

(e) $a = 0.14$

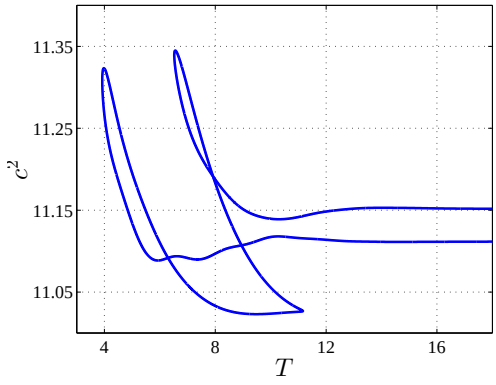

(f) $a = 0.12$

Figure 4.14: The results of continuation in $(T - c)$ plane for different values of parameter a.

the difference between the speed that corresponds to the pulses in the upper branch and those in the lower branch becomes smaller as a becomes smaller.

We discuss the difference between the curves for $a = 0.22$ and $a = 0.20$ that are shown in figure 4.14(a)-(b), respectively. We see clear different behaviour in the curve in $(T, c)-$plane. The period for the case $a = 0.22$ does not fall behind $T \approx 5.5$ while it does for $a = 0.20$ and reaches $T \approx 5$.
Moreover, the curve in $a = 0.22$ has no loop while there is a tiny loop in $a = 0.20$ appearing at the minimum value of period. However, this loop becomes bigger for smaller values of a. In general, the number of loops in the 'parabolic' curve increases as a decreases.

The profiles of pulses from the lower branch and the upper branch for each value of a are shown in figure 4.15.

The amplitude in all the pulses in figure 4.15 is less than 0.5 except the pulse which corresponds to the lower branch for $a = 0.22$. Moreover, for all different values of a the pulses that coincide to the upper branch has more oscillation than the pulses that coincide to the lower branch except for $a = 0.22$.

In [55] it is found that by direct numerical simulation, for $a = 0.12$ the propagating pulse has taken a form of envelope quasi-soliton, which is different from what we have obtained here in 4.15(f). This difference between those waves requires more investigation, which is out of the scope of this thesis.

4.6.1 Continuation in a - c Plane

As the numerical continuation shows no convergence to $a = 0.10$ in $(a, T)-$plane, we then continue in $(a, c)-$plane and fixed a large period. We aim to obtain the results of the continuation for smaller values of a. Also, we aim to see the change in the wave profiles for different values of a and c.
The start point of this continuation is the red dot in the lower branch in figure 4.10(a).

The result of this step is that the parameters a and c are bounded. In particular, in this case we can not reach $a = 0.10$. This process resulted a closed curve as shown in

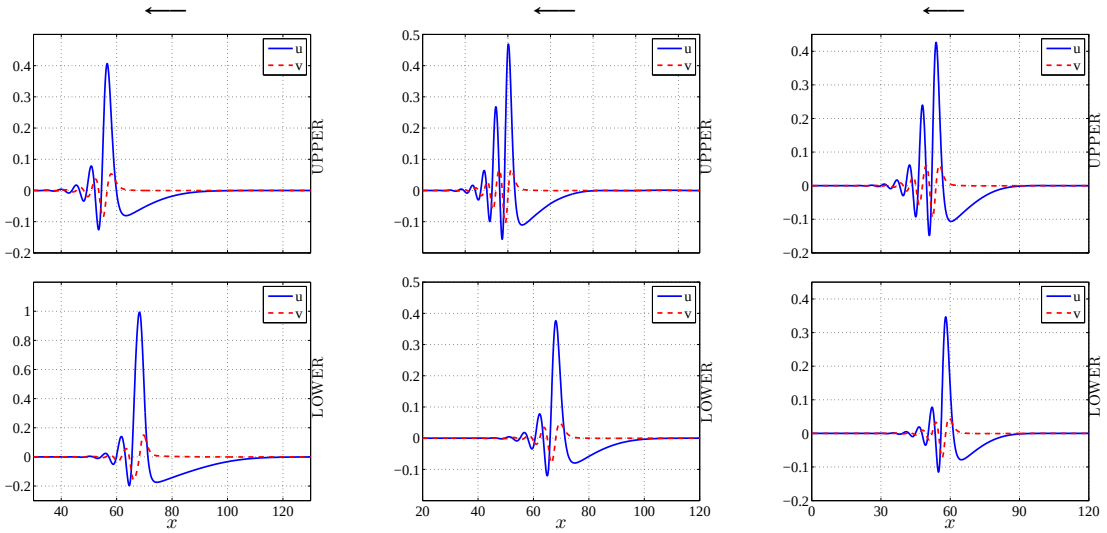

(a) $a = 0.22$ (b) $a = 0.20$ (c) $a = 0.18$

(d) $a = 0.16$ (e) $a = 0.14$ (f) $a = 0.12$

Figure 4.15: Profiles of pulses correspondent to lower and upper branch for each panel in figure 4.14.Top arrows indicate to the direction of propagation.

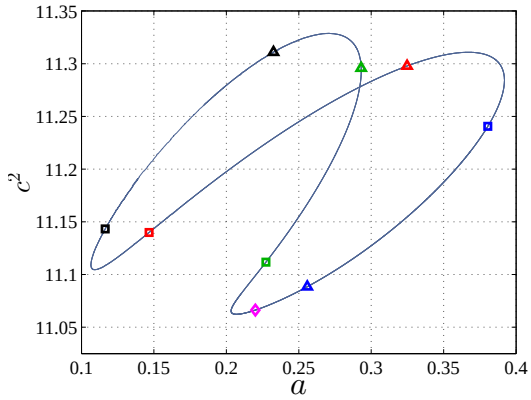

Figure 4.16: The continuation of the reaction cross-diffusion system. The starting point of the continuation is the red dot in the lower branch of parabolic curve 4.10. We fix $T = 97.9945$ and free the parameters a and c. At the initial value of the continuation the values of the free parameters are $a = 0.22$ and $c^2 = 11.0662$. The coloured dots show the positions of picked the pulses that represented in figure 4.17. The magenta diamond is the start point of the continuation.

Symbols	c^2	a
△	11.0884	0.255843
□	11.2406	0.380492
△	11.2959	0.293114
□	11.1118	0.227341
△	11.2978	0.324748
□	11.1399	0.146683
△	11.3109	0.232547
□	11.1432	0.116368

Table 4.3: The values of parameters c and a correspond to the pulses in figure 4.17.

4.16. The place of the start point in the continuation is allocated by magenta diamond, which corresponds to the stable pulse from the lower branch in the parabolic curve (see figure 4.10). A selection of the corresponding pulses are shown in figure 4.17. The corresponding values of speed and a for each pulse are presented in the table 4.3

From figure 4.16 we can see that for an interval of values of a approximately between 0.21 and 0.28, there are four propagating wave solutions, whereas figure 4.14(a) shows two distinct solutions of large periods for $a = 0.22$ which is within this interval. Thus, we conclude that mere continuation of solutions in the (T, c)-plane, or indeed any other particular continuation protocol, is not guaranteed to be fully comprehensive, and continuation in different parameters in this nonlinear problem may produce new distinct

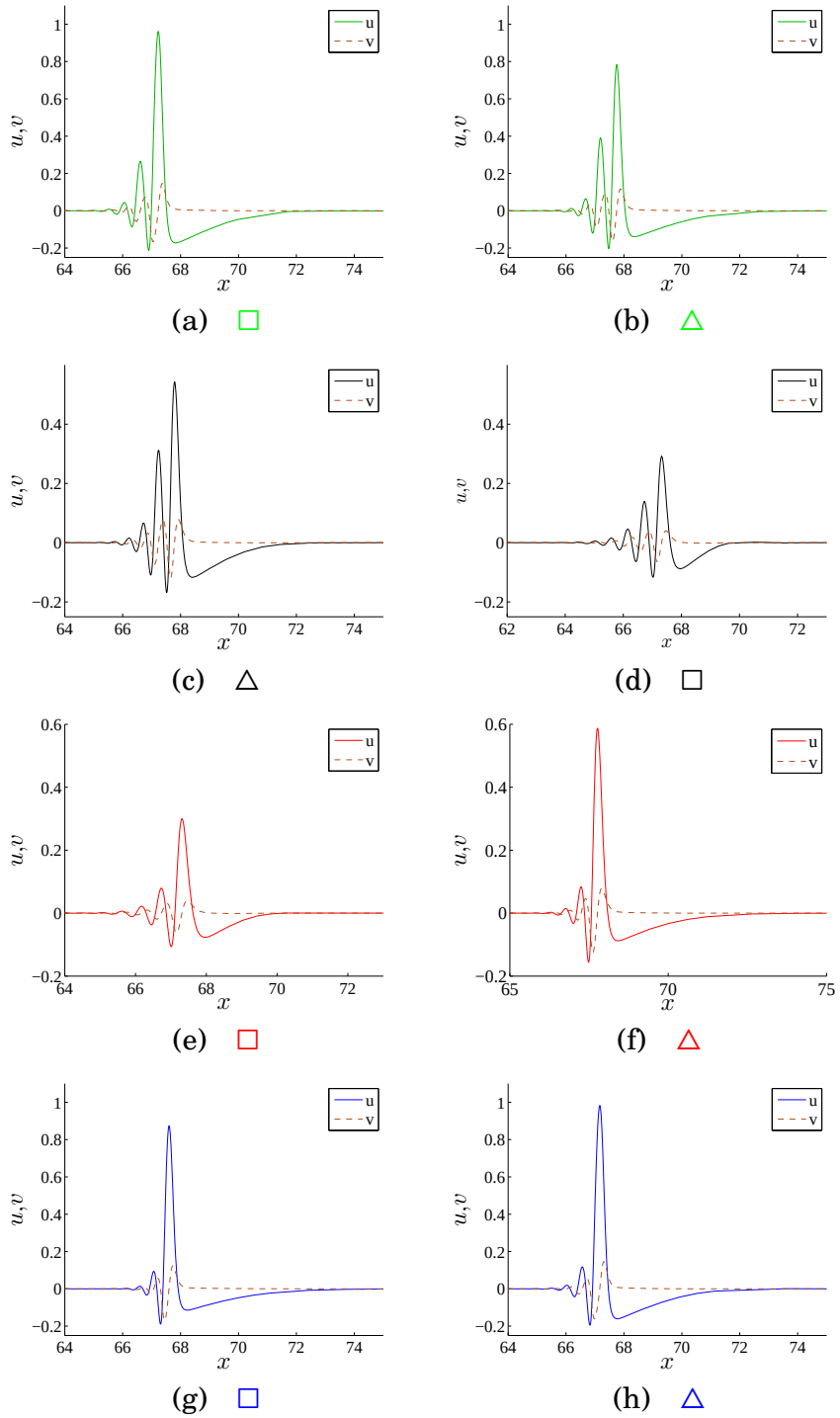

Figure 4.17: The profile of the pulses that are picked from the curve in 4.16. The profiles (a) - (h) are corresponding to the point on the caption, as shown in on the branches of 4.16. The waves are propagating from right to left.

solutions. Moreover, the problem is nonlinear, multiple solutions to the same problem ought to be expected, and it is not known how many solutions there are for any given set of parameters. One method (e.g. direct numerical simulations, [55]) produces one solution, another method (continuation in the (T, c)-plane) produces two solutions, and a third method (continuation in the $((a, c)$-plane)) produces four solutions. So perhaps continuing in some other parameters may produce even more solutions.

We see that, each point in the closed curve 4.16 corresponds to a wave pulse that is not similar to the other pulses that corresponded to other points on this closed curve. This deduction comes from the appearance of the wave pulses in figure 4.17.

We found that each branch on the closed curves corresponds to a wave pulse that has a different amplitude. For instance, moving continuously from green square to green triangle decreases the amplitude approximately from 1.0 to 0.8. And if we turn over to another branch we see that not only did the amplitude change but the number of oscillations changed as well.

So, one could conclude that each branch on the closed curve corresponds to pulses that have a monotonic tail and the same number of oscillations in front that are clearly seen by eye (i.e. oscillations that exceed a certain magnitude, say $u = 0.01$) but with a different amplitude. It might happen that two wave pulses in two different branches have the same amplitude as in figure 4.17(a) and (h), but in this case they do not have same wave profile.

The variation of parameters and change of the shape of the homoclinic solution has been discussed by Kuznetsov in chapter 6 in [33]. Kuznetsov has provided theorems that illustrate some features of the homoclinic solution in relation with the eigenvalues and the splitting function. Actually, the homoclinic orbit coincides with either saddle or saddle focus equilibrium. All those theorems are based on non-zero saddle quantity, which is defined as the sum of the real parts of the eigenvalues. These theorems revolve around proving the existence of stable limit cycle(s) in the neighbourhood of the homoclinic solution. In some cases there is a change in the number of rotations. There are infinite stable limit cycles if the equilibrium is saddle focus and the saddle quantity is

positive. In the other cases there is only one stable limit cycle.

In our case we have zero saddle quantity. This could be deduced by linearising (4.15) about the equilibrium with absence of the self diffusion terms, i.e ($D_{uu} = D_{vv} = 0$), that yields the following matrix

$$A = \begin{bmatrix} 0 & 1 & 0 & 0 \\ \frac{c^2 D_{uv}}{\Delta} \frac{\partial g(U,V)}{\partial U} & 0 & \frac{c^2 D_{uv}}{\Delta} \frac{\partial g(U,V)}{\partial V} & -\frac{c^2 D_{uv}}{\Delta} \\ 0 & 0 & 0 & 1 \\ -\frac{c^2 D_{vu}}{\Delta} \frac{\partial f(U,V)}{\partial U} & \frac{c^2 D_{vu}}{\Delta} & -\frac{c^2 D_{vu}}{\Delta} \frac{\partial f(U,V)}{\partial V} & 0 \end{bmatrix}, \tag{4.19}$$

where $\Delta = -D_{uv} D_{vu}$. As the trace of A is equal to the sum of the eigenvalues, it is obvious that we have zero saddle quantity.

Although our case is not corresponding to Kuznetsov's work as we have zero saddle quantity, but we have the numerical evidence that there is change in the number of rotations according to change the values of parameters (a, c) as shown in figure 4.16 and the correspondent travelling pulses in figure 4.17. Kuznetsov has shown similar change by using reaction self diffusion FHN model, that has positive saddle quantity.

4.7 Chapter Summary

In this chapter we have explored more features of reaction cross-diffusion system with FHN model. We have started by recomputing the speed of the stable of travelling pulse that were has been established in [55] to show better approximation to the value of the speed. Also, we have stated some of the types of the propagating pulse that obtained by the system. We have added the linearisation of the system about the equilibrium and connected the results to the different types of the pulses.

We have shown the results of applying numerical continuation on the system. The first result is obtained by continuing the parameters to be the same as those in [55] which gave a stable propagating pulse. The result is that we have obtained a pulse wave that is identical to that stable pulse in [55]. We have proved the identification between

them through comparing their speeds and profiles. Moreover, we have demonstrated the stability of the pulse that we have obtained by using direct numerical simulation.

The stable pulse is continued in (T,c)-plane. This step provided a parabolic curve, where its lower branch corresponds to the stable pulse that we have already found in the first step. The upper branch corresponds to a pulse that has a smaller amplitude. By direct numerical simulation we have established that the upper branch corresponds to a stable pulse, too. This feature is different to the reaction self diffusion system with FHN model where the two branches of the curve in (P,c)-plane correspond to two pulses, one of them is stable and the other is not.

We have shown the result of varying the threshold parameter a and the speed in $(a,c)-$plane. In this step we have obtained a closed curve. This closed curve coincides with what we have faced when AUTO fails to reduce the parameter a to 0.10. Each branch of this closed curve corresponds to pulses that are similar in the number of oscillations but different in the amplitude. We have not checked the stability of those pulses except for $a = 0.22$. So,we only know that the starting point, which is magenta diamond in the closed curve, corresponds to stable propagating pulse.

Furthermore, we have shown that in our case we have always zero saddle quantity. Although we have zero saddle quantity, we have obtained propagating pulses that have changed in the number of rotations as the parameters varied, which is a property has been proved for non-zero saddle quantity.

CHAPTER 5

DISCUSSION

5.1 Main Results

Reaction diffusion systems attracted a huge attention because such systems are helpful for us to understand many real-world problems. This thesis is dedicated to explore more features of reaction cross-diffusion systems. Reaction cross-diffusion systems have received less attention than what reaction self-diffusion systems have received. Few of reaction diffusion systems have exact analytical solutions known. In this thesis we have added one reaction diffusion system with its analytical solution. In fact, in this thesis we have obtained analytical and numerical results.

We have introduced a reaction cross-diffusion system with a continuous polynomial function as a kinetic term in the system aiming to find an analytical solution. We have shown that the quartic polynomial is the easiest suitable polynomial function that makes the problem has an exact analytical solution. We have exhibited the analytical solution in a front wave profile.

We have paid an attention to make this front wave imitate well-knowns wave fronts such as Fisher-KPP and ZFK-Nagumo. We have proven that the front wave, that is obtained from the analytical solution of reaction cross diffusion system with quartic

polynomial, could have either stable resting state ahead the front and unstable resting state behind the front or unstable resting state ahead the front and stable resting state behind the front. Therefore, it is possible to mimic Fisher-KPP regarding to the stability of the resting states of the front. On the other hand, the front wave by reaction cross-diffusion system with quartic polynomial mimics the ZFK-Nagumo front wave in that both have discrete speed rather than continuous spectrum of speeds as in Fisher-KPP. We have presented that the existence of quartic polynomial could give four different cases; inner roots, outer roots, double roots and complex roots depending on the choices of values of free parameters.

In chapter 3, we have provided the conditions of the choices of free parameters that corresponds to each case. We have simulated each case two times with different choices of free parameters. The type of the instability is identified by direct numerical simulation. We observed no qualitative difference in the behaviours of the propagating waves when we chose other values of the free parameters for outer,double and complex cases. For inner roots case, the post front state is unstable, and the system is attracted by one stable equilibrium but for other choice of values of the free parameters we have seen that it is attracted by one stable equilibrium then after a period of time it is attracted by the other stable equilibrium. All the propagating fronts of each of these cases are subject to dynamical instability, for all choices of free parameters we tried.

In chapter 4 we have presented some results of bifurcations analysis in reaction cross-diffusion system with cubic FHN nonlinearity. To do that, we have used numerical continuation software.
After continuing the parameters to the target values we continue the system in period and speed plane, that yields 'parabolic' curve. We have found that the upper branch of the 'parabolic' curve corresponds to a stable propagating pulse that has not been found by direct numerical simulation in [55]. Moreover, we have proved that the lower branch corresponds to the stable propagating pulse that is found by direct numerical simulation in [55]. Having stable propagating pulses from both (lower and upper) branches in the 'parabolic' curve in the period and speed plane is not the case in the reaction

self-diffusion system. We have found the behaviour of the curve of continuation in period and speed plane being more complicated as we decrease the value of the threshold parameter a.

By fixing a large period and make the continuation run for ($a$and speed) plane we have found a closed curve, which coincides with the inability to decrease the parameter a to 0.10.

5.2 Further Work

We have described unstable propagating waves, that happened in the propagating front in reaction cross-diffusion system with quartic polynomial function and also happened in reaction cross-diffusion system with FHN model. We have demonstrated numerically the existence of the dynamical instability but the details of this instability deserve further investigation.

One possible reason for lack of exact stable analytical solutions in our polynomial model: we assumed solutions in the shape of a monotonic front, whereas all stable solutions observed numerically have oscillatory fronts. Perhaps our method can be used to design a polynomial model, if the exact analytical solution is postulated in a more realistic form. Another possible reason is that, our choices of the parameters were not from the region which corresponds to stable propagating front.

Studying the spectrum of linear operator in the manner similar to that in Sandstede [42] will help us to answer these interesting questions. Furthermore, we could answer these questions by using numerical continuation softwares that are built to study the bifurcation of propagating waves such as WAVETRAIN [46].

The oscillation in the pulses that are obtained from reaction cross-diffusion systems with FHN model could exhibit a phenomenon similar to the 'snakes-and-ladders bifurcation' [30] [3]. In fact, this type of bifurcation is quite new field and very little literature on snakes-and-ladders bifurcation in excitable media. The only work we only found in studying the snakes-and-ladders bifurcation in excitable media is [63], that makes the

case more interesting to be searched on.

There are consideration of reaction cross-diffusion system with Truscott and Brindely model [56] and [7] and Lengyel-Epstein model [8]. Those results are obtained by direct numerical solution. We could reconsider those models in reaction cross-diffusion system and study them by using numerical continuation methods.

Last but not least, as we solve the reaction diffusion systems using travelling waves technique, we could approximate the travelling wave solution and do analysis on the waves solution by using asymptotic methods such as Wentzel, Kramer and Brillouin (WKB) method.

CHAPTER 6

APPENDIX

6.1 Analytical Solution of ZFK-Nagumo Model

The computation of analytical wave solution of ZFK-Nagumo model (1.13) will be shown in details. By applying the wave variable on (1.13) we obtain

$$U_{\xi\xi} + cU_{\xi} - U(U-\alpha)(U-1) = 0, \qquad U(\pm\infty) = u_{1,2} \qquad u_{1,2} \in \mathbb{R}, \tag{6.1}$$

where $U(\xi) = u(x,t)$ and $\xi = x - ct$.

The analytical solution of (6.1) been found in, e.g. [36]. Here we show the steps of the analytical solution in details.

The equation (6.1) could be solved by reduction of order such as follows. Let

$$U_{\xi} = y\,, \tag{6.2}$$

then

$$U_{\xi\xi} = \frac{d}{d\xi}y = \frac{dy}{dU}\frac{dU}{d\xi} = y\frac{dy}{dU}\,. \tag{6.3}$$

Substituting (6.2) and (6.3) in (6.1) yields

$$y(\frac{dy}{dU} + c) = U(U-\alpha)(U-1)\,. \tag{6.4}$$

These factorised polynomials on both sides of (6.4) suggests that y is a quadratic polynomial. So, let

$$y(U) = A(U-u_1)(U-u_2), \tag{6.5}$$

$$y'(U) = A(2U-(u_1+u_2)), \tag{6.6}$$

where $A \in \mathbb{R} \setminus \{0\}$.
Substituting (6.5) and (6.6) in (6.4) yields

$$A^2(U-u_1)(U-u_2)\left[(2U-(u_1+u_2)) + \tfrac{c}{A}\right] = U(U-\alpha)(U-1). \tag{6.7}$$

Choosing $u_1 = 0$ and $u_2 = 1$ that coincide with the resting states of the front wave solution leads to the following

$$A^2(2U-1+\tfrac{c}{A}) = U-\alpha. \tag{6.8}$$

By equating the coefficients of U in (6.8), we obtain the following relation

$$2A^2 = 1 \tag{6.9}$$

$$A^2(-1+\tfrac{c}{A}) = -\alpha \tag{6.10}$$

From (6.9) we have $A = \frac{1}{\sqrt{2}}$. Consequently ,

$$c(\alpha) = \frac{\sqrt{2}}{2}\big(1-2\alpha\big). \tag{6.11}$$

It is clear that the speed of front wave in ZFK-Nagumo model is discrete and for $c > 0$ it is required that $\alpha \in (0, 1/2)$.

The formula of the exact solution is obtained by integrating the right hand side of (6.5) with respect to ξ, that gives

$$U(\xi) = \frac{1}{1+\exp\big(C + \frac{\xi}{\sqrt{2}}\big)}, \tag{6.12}$$

where C is an arbitrary constant.

6.2 Two Travelling Wave Variables for Continuation

In section 4.3 we have applied the wave variable

$$\xi = t - \frac{1}{c}x, \tag{6.13}$$

instead of the wave variable

$$\eta = x - ct. \tag{6.14}$$

Here we present the reason why (for large c) the wave variable ξ is better to be applied on reaction cross-diffusion system rather than η.

Applying η on the reaction cross-diffusion system (4.1), yields the following system

$$\begin{aligned} f(U,V) + D_{uv}V_{\eta\eta} + cU_\eta = 0, \\ g(U,V) - D_{vu}U_{\eta\eta} + cV_\eta = 0. \end{aligned} \tag{6.15}$$

From the system (6.15), if the parameter c is very large ($c \to \infty$), then

$$U_\eta \to 0 \quad , V_\eta \to 0. \tag{6.16}$$

We see from (6.16) when we have very large c as we have then a constant solution that is not interesting case.

On the other hand, applying ξ in the system (4.1), yields

$$\begin{aligned} f(U,V) + \frac{D_u v}{c^2}V_{\xi\xi} - U_\xi = 0, \\ g(U,V) - \frac{D_v u}{c^2}U_{\xi\xi} - V_\xi = 0, \end{aligned} \tag{6.17}$$

For $c \to \infty$, we have

$$U_\xi = f(U,V) \quad , \quad V_\xi = g(U,V). \tag{6.18}$$

which is the system of interest.

6.3 Algorithm in Direct Numerical Simulation

Here we present the algorithm of direct numerical simulation using finite difference scheme to solve (4.18) with operator splitting, where we split each step to two sub-steps. In the first half step we apply fully explicit scheme on the kinetic terms and in

the second half step we apply fully implicit scheme on the linear cross-diffusion terms

- Fully explicit scheme: (1^{st} half-step)

$$u^{n+\frac{1}{2}} = u^n + \Delta t u^n (u^n - a)(1 - u^n) - k_1 v^n$$
$$v^{n+\frac{1}{2}} = v^n + \epsilon \Delta t u^n$$

- Fully implicit scheme: (2^{nd} half-step)

$$u^{n+1} - u^{n+\frac{1}{2}} = A v^{n+1} \tag{6.19}$$
$$v^{n+1} - v^{n+\frac{1}{2}} = B u^{n+1} \tag{6.20}$$

where

$$A = \begin{bmatrix} -2\rho & 2\rho & 0 & \cdots & \cdots & 0 \\ \rho & -2\rho & \rho & \ddots & & \vdots \\ 0 & \rho & -2\rho & \rho & \ddots & \vdots \\ \vdots & \ddots & \ddots & \ddots & \ddots & 0 \\ \vdots & \ddots & \ddots & \ddots & \ddots & \rho \\ 0 & \cdots & \cdots & \cdots & 2\rho & -2\rho \end{bmatrix} \qquad B = \begin{bmatrix} -2\gamma & 2\gamma & 0 & \cdots & \cdots & 0 \\ \gamma & -2\gamma & \gamma & \ddots & & \vdots \\ 0 & \gamma & -2\gamma & \gamma & \ddots & \vdots \\ \vdots & \ddots & \ddots & \ddots & \ddots & 0 \\ \vdots & \ddots & \ddots & \ddots & \ddots & \gamma \\ 0 & \cdots & \cdots & \cdots & 2\gamma & -2\gamma \end{bmatrix}$$

where $\left(\rho = \frac{\Delta t D_v}{\Delta x^2}\right)$ and $\left(\gamma = -\frac{\Delta t D_u}{\Delta x^2}\right)$.

By arranging (6.19)

$$u^{n+1} = A v^{n+1} + u^{n+\frac{1}{2}} \tag{6.21}$$

and by substituting (6.21) in (6.20) we have

$$v^{n+1} = Q^{-1}(v^{n+\frac{1}{2}} + B u^{n+\frac{1}{2}}), \tag{6.22}$$

where $Q = I - BA$ and I is the identity matrix.

Then u^{n+1} is computed by substituting (6.22) in (6.21). These steps is summarised in the following chart

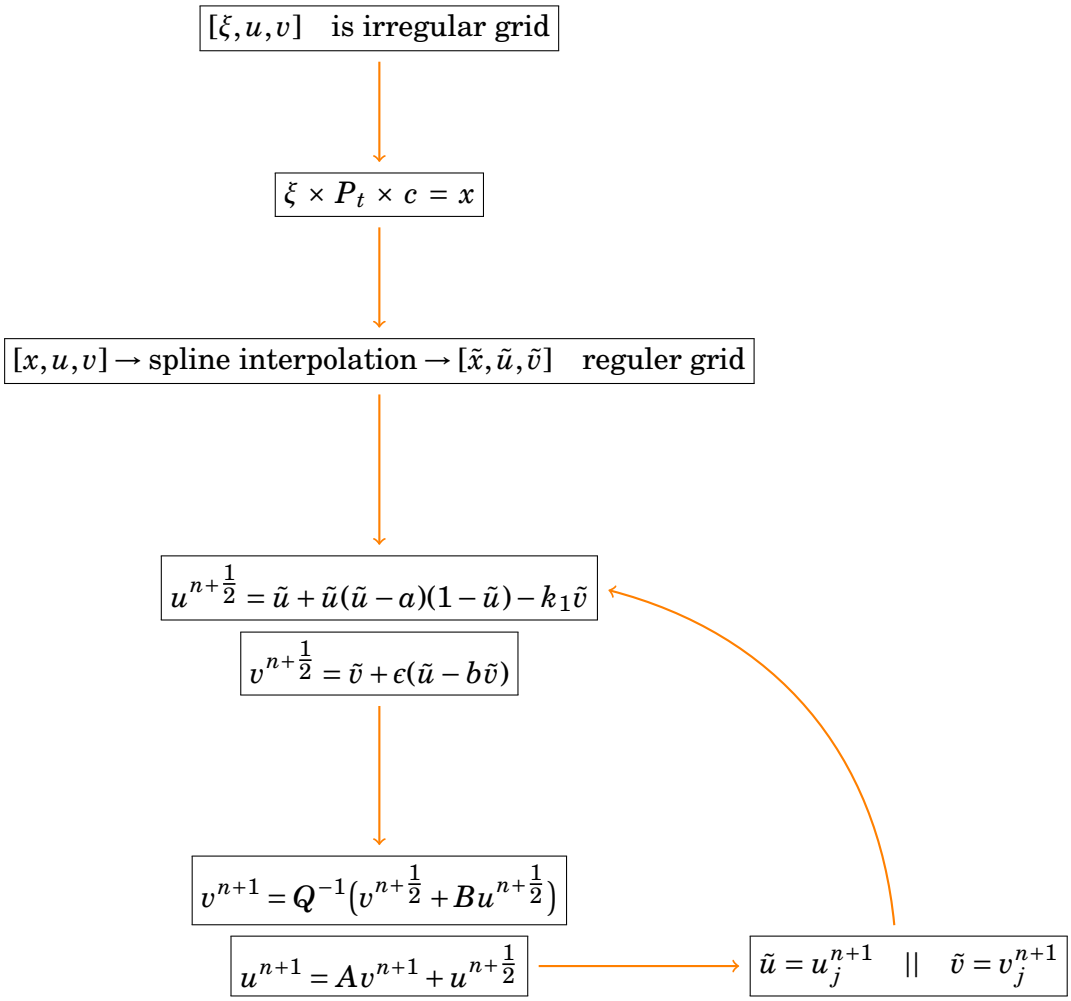
$[\xi, u, v]$ is irregular grid
$\xi \times P_t \times c = x$
$[x, u, v] \rightarrow$ spline interpolation $\rightarrow [\tilde{x}, \tilde{u}, \tilde{v}]$ reguler grid
$u^{n+\frac{1}{2}} = \tilde{u} + \tilde{u}(\tilde{u} - a)(1 - \tilde{u}) - k_1\tilde{v}$
$v^{n+\frac{1}{2}} = \tilde{v} + \epsilon(\tilde{u} - b\tilde{v})$
$v^{n+1} = Q^{-1}\left(v^{n+\frac{1}{2}} + Bu^{n+\frac{1}{2}}\right)$
$u^{n+1} = Av^{n+1} + u^{n+\frac{1}{2}}$
$\tilde{u} = u_j^{n+1}$ || $\tilde{v} = v_j^{n+1}$

BIBLIOGRAPHY

[1] M. A. ABDELKADER, *Travelling wave solutions for a generalized Fisher equation*, Journal of Mathematical Analysis and Applications, 85 (1982), pp. 287–290.

[2] M. J. ABLOWITZ AND A. ZEPPETELLA, *Explicit solutions of Fisher's equation for a special wave speed*, Bulletin of Mathematical Biology, 41 (1979), pp. 835–840.

[3] D. AVITABILE, D. J. LLOYD, J. BURKE, E. KNOBLOCH, AND B. SANDSTEDE, *To snake or not to snake in the planar Swift–Hohenberg equation*, SIAM Journal on Applied Dynamical Systems, 9 (2010), pp. 704–733.

[4] R. E. BAKER, S. SCHNELL, AND P. K. MAINI, *Waves and patterning in developmental biology: vertebrate segmentation and feather bud formation as case studies*, The International Journal of Developmental Biology, 53 (2009), p. 783.

[5] M. A. BECK, *Topics in Stability Theory for Partial Differential Equations*, PhD thesis, Boston University, 2006.

[6] B. BEZEKCI, I. IDRIS, R. SIMITEV, AND V. BIKTASHEV, *Semianalytical approach to criteria for ignition of excitation waves*, Physical Review E, 92 (2015), p. 042917.

[7] V. BIKTASHEV AND M. TSYGANOV, *Spontaneous traveling waves in oscillatory systems with cross diffusion*, Physical Review E, 80 (2009), p. 056111.

[8] ——, *Envelope quasisolitons in dissipative systems with cross-diffusion*, Physical Review Letters, 107 (2011), p. 134101.

[9] V. N. BIKTASHEV AND M. A. TSYGANOV, *Solitary waves in excitable systems with cross-diffusion*, Proceedings of the Royal Society of London A: Mathematical, Physical and Engineering Sciences, 461 (2005), pp. 3711–3730.

[10] G. BORDYUGOV, N. FISCHER, H. ENGEL, N. MANZ, AND O. STEINBOCK, *Anomalous dispersion in the Belousov–Zhabotinsky reaction: Experiments and modeling*, Physica D: Nonlinear Phenomena, 239 (2010), pp. 766–775.

[11] P. BRESSLOFF, *Waves in Neural Media: From single Neurons to Neural Fields. Lecture notes on mathematical modeling in the life sciences*, Springer-Verlag, New York, 2014.

[12] R. BURRIDGE AND L. KNOPOFF, *Model and theoretical seismicity*, Bulletin of The Seismological Society of America, 57 (1967), pp. 341–371.

[13] R. BUTT, *Introduction to Numerical Analysis Using MATLAB®*, Jones & Bartlett Learning, Sudbury, Massachusetts, 2009.

[14] J. H. CARTWRIGHT, V. M. EGUÍLUZ, E. HERNÁNDEZ-GARCÍA, AND O. PIRO, *Dynamics of elastic excitable media*, International Journal of Bifurcation and Chaos, 9 (1999), pp. 2197–2202.

[15] J. H. CARTWRIGHT, E. HERNÁNDEZ-GARCÍA, AND O. PIRO, *Burridge-Knopoff models as elastic excitable media*, Physical Review Letters, 79 (1997), p. 527.

[16] F. DIAS AND C. KHARIF, *Nonlinear gravity and capillary-gravity waves*, Annual Review of Fluid Mechanics, 31 (1999), pp. 301–346.

[17] E. J. DOEDEL, T. F. FAIRGRIEVE, B. SANDSTEDE, A. R. CHAMPNEYS, Y. A. KUZNETSOV, AND X. WANG, *Auto-07p: Continuation and bifurcation software for ordinary differential equations*.
`http://www.dam.brown.edu/people/sandsted/auto/auto07p.pdf`.
Accessed: 06-01-2018.

[18] D. R. DURRAN, *Numerical methods for fluid dynamics: With applications to geophysics*, vol. 32, Springer Science & Business Media, New York, 2010.

[19] L. EDELSTEIN-KESHET, *Mathematical models in biology*, SIAM, Philadelphia, 2005.

[20] P. C. FIFE, *Propagator-controller systems and chemical patterns*, in Non-equilibrium Dynamics in Chemical Systems, C. Vidal and A. Pacault, eds., Springer-Verlag, Berlin Heidelberg New York Tokyo, 1984, pp. 76–88.

[21] R. A. FISHER, *The wave of advance of advantageous genes*, Annals of Eugenics, 7 (1937), pp. 355–369.

[22] R. FITZHUGH, *Impulses and physiological states in theoretical models of nerve membrane*, Biophysical Journal, 1 (1961), pp. 445–466.

[23] R. FUTRELLE, *Dictyostelium chemotactic response to spatial and temporal gradients. theories of the limits of chemotactic sensitivity and of pseudochemotaxis*, Journal of Cellular Biochemistry, 18 (1982), pp. 197–212.

[24] B. H. GILDING AND R. KERSNER, *Travelling waves in nonlinear diffusion-convection reaction*, vol. 60, Birkhäuser, Basel Boston Berlin, 2012.

[25] A. L. HODGKIN AND A. F. HUXLEY, *A quantitative description of membrane current and its application to conduction and excitation in nerve*, The Journal of Physiology, 117 (1952), pp. 500–544.

[26] P. KALIAPPAN, *An exact solution for travelling waves of* $u_t = d u_{xx} + u - u^k$, Physica D: Nonlinear Phenomena, 11 (1984), pp. 368–374.

[27] R. KAPRAL AND K. SHOWALTER, *Chemical waves and patterns*, Springer Science & Business Media, Dordrecht, Netherlands, 2012.

[28] T. KAWAHARA AND M. TANAKA, *Interactions of traveling fronts: an exact solution of a nonlinear diffusion equation*, Physics Letters A, 97 (1983), pp. 311–314.

[29] E. F. KELLER AND L. A. SEGEL, *Initiation of slime mold aggregation viewed as an instability*, Journal of Theoretical Biology, 26 (1970), pp. 399–415.

[30] E. KNOBLOCH, *Spatially localized structures in dissipative systems: open problems*, Nonlinearity, 21 (2008), p. T45.

[31] A. KOLMOGOROV, I. PETROVSKII, AND N. PISCOUNOV, *A study of the diffusion equation with increase in the amount of substance, and its application to a biological problem*, in Selected works of A.N. Kolmogorov, V. Tikhomirov, ed., Springer, Dordrecht, 1991, pp. 242–270.

[32] N. KOPELL AND L. HOWARD, *Plane wave solutions to reaction-diffusion equations*, Studies in Applied Mathematics, 52 (1973), pp. 291–328.

[33] Y. A. KUZNETSOV, *Elements of applied bifurcation theory*, Springer-Verlag, New York, 1998.

[34] C.-M. LIN, T. X. JIANG, R. E. BAKER, P. K. MAINI, R. B. WIDELITZ, AND C.-M. CHUONG, *Spots and stripes: pleomorphic patterning of stem cells via p-ERK-dependent cell chemotaxis shown by feather morphogenesis and mathematical simulation*, Developmental Biology, 334 (2009), pp. 369–382.

[35] J. D. LOGAN, *An introduction to nonlinear partial differential equations*, vol. 89, John Wiley & Sons, Hoboken, New Jersey, 2008.

[36] H. P. MCKEAN, *Nagumo's equation*, Advances in Mathematics, 4 (1970), pp. 209–223.

[37] J. D. MURRAY, *Mathematical Biology. II Spatial Models and Biomedical Applications* {*Interdisciplinary Applied Mathematics V. 18*}, Springer-Verlag, New York, 2001.

[38] J. D. MURRAY, *Mathematical biology [electronic resource] I: An introduction*, Springer-Verlag, New York, 2002.

[39] L. PERKO, *Differential equations and dynamical systems*, Springer-Verlag, New York, 2001.

[40] A. RALSTON AND P. RABINOWITZ, *A first course in numerical analysis*, Dover Publications Inc., Mineola, New York, 2001.

[41] M. RODRIGO AND M. MIMURA, *Exact solutions of reaction-diffusion systems and nonlinear wave equations*, Japan Journal of Industrial and Applied Mathematics, 18 (2001), pp. 657–696.

[42] B. SANDSTEDE, *Stability of travelling waves*, in Handbook of dynamical systems, B. Fiedler, ed., Elsevier Science, Amsterdam etc, 2002, pp. 983–1055.

[43] M. SCHNITZER, S. BLOCK, AND H. BERG, *Strategies for chemotaxis*, Biology of The Chemotactic Response, 46 (1990), pp. 15–34.

[44] J. SCOTT RUSSELL, *Report on Waves: Made to the Meetings of the British Association in 1842-43*, Richard and John E Taylor, London, 1845.

[45] L. A. SEGEL, *Distant side-walls cause slow amplitude modulation of cellular convection*, Journal of Fluid Mechanics, 38 (1969), pp. 203–224.

[46] J. A. SHERRATT, *Numerical continuation methods for studying periodic travelling wave (wavetrain) solutions of partial differential equations*, Applied Mathematics and Computation, 218 (2012), pp. 4684–4694.

[47] J. A. SHERRATT AND G. J. LORD, *Nonlinear dynamics and pattern bifurcations in a model for vegetation stripes in semi-arid environments*, Theoretical Population Biology, 71 (2007), pp. 1–11.

[48] J. A. SHERRATT AND M. J. SMITH, *Periodic travelling waves in cyclic populations: field studies and reaction–diffusion models*, Journal of The Royal Society Interface, 5 (2008), pp. 483–505.

[49] N. SHIGESADA, K. KAWASAKI, AND E. TERAMOTO, *Spatial segregation of interacting species*, Journal of Theoretical Biology, 79 (1979), pp. 83–99.

[50] G. D. SMITH, *Numerical solution of partial differential equations: finite difference methods*, Oxford University Press, Oxford, 1985.

[51] J. C. STRIKWERDA, *Finite difference schemes and partial differential equations*, SIAM, Philadelphia, 2004.

[52] J. W. THOMAS, *Numerical partial differential equations: finite difference methods*, vol. 22, Springer-Verlag, New York, 2013.

[53] L. N. TREFETHEN, *Spectral methods in MATLAB*, Society for Industrial and Applied Mathematics (SIAM), Philadelphia, 2000.

[54] M. TSYGANOV AND V. BIKTASHEV, *Half-soliton interaction of population taxis waves in predator-prey systems with pursuit and evasion*, Physical Review E, 70 (2004), p. 031901.

[55] ——, *Classification of wave regimes in excitable systems with linear cross diffusion*, Physical Review E, 90 (2014), p. 062912.

[56] M. TSYGANOV, J. BRINDLEY, A. HOLDEN, AND V. BIKTASHEV, *Quasisoliton interaction of pursuit-evasion waves in a predator-prey system*, Physical Review Letters, 91 (2003), p. 218102.

[57] M. TSYGANOV, I. KRESTEVA, A. MEDVINSKII, AND G. IVANITSKII, *A novel mode of bacterial population wave interaction*, Doklady Akademii Nauk, 333 (1993), pp. 532–536.

[58] A. M. TURING, *The chemical basis of morphogenesis*, Bulletin of Mathematical Biology, 52 (1990), pp. 153–197.

[59] J. J. TYSON AND J. P. KEENER, *Singular perturbation theory of traveling waves in excitable media (a review)*, Physica D: Nonlinear Phenomena, 32 (1988), pp. 327–361.

[60] A. I. VOLPERT, V. A. VOLPERT, AND V. A. VOLPERT, *Traveling wave solutions of parabolic systems*, American Mathematical Soc., Providence, Rhode Island, 1994.

[61] V. VOLPERT AND S. PETROVSKII, *Reaction–diffusion waves in biology*, Physics of Life Reviews, 6 (2009), pp. 267–310.

[62] D. XUE AND Y. CHEN, *Scientific computing with MATLAB*, CRC Press, Boca Raton, Florida, USA, 2016.

[63] A. YOCHELIS, E. KNOBLOCH, AND M. H. KÖPF, *Origin of finite pulse trains: Homoclinic snaking in excitable media*, Physical Review E, 91 (2015), p. 032924.

[64] N. J. ZABUSKY AND M. D. KRUSKAL, *Interaction of "solitons" in a collisionless plasma and the recurrence of initial states*, Physical Review Letters, 15 (1965), p. 240.

[65] Y. B. ZELDOVICH AND G. BARENBLATT, *Theory of flame propagation*, Combustion and Flame, 3 (1959), pp. 61–74.

[66] J. ZELDOWITSCH AND D. FRANK-KAMENETZKI, *On the theory of uniform flame propagation*, Doklady AN SSSR, 19 (1938), pp. 693–697.